ISTANBUL TECHNICAL UNIVERSITY ★ GRADUATE SCHOOL OF SCIENCE ENGINEERING AND TECHNOLOGY

UNDERSTANDING THE AERODYNAMICS AROUND A SET OF FLYING SAILS USING EXPERIMENTAL AND THEORETICAL TECHNIQUES

M.Sc. THESIS

Ersin DANIŞ

Department of Naval Architecture and Marine Engineering

Naval Architecture and Marine Engineering Programme

JANUARY 2012

ISTANBUL TECHNICAL UNIVERSITY ★ GRADUATE SCHOOL OF SCIENCE ENGINEERING AND TECHNOLOGY

UNDERSTANDING THE AERODYNAMICS AROUND A SET OF FLYING SAILS USING EXPERIMENTAL AND THEORETICAL TECHNIQUES

M.Sc. THESIS

Ersin DANIŞ
(508091012)

Department of Naval Architecture and Marine Engineering

Naval Architecture and Marine Engineering Programme

Thesis Advisor: Prof. Dr. Mustafa İNSEL

JANUARY 2012

İSTANBUL TEKNİK ÜNİVERSİTESİ ★ FEN BİLİMLERİ ENSTİTÜSÜ

DENEYSEL VE TEORİK YÖNTEMLERİ KULLANARAK BİRTAKIM YELKEN MODELLERİNİN ETRAFINDAKİ AERODİNAMİK AKIŞININ İNCELENMESİ

YÜKSEK LİSANS TEZİ

Ersin DANIŞ
(508091012)

Gemi İnşaatı ve Gemi Makinaları Mühendisliği Anabilim Dalı

Gemi İnşaatı ve Gemi Makinaları Mühendisliği Programı

Tez Danışmanı: Prof. Dr. Mustafa İNSEL

OCAK 2012

Ersin Danış, a **M.Sc.** student of ITU **Institute of / Graduate School of Science Engineering and Technology** student ID 508091012, successfully defended the **thesis/dissertation** entitled "**UNDERSTANDING THE AERODYNAMICS AROUND A SET OF FLYING SAILS USING EXPERIMENTAL AND THEORETICAL TECHNIQUES**", which he prepared after fulfilling the requirements specified in the associated legislations, before the jury whose signatures are below.

Thesis Advisor :	**Prof. Dr. Mustafa İNSEL** İstanbul Technical University	.....
Jury Members :	**Prof. Dr. Abdi KÜKNER** Istanbul Technical University	.....
	Asst. Prof. Şebnem HELVACIOĞLU Istanbul Technical University	.....

Date of Submission : 19 December 2011
Date of Defense : 31 January 2012

To my family and friends,

FOREWORD

This dissertation project would not have been possible without the support of many people. The author wishes to express his gratitude to his supervisor, Prof. Dr. M. Insel who was abundantly helpful and offered invaluable assistance, support and guidance. Deepest gratitude is also due to Prof. P. Wilson and Mr Lester Gilbert without their knowledge and assistance this project would not have been successful. Special thanks also to all his post-graduate friends and best friends. The author would also like to convey thanks to Mr I. Campbell and Dr Z. Xie for sharing the literature and invaluable assistance. The author wishes to express his love and gratitude to his beloved family members; for their understanding and endless love through the duration of his studies.

December 2011

Ersin DANIŞ
(Naval Architect)

TABLE OF CONTENTS

Page

ABBREVIATIONS

A : Area of Sail
AR : Aspect Ratio
C : Wind Tunnels Cross Sectional Area
C_D : Drag Coefficient
C_{DI} : Induced Drag Coefficient
C_{D0} : Zero-lift Drag Coefficient
C_{DS} : Separated Drag Coefficient
CFD : Computational Fluid Dynamics
C_L : Lift Coefficient
D : Drag (Aerodynamic)
D_F : Driving Force
D_I : Induced Drag
E : Energy
F : Body Force
F : Net Force
F_A : Total Aerodynamic Force
F_H : Total Hydrodynamic Force
H_E : Effective Rig Height
H_F : Heeling Force; Aerodynamic Side Force
g : Acceleration of Gravity
GUI : Graphical User Interface
m : Mass of the Body
L : Lift (Aerodynamic)
Le : Characteristic Linear Dimension
P : Pressure
R : Hydrodynamic Drag Force
RANS : Reynolds Averaged Navier-Stokes
Re : Reynolds Number
S_F : Hydrodynamic Side Force
SST : Shear Stress Transport
T : Temperature
V : Velocity
V_A : Apparent Wind Velocity
Ve : Equivalent Airspeed
V_S : Velocity of Sailboat
V_T : True Wind Velocity

LIST OF TABLES

Page

LIST OF FIGURES

Page

NOMENCLATURE

λ	: Leeway Angle
β_A	: Apparent Wind Angle
β_T	: True Wind Angle
ϕ	: Heeling Angle
γ	: Angle of Attack (True Wind Angle)
ε_A	: Aerodynamic Drag Angle
ε_H	: Hydrodynamic Drag Angle
ρ_{air}	: Density of Air
δ	: Boundary Layer Thickness
δ	: Downwash Boundary Correction Factor
ε_{WB}	: Wake Blockage Factor
π	: Pi Number
ρ	: Density of the Fluid
δ_M	: The Sheeting Angle of the Mainsail
δ_F	: The Sheeting Angle of the Foresail (or Jib Sail)
υ	: Mean Velocity
μ	: Dynamic Viscosity of the Fluid
ν	: Kinematic Viscosity of the Fluid
τ	: Shear Stress
τ_{xx}	: Normal Stress in the x-direction on x-plane
τ_{xy}	: Shear Stress in the y-direction on x-plane
a	: Acceleration of the Body
e	: Oswald Efficiency Number, typically 0.85 to 0.95
h	: Elevation
i, j, k	: Ordering Grid Points in Structure Mesh
k	: Material's Conductivity
q	: Dynamic Pressure
t	: Time
u,v,w	: Components of Velocity
x,y,z	: Cartesian Coordinates

UNDERSTADING THE AERODYNAMICS AROUND A SET OF FLYING SAILS USING EXPERIMENTAL AND THEORETICAL TECHNIQUES

SUMMARY

The aim of this study is to perform experimental testing by using A Class model and to validate data from wind tunnel tests using a computational fluid dynamics (CFD) code. The wind tunnel testing for heeled upwind condition is conducted for various twist and sheeting configurations for both main and jib sails in order to compare the wind tunnel test data with CFD calculations.

A number of changing twist and sheeting configurations are tested in the wind tunnel, and it has showed that the sails having too much twist and sheeting cause of a reduction in the performance of the sails. It also must be pointed out that 28° apparent wind angle compared to 20° has a better performance in terms of lift and drag forces. In this study, only one heel angle (30°) is tested, and it could be possible to test different heel angles and study their effects on the performance of the upwind sailing conditions unless there were some constraints of the project time. In addition to these, it has been observed in the wind tunnel throughout the experiments and checked by analysis results so that 7 m/s wind speed is too strong for those tested sail configurations. 3 m/s wind speed is therefore chosen for CFD simulations.

A number of digital images taken in the wind tunnel are used to create a three-dimensional computational model for the simulation of the wind tunnel testing conditions. Firstly, the pictures are used to create three-dimensional model in Cartesian coordinates (x,y,z) by using Excel software, and then the three-dimensional model is finalised in Rhinoceros software with previously created coordinates. However, the 3D model created in Rhinoceros is an initial surface model which is re-meshed in STAR-CCM+ software after being imported. The final three-dimensional model created in STAR-CCM+ is simulated for compressible flow and discretized on unstructured hexahedral grids to provide estimates of lift and drag for upwind sail configurations. The results are then analysed to draw a comparison between the wind tunnel testing and CFD.

Much time is spent on learning how to simulate desired models in the STAR-CCM+ software, and also on studying backgrounds of the sail aerodynamics and CFD. Due to this, the limitation of the project time is considerably a significant parameter for more accurate CFD simulations to be carried out; most probably less than 8% error could be succeeded. Additionally, there is a need of much developed 3D model creating method. Even though CFD calculations need to be validated, they have proved that CFD is able to estimate the forces developed by the sails. Furthermore, CFD enables the users to visualize the flow behaviours around the sails, although it is very difficult to demonstrate visually the flow behaviours in the wind tunnel. To perform this in the wind tunnel, it should be attached some sensors on the sail surfaces, and thus a new problem will arise by doing this due to fluid-structure interactions.

DENEYSEL VE TEORİK YÖNTEMLERİ KULLANARAK BİRTAKIM YELKEN MODELLERİNİN ETRAFINDAKİ AERODİNAMİK AKIŞIN İNCELENMESİ

ÖZET

Bu çalışmanın amacı A Class yelken modelini kullanarak rüzgâr tüneli deneylerini gerçekleştirmek ve rüzgâr tüneli deneyinden alınan sonuçları hesaplamalı akışkanlar dinamiği yöntemini kullanan CFD programı ile teyit etmektir. Eğimli ve rüzgârın geliş yönüne doğru olarak hazırlanmış rüzgâr tüneli deneyi değişik twist (kıvrımlı) ve sheeting (bumba direğinin açılması) açıları kullanılarak hem ana yelken hem de ön yelken için gerçekleştirilmiştir.

Rüzgâr tüneli deneyinde kullanılan parametreler olan değişik twist ve sheeting açıları bir noktaya işaret etmektedir. Bu nokta, eğer yelkene çok fazla twist ve sheeting yaptırılır ise bu yelken performansında azalmaya sebep olmaktadır. Buradaki önemli nokta rüzgârın yelkene yeterince temas etmeden gitmesini engellemektir. Ayrıca başka bir noktaya değinmek gerekirse, 28° olan görünen rüzgâr açısı 20° olandan daha verimli sonuçlar vermektedir lift (emme) ve drag (direnç) kuvvetleri cinsinden.

Bu çalışmada sadece bir eğim açısı (heeling angle) olarak 30° kullanılarak test edilmiştir. Ancak projenin gerçekleştirilmesinde daha fazla zaman olması halinde değişik eğim açıları da kullanılarak rüzgâr tüneli deneyinde test edilebilirdi. Farklı eğim açıları yelken performansını anlamak açısından önemli bir nokta oluşturmaktadır. 30°'lik heeling angle seçilmesinin sebebi ise bu açının genel yelken performansında kabul edilen bir değer olduğundan dolayıdır. Buna ek olarak, gerek deney yapımı esnasında gerekse de deney sonuçları incelenirken gözlemlenen bir nokta ise 7 m/s rüzgâr hızın test edilen twist ve sheeting konfigürasyonları için oldukça fazla olduğu gerçeği ortaya çıkmıştır. Yelkenler 7 m/s rüzgâr hızı ile oldukça fazla dalgalanma yapmıştır. Bu durum test koşulların doğru bir şekilde analiz edilmesini engellemektedir. Bundan dolayı 7 m/s hızla yapılan testler CFD ile doğrulama yapılmamıştır ve 3 m/s rüzgâr hızı CFD hesapları için seçilmiştir. 3 m/s ile yapılan deneyler oldukça düzgün bir akış sergilemekle birlikte istenilen akış biçimidir. 7 m/s hızın deneyde kullanım amacı ise daha yüksek bir hızda ayarlanan yelken para metlerinin nasıl tepki verdiğini gözlemlemektir.

Rüzgâr tüneli deneyi için ilk olarak 3 gün izin alınabilmiştir Southampton Üniversitesinden. Ancak deney hazırlama sürecinin uzaması nedeniyle 1 gün daha ek bir süre alımı gerçekleşmiştir. Deneyde kullanılan yelken modeli L. Gilbert Bey tarafından tedarik edilmiştir. Yelken modeli genel olarak kullanıma hazır olduğundan dolayı model inşasına zaman ve para harcanmamıştır. Yapılan iş modeli uygun kısımlarını bir araya getirmek ve rüzgâr tüneli monte etmektir. Tünelde kurulu olan 6 degrees of freedom dynamometer (dinamometre) deneyde elde edilen 3 moment ve 3 kuvvet değerlerinin alınması için kullanılmıştır. Dinamometre kullanılmadan önce gerekli kalibrasyonların yapılması gerekmektedir. Ayrıca farklı twist ve sheeting açıları test edildiğinden dolayı her deney sırasında bu değerlerin değişiminin

yapılması gerekmektedir. Bunun için bir cihaz Southampton Üniversitesine bağlı Wolfson Unit bölüminde mevcut olup oradan tedarik edilmiştir. Ancak gerekli bağlantıların model üzerinde etkili olamamasından dolayı bu değişim elde bulunan bazı sağlamlığını koruyabilen kablolar yardımı ile rüzgâr tüneline girmek suretiyle değiştirilmiştir. Bu değişim yapılırken metre yardımıyla da gerekli değişimler yapılmıştır. Bu değişimleri hızlıca yapabilmek için deney için belirlenen açıların yelken üzerindeki mesafe olarak değerleri önceden hesaplanıp deney sırasında seri bir biçimde değiştirilmiştir.

Elde edilen ham (raw data) bilgiler daha sonra tüneldeki data alımı programıyla kayıt altına alınmıştır. Elde edilen bu raw data gerekli düzeltmeler yapılmadan kullanılamamaktadır. Bundan dolayı gerek rüzgâr tüneli düzeltmeleri gerekse de dinamometre düzeltmeleri uygulanmıştır. Dinamometre düzeltmesi her deneyden önce bir rüzgârsız bir ölçüm alınmasını gerektirmiştir. Bunun nedeni ise yapılan herhangi bir ölçümden sonra dinamometre kalibre edilen ilk haline yani sıfır koşullarına geri dönmemesidir.

Bu çalışmanın bir diğer amacı olan rüzgâr tüneli koşullarının bilgisayar ortamında modellenmesini gerçekleştirmek için ilk olarak deney sırasında belirli bir sayıda fotoğraf çekilmiştir. Bu fotoğraflar çekilmeden önce nereden ve hangi açıdan çekileceği belirlenip ondan sonra rüzgâr akımı devam ederken rüzgâr tüneline girmek suretiyle çekilmiştir. Burada önemli olan ise nokta akış devam ederken akışı bozmadan fotoğrafların çekilmesidir. Bu çalışmada içeri girilmeden fotoğraf çekilmeye çalışılmış ancak elde mevcut bulunan fotoğraf makinesinin yeterince geniş açı lens barındıramamasından dolayı bir başarı sağlanamamıştır. Eldeki mevcut yüksek çözünürlükteki fotoğraf makinesi rüzgâr tüneli içinde uygun bir yerde sabitlenmiştir. Bu makinenin istenilen açıda fotoğraf çekememesi sonucunda daha kompakt bir makine ile içeri girmek suretiyle fotoğraflar elde edilmiştir. Kompakt olan makinenin gerekli kablo bağlantılarının olmamasından dolayı rüzgâr tüneline girilmiştir. Fotoğraflar çekilirken uygun bir yerde konum alınarak rüzgârın akış tipinin bozulmaması için çaba sarf edilmiştir.

Çekilen fotoğraflar daha sonra AccuMeasure programı kullanılarak gerekli yelken kıvrımları elde edilmiştir. AccuMeasure programı oldukça basit bir program olmakla beraber bizlere sunduğu olanaklar çok fazladır. Çok önemli bir nokta AccuMeasure programını kullanmadan önce, fotoğraflar çekilirken olabildiğince kamera lensi yelken yüzeyine yakın olmasıdır. Bu yelken kıvrımlarının net ve düzgün bir şekilde okunması açısından önemlidir. AccuMeasure programı ile maksimum yelken kavisi, draft pozisyonu, 15% ve 75% kavis pozisyonları ve de twist değerleri tespit edilebilmektedir. Ancak elde edilen bu değerler bir takım düzeltme basamakları kullanılarak modellemede kullanılmalıdır. Bu düzeltmelerden birincisi kamera lensinden yelken direğinin bumba ile birleştiği noktaya olan mesafenin belirlenip düzeltmede uygulanmasıdır. Diğer bir düzeltme ise kamera lensinden yelken direğinin üst kısmına olan mesafenin belirlenmesidir. Bu deney yapılırken elde edilmesi gereken mesafelerin uygulama yeri ise Excel programı kullanılarak yazılan formüllerin içinde uygulanmasıdır. Excel'de yazılan program otomatik olarak gerekli datanın girilmesi koşulu ile hem ana yelken hem de ön yelken modellemesi için gerekli Kartezyen koordinatlarını vermektedir. Elde edilen bu koordinatlar x,y ve z düzleminde olmakla birlikte üç boyutlu ilk modelin yapılmasına olanak sağlamaktadır. Üç boyutlu ilk meshed model Rhinoceros programı kullanılarak yapılmıştır. Rhinocerosta yapılan modelde 1 mm yelken kalınlığı verilmiştir, çünkü STAR-CCM+ 2 boyutlu işlem yapamamaktadır ve bunu önlemek amacıyla 1 mm

yelken kalınlığı verilmiştir. Bu kalınlık yelken boyutları düşünüldüğünde ihmal edilebilecek bir değer olmakla birlikte bu önemli sorunda bir çözüme kavuşturulmuş olmaktadır.

Rhinoceros programı ile tasarlanan ilk model daha sonra stereolithography CAD (.stl) uzantılı bir dosya ile kaydedilip daha sonra STAR-CCM+ e aktarım yapılmıştır. Aktarılan bu model doğal olarak iyi yapılmamış ise CFD programında tekrardan mesh yapılırken bir sürü kötü yüzey oluşacaktır. STAR-CCM+ in güzel bir özelliği bu kötü yüzeylerin bir nebzede olsa düzeltme imkânı vermesidir. Şayet bu mesh kalitesi açısından kötü olan yüzeyler düzeltilmeyip tekrardan mesh yapılırsa bu analiz sonuçlarının yakınsaması açısından problem oluşturmaktadır. İyi bir yakınsama isteniyorsa temiz bir yüzey elde edilmek zorundadır.

Bu çalışmanın temel amacı olan rüzgâr tüneli modellemesi doğal olarak yelken özelliklerinden dolayı 3 boyutlu olmak zorundadır. Ancak 3 boyutlu analiz oldukça karmaşık ve analiz yapılması zaman almaktadır. Bu aşamada zamandan tasarruf edilebilmesi için ve genel olarak hesaplamalı akışkanlar dinamiğini (CFD) anlamak açısından 2 boyutlu bir ön çalışma yapılmıştır. Bu 2 boyutlu çalışmanın amacı 3 boyutlu analize başlamadan önce bir fikir sahibi olmak ve zamandan tasarruf sağlamaktır. 2 boyutlu analiz yapabilmek için ana ve ön yelkenden ana yelkenin alt kısmından itibaren 700 mm yükseklikte bir kesit alınmıştır. Bu kesitler daha sonra Rhinoceros programı ile kolaylıkla modellenip hesaplamalı akışkanlar dinamiği kullanan STAR-CCM+ a aktarılmıştır. Bir kez daha 2 boyutlu bir analiz direkt olarak yapılamadığından ilk önce belli bir derinlik verilmiştir. Bu derinlik daha sonra STAR-CCM+ da yüzey ve hacim mesh yapıldıktan sonra 2 boyutlu hale dönüştürülmüştür. Dikkat edilmesi gereken nokta CAD programı ile yapılan ilk model 3 boyutlu olmak zorundadır. Eğer çalışma 2 boyutlu yapılmak isteniyorsa bu hesaplamalı akışkanlar dinamiğini kullanan herhangi bir programda yüzey ve hacim mesh yapıldıktan sonra 2 boyuta indirgenebilmektedir.

Oluşturulan 3 boyutlu model STAR-CCM+'da sıkıştırılabilir akış modeli seçilerek unstructured hexahedral gridlerinin üzerine uygulanarak simülasyonlar yapılmıştır drag ve lift katsayılarını elde edebilmek için. CFD simülasyonlardan gelen veriler ile rüzgâr tünelinden gelen deneysel sonuçlar daha sonra bir karşılaştırma yapılmıştır. Hesaplamalı akışkanlar dinamiği (CFD) ve yelken teorisi hakkında yeterli bilgi elde edilmesi amacıyla çok zaman harcanmıştır. Harcanan bu oldukça fazla zaman neticesinde proje zamanı önem kazanmaktadır. Şayet projeyi gerçekleştirmek için daha fazla zaman olması halinde CFD sonuçları daha iyi bir oranda doğru olabilirdi %8'lik bir hata payı yerine.

CFD analiz sonuçları göstermiştir ki iyi bir mesh ve uygun akış parametleri seçildiği takdirde yelken tarafından üretilen kuvvetlerin tahmin edilmesi mümkündür. Bu ek olarak, CFD yelken etrafındaki akışın görselleşmesi olanağı sağlamakta oysaki rüzgâr tüneli deneyinde bu kolaylıkla mümkün olamamaktadır. Bu görselleşmenin rüzgâr tünelinde yapılabilmesi ancak yelken üzerine sensorler koyularak elde edilebilir, ancak bu durumda başka bir problem ortaya çıkmaktadır ki bu problem akış-yapı etkileşimidir. Bu etkileşimde akışın bozulmasına neden olmaktadır.

1. INTRODUCTION

1.1 Design Parameters of Sailing Yachts

Sailing races have seen significant improvements in the designs of the sails and hulls more than the last three decades. The races like the America's Cup (AC) and Volvo Ocean Race (VOR) have not only been a technological development for the engineers and designers but also receiving increased public interest [1]. In a sailing race, performance measure of a sailing boat is the distance that the boat sails. The distance depends on the sailing direction and the boat's speed, which they are basically dependent on the hydrodynamics and aerodynamics forces. Additionally, reducing the sail drag and hull resistance increase the overall performance of a sailing boat. Yacht engineers and designers generally assume a steady state sailing condition, using the fact that a sailing yacht moving in a steady state represents an equilibrium condition and the sum of all the forces and the moments is zero [2]. The program using a steady state sailing condition is widely known as a Velocity Prediction Program (VVP). These programs enable the users to estimate the aerodynamic and hydrodynamics forces by using potential flow solvers. Although they estimate the forces fast, the potential flow has basic problems to solve rotational flow and viscous effects.

Wind tunnel testing is an experimental technique having been a good approach to estimate the aerodynamic and hydrodynamic forces produced by the sailing yacht. The wind tunnel tests are accurately used for downwind sail calculations. This method assumes no physical property approximation and hence accurately carried out experimental technique measurements can verify good approximations of the aerodynamic and hydrodynamic forces. However, it is indeed very expensive to build and maintain experimental models comparing with computational models. In addition, the experimental tests do not produce good estimations of the pressure and velocity gradients on the sail geometry, because it is difficult to mount sensors on the flying sail shapes without interfering with the flow.

An alternate design technique is computational fluid dynamics (CFD) that is being frequently used in the sail and maritime industry. The cost of computational models constantly decreasing makes this alternate design method much more acceptable than the other methods [1]. The previous computational programs generally rely on panel or vortex-lattice methods in the sail design. These methods are computationally inexpensive whilst enabling the engineers and designers to obtain significant understanding of the problem during the early stage of the design. However, as the these methods are not suitable to be applied to viscous and rotational flows, hence new CFD programs including viscous flow solvers are being popularly used in recent years by the designers and engineers. The improvements in CFD codes provide a good estimation of the viscous effects by solving the Navier-Stokes equations.

1.2 IOM A Class Boat

The International A Class is a class of radio controlled racing yacht used in sailing races. The sail plan of the A Class consists of one mainsail and one headsail (jib sail). In this project, the International A Class was used due to its special characteristics, which are being a full-size boat and availability to use easily in wind tunnel. These characteristics are detailed in the below list:

- A full scale racing yacht enables the users to ignore all the scaling problems in wind tunnel.
- A Class boat was provided by Mr Lester Gilbert [3] and it was well maintained so that makes it to mount easily in the wind tunnel. All the fitting apparatuses on the boat were perfectly placed.

The A Class boat, which was used in the project studies, can be seen in Figure 1.1.

Figure 1.1 : “Sword”, The International A Class racing boat.

1.3 Aim and Objectives

1.3.1 Aim

- Understand and study the aerodynamic lift and drag forces developed by a set of sail shapes on a sailing yacht by conducting experimental tests in wind tunnel.
- Assess the effects of a range twist configurations upon the sail performance.
- Assess the effects of a range sheeting configurations upon the sail performance.
- Investigate the effects of different wind speeds and apparent wind angles (AWA) upon the performance of the sails in wind tunnel.
- Perform computational fluid dynamics (CFD) calculations as a second main part of the project.

1.3.2 Objectives

- Carry out experimental tests in wind tunnel. The experimental raw data will be obtained using the 6-component dynamometer located under the turntable and data acquisition software.
- The sail shapes will be obtained by using digital photographs taken during the experimental tests.
- Use AccuMeasure software provided by UK Sailmakers to read sail's sectional shapes from the digital photographs.
- Calculate a three dimensional geometry in terms of numbers in Excel software, and apply some corrections to obtain the final geometry.
- Draw the three dimensional geometry of the sail shapes by using Rhinoceros software.
- Conduct CFD analysis of the created sails, and draw a comparison between wind tunnel and CFD.

1.4 Report Outlines and Time Plan

These outlines are mentioned in the aims and objectives part. Schematic view of the outlines is presented in Figure 1.2.

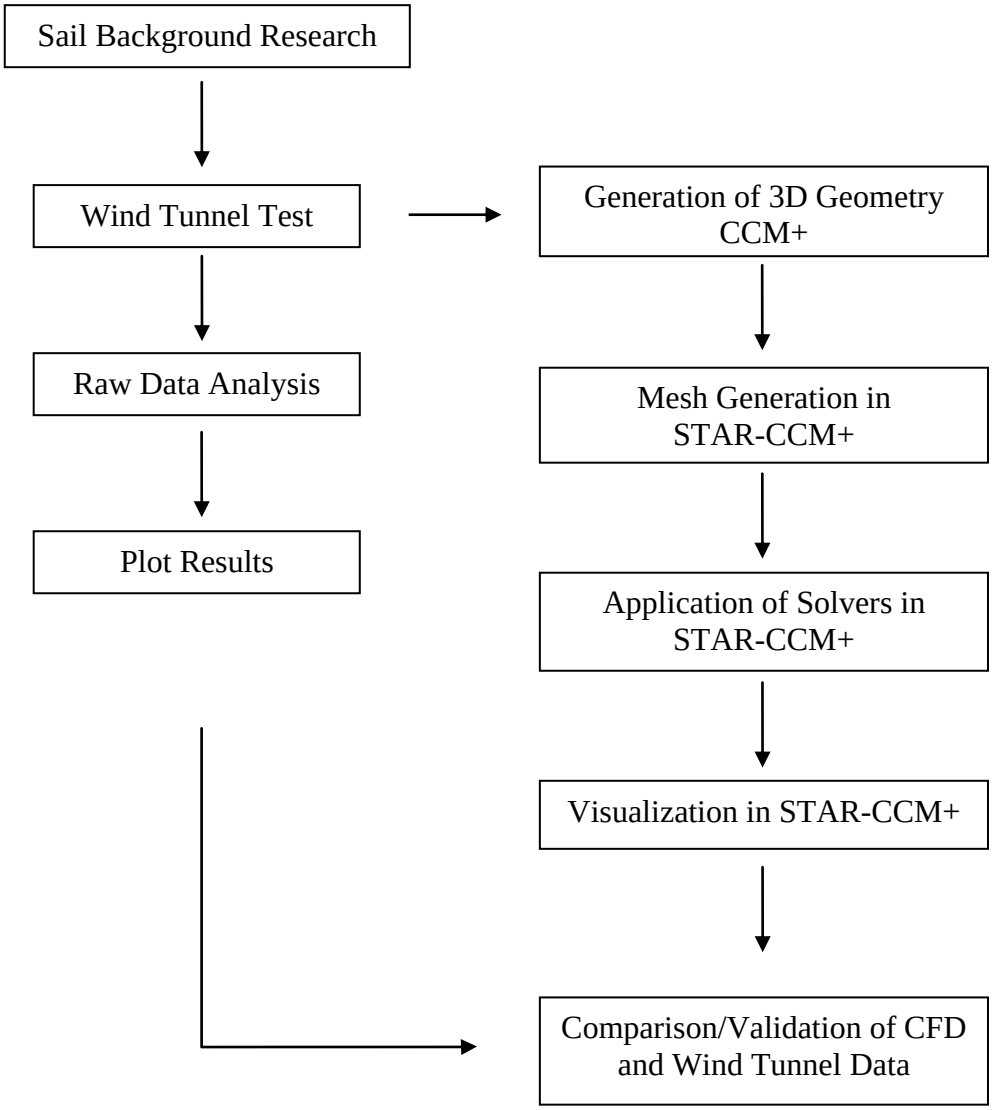

Figure 1.2 : Schematic view of report outlines.

Time planning is a significant topic in this study. To use time in an effective way, Gantt chart is used to schedule the work flow from start to finish, and to ensure all the work is done in an appropriate way. In the Gantt chart, the plan is given monthly information due to uncertainty in CFD work, and much time spent learning how to use STAR-CCM+. The Gantt chart is presented in Appendix A.1.

2. SAILING YACHT AERODYNAMICS

2.1 Introduction

Sailing boats have been used as a means of transportation and leisure for many millenniums. Since then, the science behind the sailing system is still not utterly understood due to their complex structure of strongly relying on both water and air fluids. The sail performance depends on a balance of aerodynamic forces occurring around the sails and hydrodynamic forces occurring around the sailing yacht's hull [2]. The sea can be very tough with storms or smoothly flat, and the wind can blow severely and cause rough waters.

The sailing designers and engineers have been dealing with not only the fluid dynamics, but also dealing with the solid mechanics effects on the sailing yacht's aerodynamic and hydrodynamic performance. This study will only focus on the sail aerodynamics.

2.2 Sail Definitions

2.2.1 Sail twist

Sail twist is used to change the lift distribution around a sail by using different angles of incidence for the head and foot of the sail. Sail twist can be measured by using a straight line between the leading and trailing edges of the sail boom. In order to measure twist angles, the angles between these edges at the boom are compared and determined the sail twist.

Wind gradient shows different effects on a sail that the wind is at the top of the sail much stronger than at the bottom of the sail. Hence, whilst the wind gets closer to sea surface, the wind gradient gets slower. That is why; the sail should twist to keep the sail's angle of attack stable through the rest of the sail, while the apparent wind increases with the height of the sail [3]. To obtain optimum performance from the sail, it should be accepted that consists of several different two dimensional foil

shapes. Therefore, the different foil shapes make it easier to study flow around each divided part of the sail. Figure 2.1 shows how different twist angles change throughout the surface of a sail geometry.

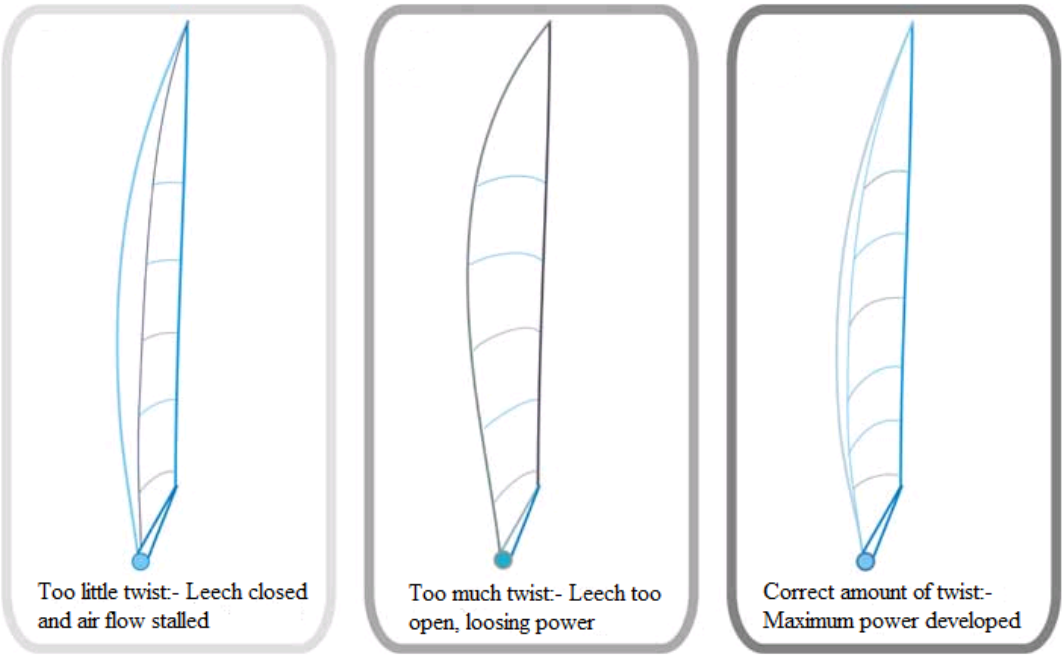

Figure 2.1 : Different twists on a mainsail [7].

2.2.2 Sail draft

The entry and exit angles of the wind onto the sail depend on the draft position of the sail. When the wind blows over the sail, the position of the draft continually changes. Therefore, the maximum draft position needs to be adjusted often to control the entry and exit angles of the wind. It must be pointed out that producing maximum driving forces rely on the right angle of attack which is related with the entry angles of the wind onto the sail. Figure 2.2 illustrates the maximum draft position of the sail, the entry and exit angles of the wind.The draft position can be adjusted by using cunningham and halyard. When flow of the wind increases, draft position will be repositioned and the halyard tension needs to be readjusted to keep appropriate angle of attack [3]. Hence, ideal draft position can be obtained about 50-60 % away from the leech side of the sail.

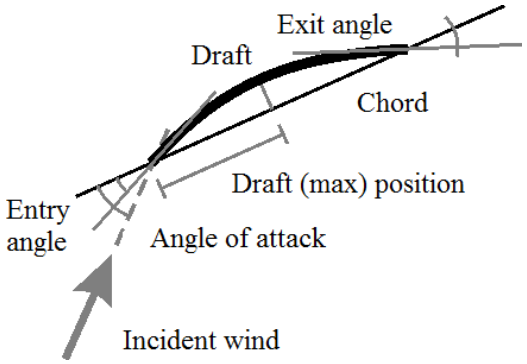

Figure 2.2 : Maximum draft position of a 2D sail section [3].

2.2.3 Sail camber

Sail camber has two aspects which are the depth and chord. As it can be seen in Figure 2.3, the depth is the perpendicular distance from the chord to the deepest point of the sail's curve. The chord is the straight line between the luff and leech sides of the sail [4].

To control sail's camber, boom vang, outhaul and mast bend are used to adjust sail's camber. The deepest curvature's position depends on the tensioning the Cunningham or boom vang.

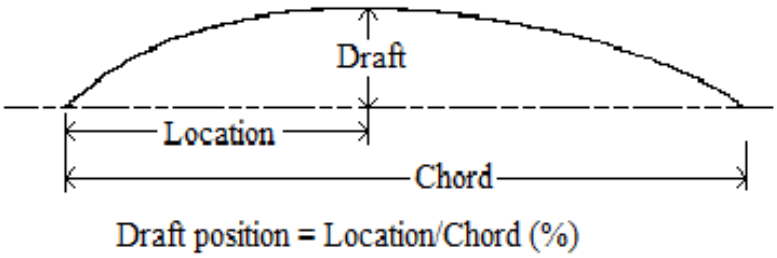

Figure 2.3 : Sail camber [3].

2.2.4 Slot effect

Slot effect occurs due to flow interaction between main and jib sails. Figure 2.4 shows the slot effect clearly by pointing out streamlines when both the main and jib sails used together. Both sails have their own circulation areas that creates the interactions and slot effects between the main and jib sails (head sail) [5].

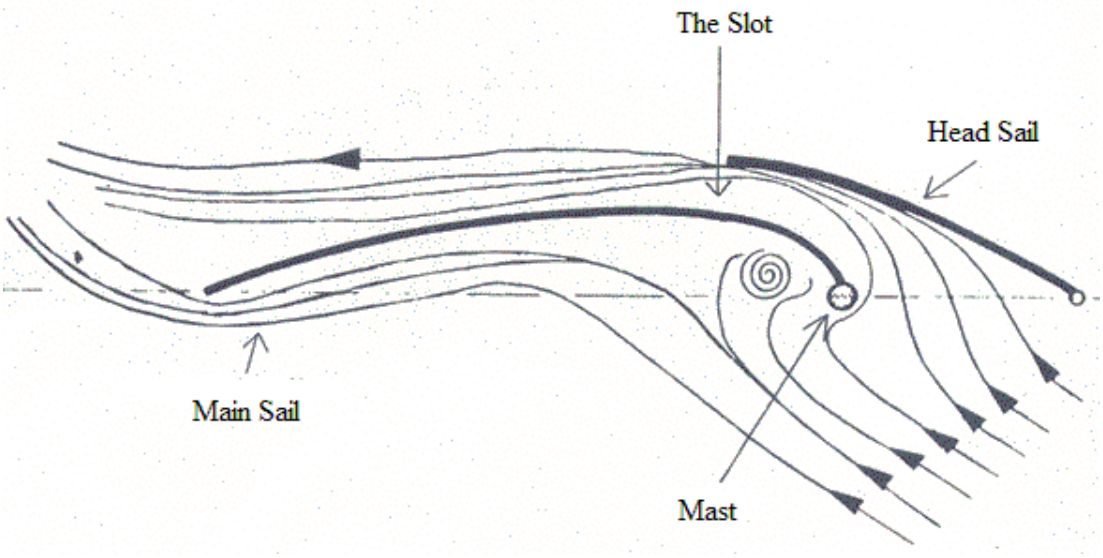

Figure 2.4 : Slot effects onto the main and jib sail [6].

In Figure 2.4, the velocity of the flow apparently reduces in the slot field that increases pressure on the leeward side of the mainsail. The high pressure and low velocity between the sails produce suction that causes the airflow in return [5,6]. This effect is very significant when it comes to keep the sails trimmed.

2.2.5 Tell-tales

A tell-tale is a piece of cloth that is used to determine the direction of the airflow. It is generally attached to wires which are connected to mast [7]. The tell-tales on the wires normally are on both starboard and port side of a sailboat. The tell-tales are used often on the surface of the sails as well. They enable the sailors to trim the sails and steer the boat easily. Although the system behind using the tell-tales is simple, the benefits are huge enough. Additionally, they are sufficient and essential to monitor the conditions of the sails and adjust the sail slot and twist.

2.3 Sail Drag

The sail performance depends on generating large amounts of aerodynamic lift and simultaneously possible low amount of aerodynamic drag. In sail aerodynamics' field, viscous effects determine the maximum lift and minimum drag in the boundary layer. The drag is very significant parameter that should be carefully examined. One way of the drag examining, indeed very appropriate way, is to divide the total aerodynamic drag into the following main two parts:

- Induced Drag
- Frictional Drag

In the following next parts, these drag components will be comprehensively mentioned.

2.3.1 Induced drag

Induced drag occurs when using an aerofoil to produce aerodynamic lift. The reason of the induced drag is that higher pressure underneath of an aerofoil makes low pressure (suction) kept at the upper part of an aerofoil [6]. At the trailing edge of the aerofoil, the low and high pressures inevitably meet around the end of the aerofoil. The pressure differences at the trailing edge gets smaller that the lift producing decreases at this time, and it causes the tip vortex problem. As long as there are pressure differences between the lower and upper parts of the aerofoil, these vortices will continue to happen. It can be showed that the magnitude of the induced drag (tip vortex drag) can be calculated by using the formula in equation **(2.1)**.

$$D_I = L^2 / (0{,}5\ \rho_{air}\ V_e\ A\ \pi\ e\ AR) \qquad \textbf{(2.1)}$$

In some cases, airflow does not follow the desired way, where the airflows over the aerofoil surface. It results in some amount of energy lost around the aerofoil. It is no longer producing lift. Although this expanded energy does not produce enough lift, it causes induced drag.

Another consequence of the tip vortex drag is downwash. It is developed by the aerofoil's action to produce lift. By deflecting the air as downwash, the aerofoil or the sail produces lift. The direction of downwash is opposite side to the direction of lift. Downwash theoretically depends on two main factors: lift coefficient and aspect ratio [3]. Figure 2.5 shows the tip vortices and downwash happening behind a sail.

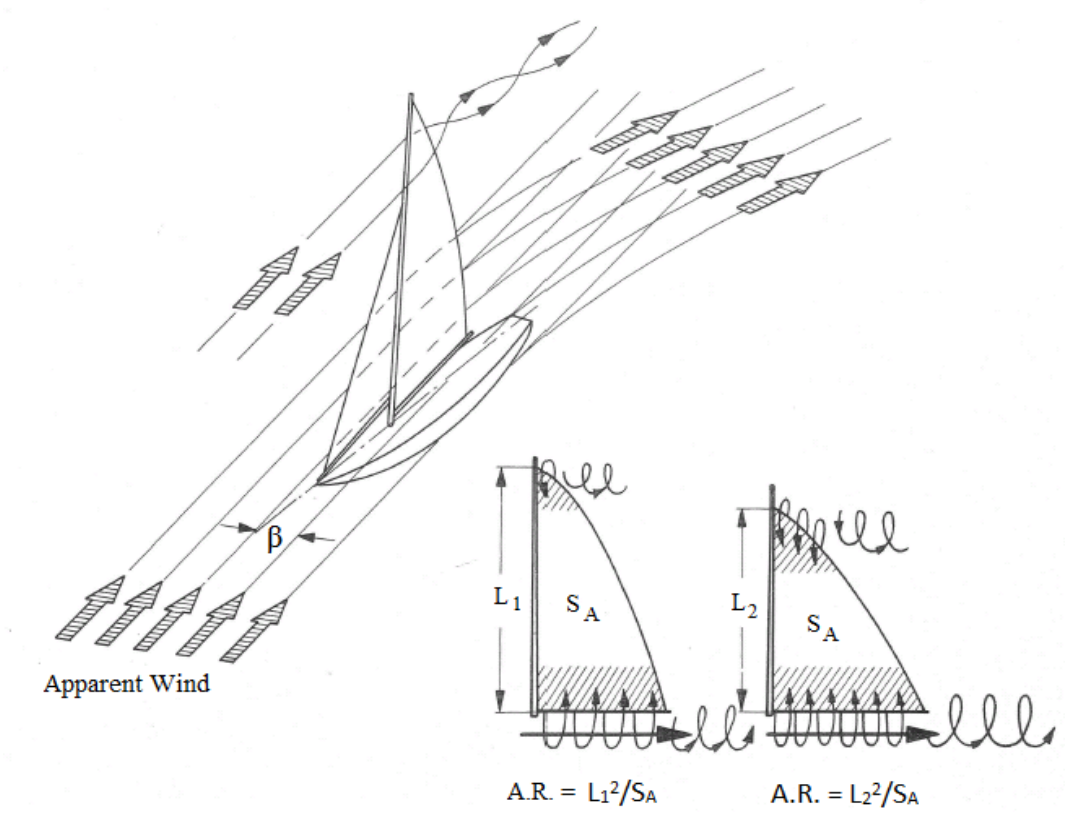

Figure 2.5 : Tip vortices and downwash behind a sailboat [6].

2.3.2 Frictional drag

Frictional drag happens due to the interaction between a solid body surface and airflow [6]. It can be said that this drag component is similar with the friction, which is a result of any interacted two surfaces. In sail aerodynamics, the characteristics of the friction drag change due to fact that the properties of a sail and airflow mainly effect on the produced amount of the drag. Furthermore, to minimize the frictional drag on the side of the solid body, the sail surface can be produced frictionless as much as possible. By doing this, it increases the sail speed and decreases the frictional drag.

On the other hand, however, air characteristics depend on the viscosity of air in the boundary layer, and these effects should be taken into account as well. Whilst air particles flow over a sail, these particles pass very closely to the sail surface. These air particles normally should slip without any sticking effect along the surface. However, they stick on the surface and do show no slip effect. All these interactions between a solid surface (sail surface) and airflow are happening in the region, which is named boundary layer [6].

2.4 Apparent Wind

Apparent wind is the wind experienced by a sailboat, and it is the resultant component of the vectors of sailboat's velocity and true wind velocity [6]. Figure 2.6 simply illustrates the schematic view of the wind structure of a sailboat.

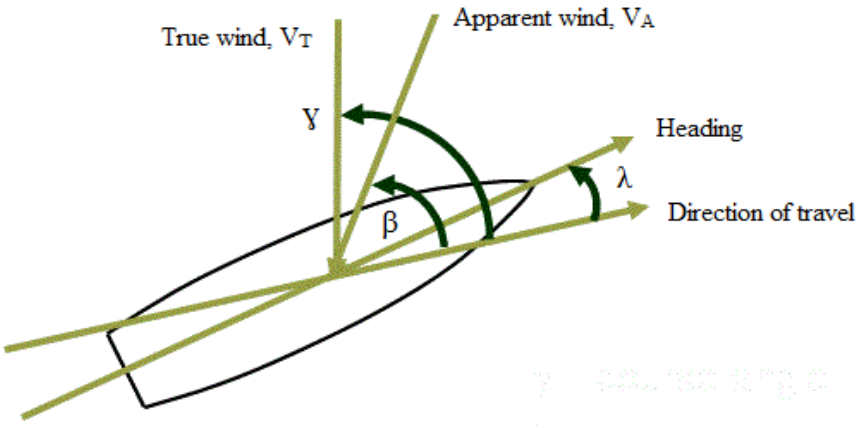

Figure 2.6 : Apparent and true wind diagram on a sailboat [8].

The diagram in Figure 8 shows the relationship between apparent wind and true wind angles as well as the boat's course. The real direction of the travel has a heading angle which is called leeway angle (λ).

Equations **(2.2)** and **(2.3)** show how apparent wind velocity (V_A) and apparent wind angle (β_A) are calculated [1].

$$\beta_A = tan^{-1}\left[(V_T\ sin\beta_T\ cos\phi)/(V_T\ cos\beta_T + V_S)\right] \quad \textbf{(2.2)}$$

$$V_A = \sqrt{[(V_T\ sin\beta_T\ cos\phi)^2 + (V_T\ cos\beta_A + V_S)^2]} \quad \textbf{(2.3)}$$

In the equations **(2.2)** and **(2.3)**, the sign (ϕ) implies heel angle of a sailboat, and the equations consist of the heel angle due to fact that apparent wind area is considered to move with the centre plane of the boat whilst aerodynamic behaviours are estimated [1].

2.5 Balance of Forces on a Sailing Yacht

In Figure 2.7, forces on an un-heeled sailing boat are illustrated. When the sail boat is in equilibrium (in a steady state condition), total hydrodynamic force (F_H) and total aerodynamic force (F_A) must be equal as being showed in equation **(2.4)** and must be in opposite directions at which the angle between these directions is 180° [6,8,9].

These requirements can be summarized below [8]:

1. F_H and F_A are equal.

$$F_A = F_H \tag{2.4}$$

2. F_H and F_A are opposite vectors. This requires the directions are 180° apart.

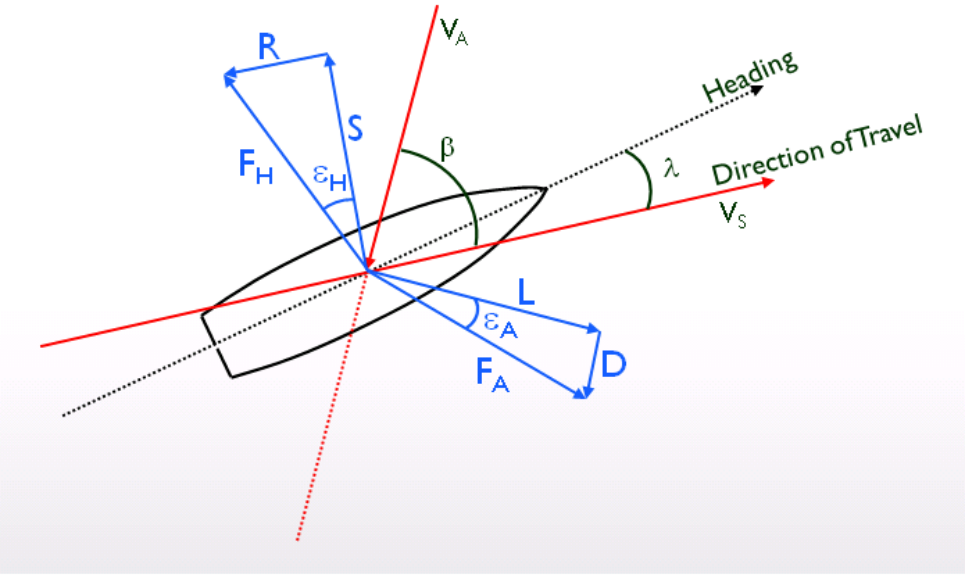

Figure 2.7 : Balance of forces on a sailing yacht [8].

Relying on the balance of forces, in a steady state condition hydrodynamic side force (S_F) and hull drag (R) must be equal to sail heeling force (H_F) and driving force (D_F).

The formulas of D_F and H_F are shown in equations **(2.5)** and **(2.6)**, and the formula for how to calculate Lift (L) is in equation **(2.7)** as well as hydrodynamic side force (S_F) and total hull drag (R) are in equations **(2.8)** and **(2.9)**, respectively [8].

$$D_F = F_A\, cos(90° - \beta_A + \varepsilon_A) = F_A\, sin\,(\beta_A - \varepsilon_A) \tag{2.5}$$

$$H_F = F_A\, sin(90° - \beta_A + \varepsilon_A) = F_A\, cos\,(\beta_A - \varepsilon_A) \tag{2.6}$$

$$L = F_A\, cos\ \varepsilon_A = D_F\ cos\,\varepsilon_A\,/sin\,(\beta_A - \varepsilon_A) \tag{2.7}$$

$$R = F_A\, sin\,\varepsilon_A \tag{2.8}$$

$$S_F = F_A\, cos\,\varepsilon_A \tag{2.9}$$

According the Beta Theorem, the angle of apparent wind (β_A) is equal the sum of the angle of aerodynamic drag (ε_A) and hydrodynamic drag (ε_H) on the following formula in equation **(2.10)**.

$$\beta_A = \varepsilon_A + \varepsilon_H \quad \textbf{(2.10)}$$

2.6 Sail Interactions

According to C. A. Marchaj [6], the topic of the sail interactions is highly controversial subject, and there is no proper agreement on how the sails affect each other. A mainsail is often used with a foresail in sail design and construction environment. This is due to the fact that the foresail directs better flow (smooth flow) to the mainsail and mast [10].

It is the fact that when there are two sails very closely in progress, they will begin to interact each other. Sail interaction can be divided into two main parts, effects of foresail on the mainsail and effects of mainsail on the foresail.

2.6.1 Effects of foresail on the mainsail

A foresail has effects on the airflow passing the foresail and going towards to main sail. Because, there is a gap between the sails, and the air goes through the gap. As the air passes between the mains and fore sails, pressure distribution slightly changes on the both sides of the mainsail, namely the leeward and windward sides. An improved aerodynamic performance can be acquired by minimizing the slot effects occurred in the area between the fore and mainsail. However, the slot does not have too large effects on air speed increases in the gap due to the fact that the air speed in the beginning is slow and it increases in the slot [6].

According to Bernoulli's theorem, when air speeds slow down at some points, pressure simultaneously increases at same points. As a result of this, magnitude of suction is getting smaller. There must be a pressure balance between the leeward and windward sides of the mainsail so that the sail does not flatter. When the pressure on the side of the leeward is bigger than the pressure on the side of the windward, this eventually causes back winding of the mainsail.

Some experiments conducted by Gentry [11] show that sheeting angles, δ_M and δ_F, have large effect on the amount of the air which passes between the fore and main sails. δ_M indicates the sheeting angle of the mainsail, and δ_F indicates similarly the foresail's sheeting angle. Figure 2.8 clearly shows changes in the slot when sheeting angles vary.

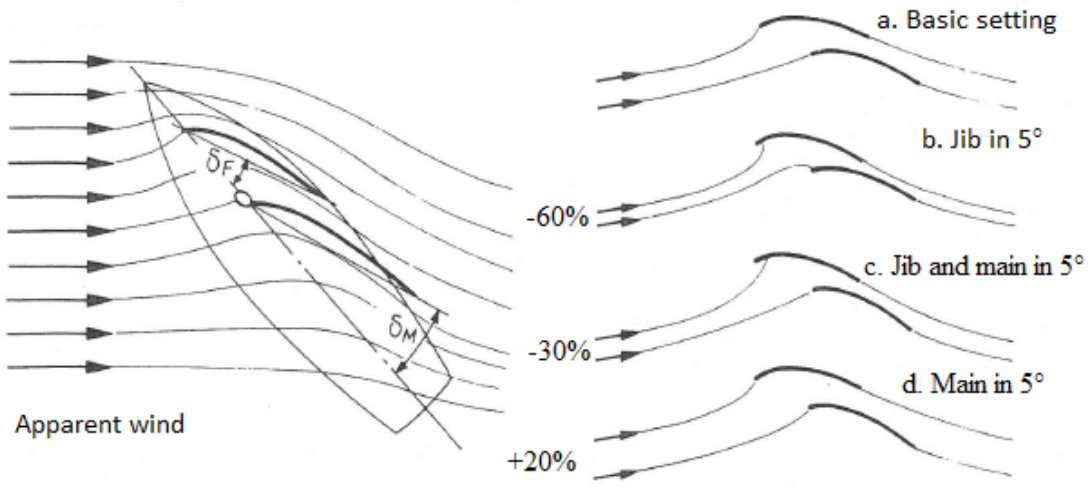

Figure 2.8 : Influences of sheeting angles, δM and δF, over the sails [11].

2.6.2 Effects of mainsail on the foresail

As a foresail causes some vital influences on mainsail, it also has some effects on foresail (jib sail). One of the influences due to the interaction of mainsail is that foresail receives the flow with high angle of attack, and this, the high angle of attack flow, causes velocity particles on the upper side of foresail faster than on the lower side [12]. This eventually increases the performance of foresail and contributes over all sail performance.

Because of the high angle of attack for foresail, it creates upwash flow towards to mainsail. The upwash flow basically prevents foresail to stall by moving the flow stagnation point on the foresail to the windward direction. Another significant effect of the foresail on the mainsail is that well fixed mainsail trim is vital for sail performance, and it increases the production of driving forces. Any reduction of the speed between sails will reduce the amount of driving force produced by sails [6, 12].

3. FLUID MECHANICS

3.1 Introduction

Fluid mechanics is the study of all fluid (both liquids and gases) under static and dynamic situations [13]. The behaviours of fluids base on the laws of fluid mechanics that these are related continuity of mass, energy, force and momentum. Fluid mechanics can be divided into three parts:

1. Fluid dynamics
2. Fluid kinematics
3. Fluid statics

Fluid dynamics deals with the study of force effects on the fluid particles. The branch of fluid dynamics is very popular research field where it can be commercially applied to many different areas. This study will mainly focus on the branch of fluid dynamics.

In fluid mechanics, flow can be either laminar (smooth flow) or turbulent flow (chaotic flow). To characterize which kind of flow is present, there is the need of a number which is called Reynolds number (Re). Re is a non-dimensional number, and it expresses the ratio of inertia forces to viscous forces in fluid motion. Laminar flow occurs at low Reynolds numbers, where viscous forces are dominant, and turbulent flow occurs at high Reynolds numbers where inertial forces are dominant.

This ratio (Reynolds number) is defined in the following equation **(3.1)**:

$$Re = (\rho\, \upsilon\, Le)/\mu = (\upsilon\, Le)/\nu \qquad \textbf{(3.1)}$$

Where kinematic viscosity (ν) is equal to μ/ρ in the equation **(3.2)**:

$$\nu = \mu/\rho \qquad \textbf{(3.2)}$$

The problems of fluid dynamics (also fluid mechanics) are complex. They can be numerically solved, and computers are very good example for numerical way.

Recently, depending on the developments of computer facilities, computational fluid dynamics (CFD) is being more popular to solve fluid dynamic problems. Furthermore, CFD makes the results to be visualised for better understanding of the fluids behaviours. Further details of CFD will be comprehensively discussed in CFD chapter.

3.2 Potential Flow Theory

Potential flow theory assumes that the fluid around an aerofoil is an ideal fluid which is incompressible, and has no viscosity (inviscid). Eventually, the flow is irrotational, and no shear forces can be applied to an inviscid fluid [14]. There is no separation between fluid and solid boundaries. Potential flow theory therefore ignores separation effects. Moreover, Newton's second law of motion which is based on the following equation **(3.3)** is applied for every point and all time intervals.

$$F = ma \tag{3.3}$$

In the aerodynamic field, potential flow is used to explain the airflow not affected by viscous effects in the boundary layer. Hence there is no way to solve properly separated flow behaviours. And also there is no such fluid exist, however these assumptions make it possible to produce mathematical models to study and understand fluid characteristics around an aerofoil or a mainsail. Figure 3.1 simply shows how airflow passes over an aerofoil as a potential flow.

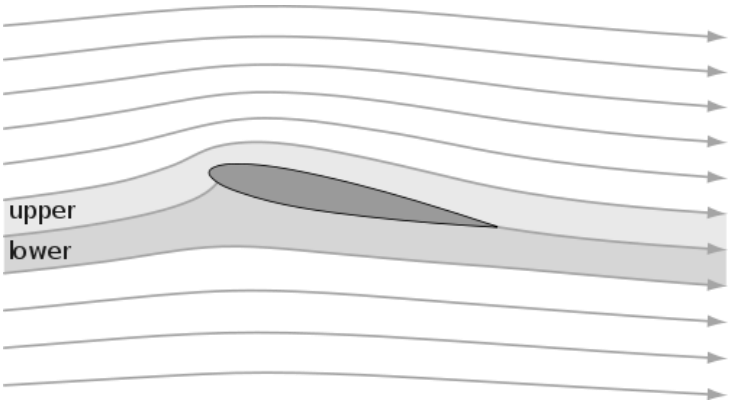

Figure 3.1 : Potential flow around an aerofoil [14].

3.3 Boundary Layer Theory

Boundary layer theory was first introduced by Ludwig Prandtl in the early 1900's. He was the first person who had realized the relative magnitude of inertial and viscous forces changed from very close wall surface to boundary layer's far surface [15].

Boundary layer theory enables the equations of fluid flow to be simplified and solved. It consists of two layers that one layer is outside boundary layer, where viscous effects can be ignored without changing the solution much, and the other one is inside the boundary layer, where the most drag forces occur and viscous forces are dominant in the boundary [16]. The boundary layer illustrates the flow characteristics over a solid aerofoil surface on the following Figure 3.2.

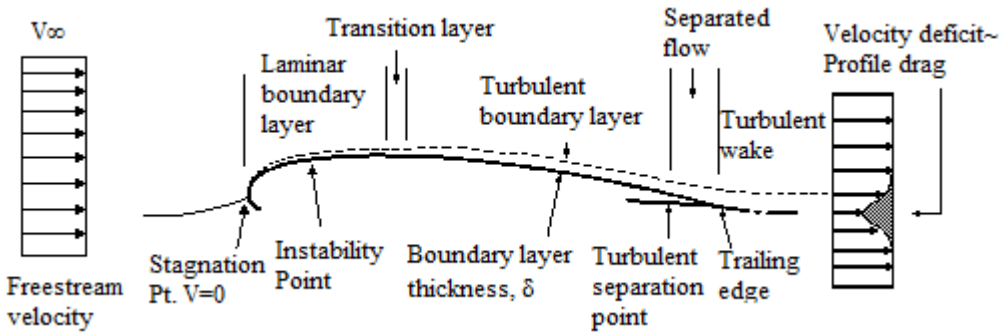

Figure 3.2 : Boundary layer [15].

The boundary layer thickness featured in Figure 3.2 is a distance from the solid body surface to free stream flow. The no slip condition assumes that the velocity at the solid body surface must be zero, and viscosity allows the flow speed to increase rapidly with moving away from the solid surface. The speed in the laminar flow is relatively slow and laminar flow provides desirably low skin friction. And also viscosity does not allow any turbulence occurred in the laminar flow. However, at high Reynolds numbers, the boundary layer grows inevitably while the fluid flowing around the solid body and viscosity no longer prevents turbulence flow.

3.4 Bernoulli's Theorem

According to Bernoulli's theorem for an inviscid flow, an increase in the speed of fluid results in with a decrease in pressure or the fluid's potential energy [14,17]. An aerofoil as a cross-section of a sail produces lift by inducing pressure gradients through the bottom and top surfaces. These pressure gradients can be expressed by Bernoulli's theorem which is expressed in equation **(3.4)**:

$$P + \frac{1}{2}\rho V^2 + \rho g h = constant \qquad \textbf{(3.4)}$$

Figure 3.3 demonstrates the relationship between pressure and velocity. Hereby, when flow velocity increases along a single streamline, pressure simultaneously must reduce. The reason for this reduction is that flow velocity at the upper part of an aerofoil is higher than velocity at the lower part of the aerofoil. Therefore, pressure area at the upper part of the aerofoil is lower than pressure area at the lower part of the aerofoil. As a result of these simultaneous changes, pressure gradient shows a movement in direction of upward on the aerofoil surface to develop necessary lift power for a sail.

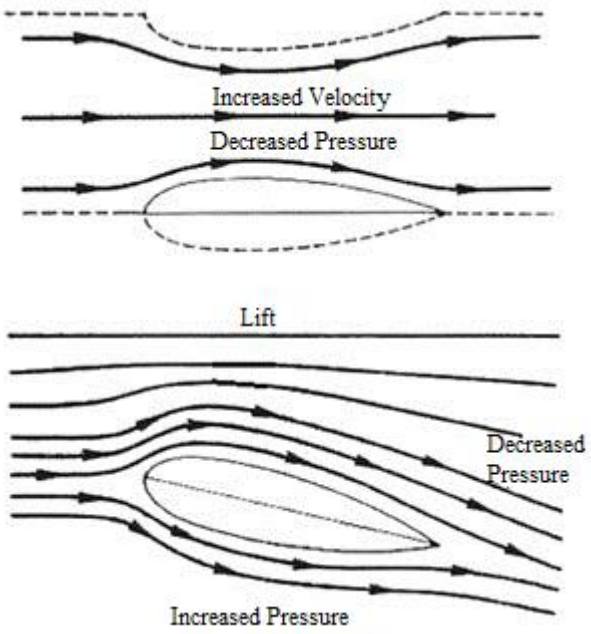

Figure 3.3 : Bernoulli's principle applied for an aerofoil [8].

3.5 Navier-Stokes Equations

The Navier-Stokes equations are a set of nonlinear partial differential equations that describe the flow behaviours of fluids. These behaviours consist of air movements, waves in the oceans and many other fluids' behaviours. The Navier-Stokes equations were derived by Claude Louis Navier and George Gabriel Stokes in the early 1800's.

The Navier-Stokes equations could be theoretically solved for a particular case problem. However, these equations indeed are incredibly difficult to be properly solved. Researchers and engineers in the past did follow some simplification methods to solve the equations and obtain solutions. In these days of having advanced high-tech computer facilities, high speed computers are being used to approximate the Navier-Stokes equations with an acceptable accuracy. In the other words, this field of research is computational fluid dynamics (CFD), which performs many different tasks with high calculation speed by using some well-known and popular methods such as finite volume, finite element and finite difference methods. Before derivation of the Navier-Stokes equations, the knowledge of Newtonian fluids is necessary. Newtonian fluid is a fluid type that has a certain constant viscosity, where viscosity is independent of shear stress [14]. Many common fluids such as water and air are Newtonian fluids. However, on the other hand, there are some fluids that behave like non-Newtonian fluid; shear stress does not linearly depend on the velocity gradient.

The Navier-Stokes equations for a compressible flow of Newtonian fluid can be derived by using the equations which are conservation of mass or continuity equation, conservation of momentum and conservation of energy.

3.5.1 Conservation of mass

Conservation of mass in three dimensions is given in Cartesian coordinates in equation **(3.5)** [18].

$$\frac{\partial \rho}{\partial t} + \frac{\partial (\rho u)}{\partial x} + \frac{\partial (\rho v)}{\partial y} + \frac{\partial (\rho w)}{\partial z} = 0 \qquad \textbf{(3.5)}$$

When flow is steady, the density of fluid (ρ) does not change in time. Hence, conservation of mass (continuity equation) is reduced to **(3.6)**:

$$\frac{\partial(\rho u)}{\partial x} + \frac{\partial(\rho v)}{\partial y} + \frac{\partial(\rho w)}{\partial z} = 0 \quad \textbf{(3.6)}$$

Similarly, when flow shows incompressible characteristic, ρ does not change with respect to space. Conservation of mass is reduced to **(3.7)**:

$$\frac{\partial(u)}{\partial x} + \frac{\partial(v)}{\partial y} + \frac{\partial(w)}{\partial z} = 0 \quad \textbf{(3.7)}$$

where,

u, v and w are the components of velocity in axes directions of x, y and z, respectively. These velocity components are the dependent variables at which they are expected to be solved.

3.5.2 Conservation of momentum

The principle of conservation of momentum is in fact an application of Newton's Second Law of motion to an element of fluid [18]. In addition, the Navier-Stokes equation is considered to be an accurate representation of Newton's Second Law applied to air and water over wide ranges of pressure and temperature [20].

Conservation of momentum in x-direction **(3.8)**:

$$\rho\left(\frac{\partial u}{\partial t} + u\frac{\partial u}{\partial x} + v\frac{\partial u}{\partial y} + w\frac{\partial u}{\partial z}\right) = -\frac{\partial P}{\partial x} + \mu\left(\frac{\partial^2 u}{\partial x^2} + \frac{\partial^2 u}{\partial y^2} + \frac{\partial^2 u}{\partial z^2}\right) + \rho f_x \quad \textbf{(3.8)}$$

Conservation of momentum in y-direction **(3.9)**:

$$\rho\left(\frac{\partial v}{\partial t} + u\frac{\partial v}{\partial x} + v\frac{\partial v}{\partial y} + w\frac{\partial v}{\partial z}\right) = -\frac{\partial P}{\partial y} + \mu\left(\frac{\partial^2 v}{\partial x^2} + \frac{\partial^2 v}{\partial y^2} + \frac{\partial^2 v}{\partial z^2}\right) + \rho f_y \quad \textbf{(3.9)}$$

Conservation of momentum in z-direction **(3.10)**:

$$\rho\left(\frac{\partial w}{\partial t} + u\frac{\partial w}{\partial x} + v\frac{\partial w}{\partial y} + w\frac{\partial w}{\partial z}\right) = -\frac{\partial P}{\partial z} + \mu\left(\frac{\partial^2 w}{\partial x^2} + \frac{\partial^2 w}{\partial y^2} + \frac{\partial^2 w}{\partial z^2}\right) + \rho f_z \quad \textbf{(3.10)}$$

3.5.3 Conservation of energy

The first law of thermodynamics observes the principle of conservation of energy which is in the equation **(3.11)**. Energy can be transformed, i.e. changed from one form to another, but can be neither created nor destroyed [19,20].

$$\rho \frac{DE}{Dt} = -\text{div}(Pu) + \frac{\partial P}{\partial z} + \begin{pmatrix} \frac{\partial(u\tau_{xx})}{\partial x} + \frac{\partial(u\tau_{yx})}{\partial y} + \frac{\partial(u\tau_{zx})}{\partial z} \\ + \frac{\partial(v\tau_{xy})}{\partial x} + \frac{\partial(v\tau_{yy})}{\partial y} + \frac{\partial(v\tau_{zy})}{\partial z} \\ + \frac{\partial(w\tau_{xz})}{\partial x} + \frac{\partial(w\tau_{yz})}{\partial y} + \frac{\partial(w\tau_{zz})}{\partial z} \end{pmatrix} + \text{div}(k\,\text{grad}T) \quad \textbf{(3.11)}$$

3.6 Flow Regions

Sails act as an aerofoil in the wind and hull of a sailing boat acts as a hydrofoil in the water. That is why; aerofoils are used to explain sail behaviours in sailing yacht design environment. Figure 3.4 demonstrates flow regions around a thin aerofoil, where flow regions consist of boundary layer region and external flow region. Boundary layer region is very close to aerofoil wall, and contains air viscosity.

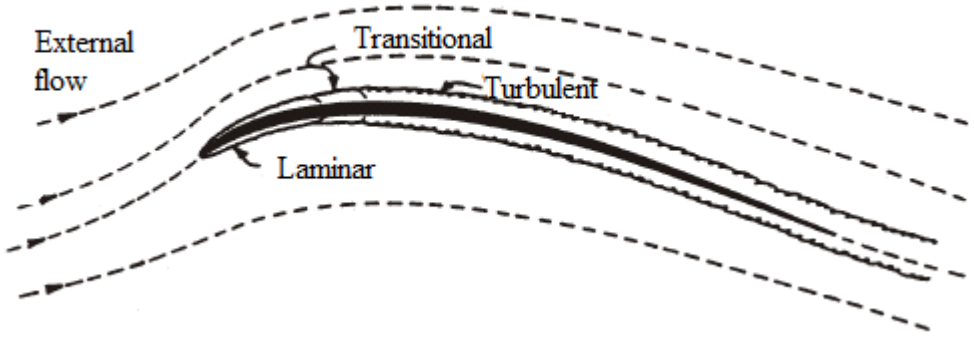

Figure 3.4 : Flow regions over a thin aerofoil [12].

Boundary layer is generally divided into three different flow parts:

1. Laminar boundary layer
2. Transitional boundary layer
3. Turbulence boundary layer

3.6.1 Laminar boundary layer

The laminar boundary layer is near the leading edge of the aerofoil, and the wind speed changes very smoothly from the aerofoil wall to the boundary layer borders in the laminar layer [12]. In this layer, there are no unsteady behaviours of the air flow.

3.6.2 Transitional boundary layer

In the transitional layer, the air starts being gradually unsteady and causes much chaotic type of flow. In the turbulence boundary layer, the air flow shows no longer laminar effects, and it becomes fully unsteady [12].

3.6.3 Turbulent boundary layer

In the turbulent layer, the lift does not change much due to the fact that the external flow is not largely affected by this. However, the important point is that the skin friction drag in the turbulent layer is much greater than the laminar layer. Furthermore, there are air separations either in the laminar or in the turbulent layers. Separations begin whilst the boundary layers start not following through the aerofoil wall surface. Figure 3.5 shows clearly laminar and turbulent separations occurred on a thin aerofoil [12].

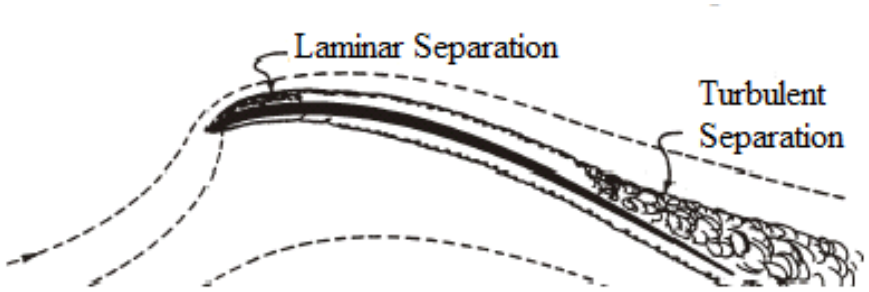

Figure 3.5 : Laminar and turbulence flow separations [12].

In the boundary layer, viscous forces try to govern and stabilize the flow. However, in contrast, inertia forces of fluid are tend to destabilize the flow into the disordered flow behaviours (turbulent flow). Reynolds number (Re) determines which flow is occurring. Re is up to 2000 for a laminar boundary layer, and when it is more than 4000, the flow can be said that is turbulent.

4. WIND TUNNEL

4.1 Wind Tunnel Testing

Wind tunnel testing is considerably significant part of the study, as its data will be compared to CFD calculations. In wind tunnel, flow is more realistic and similar to real life conditions, although CFD code uses highly assumed perfect flow conditions. Two dimensional wind tunnel tests are no longer popular among the designers and engineers because of the reliability of computational fluid dynamics (CFD). However, complete aerodynamic wind tunnel calculations are still a common use in sailing yacht design field because of highly complicated flow behaviours around sails [1].

4.2 Experimental Set-up in Wind Tunnel

The experimental tests were carried out in the 7 by 5 low speed section wind tunnel at the University of Southampton. Main dimensions of wind tunnel are 4.6m wide, 3.7m high and 3.7m long. In the low speed section, the wind speed can be adjusted between 1.5 m/s to 10 m/s. The set-up characteristics in the wind tunnel are introduced in the following sections.

4.2.1 Dynamometer set-up

The 6 degrees of freedom dynamometer (DOF) was used to obtain the forces and moments in the wind tunnel. The data acquisition software calculates forces and moments using the dynamometer. The model was attached to the 6 degrees of freedom dynamometer which is located below turntable. It can be seen that how those forces are taken from 6 degrees of freedom in Figure 4.1. The dynamometer needs to be calibrated before any measurements. In this study, the dynamometer was already calibrated by Wolfson Unit staff and there was no need to re-calibrate the dynamometer.

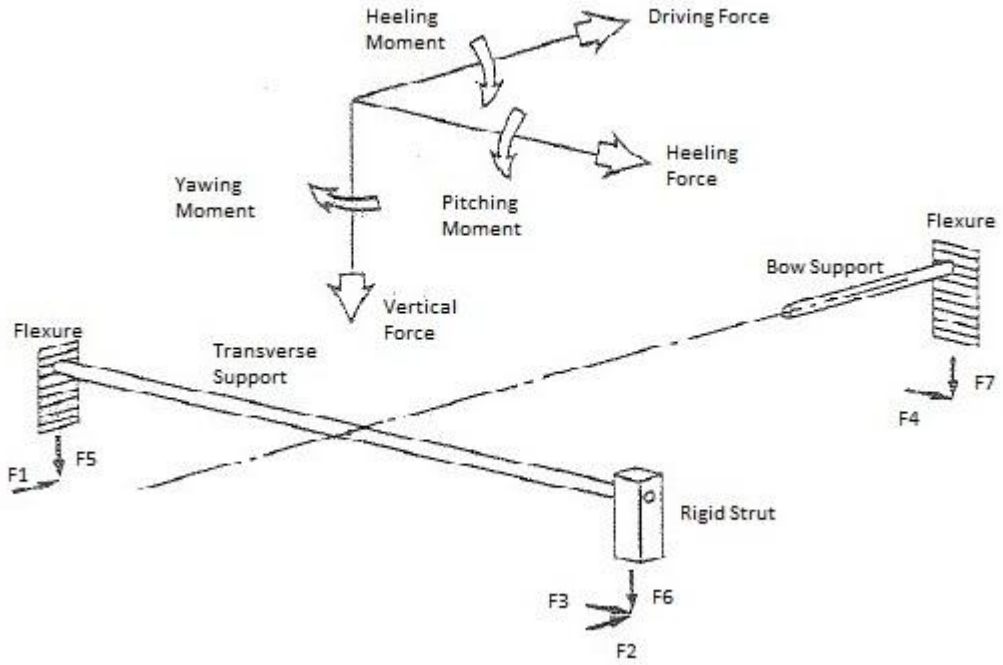

Figure 4.1 : Dynamometer schematic arrangement [9].

Moments:

- Heeling Moment (HM)
- Yawing Moment (YM)
- Pitching Moment (PM)

Forces:

- Driving Force (DF)
- Vertical Force (VF)
- Heeling Force (HF)

4.2.2 Turntable

Turntable is a useful device to adjust apparent wind angle (AWA) in wind tunnel. The turntable enables to change apparent wind angles up to 180 degree. The turntable has a water basin which enables boat to be accurately modelled at heel angles and provides a true representation of airflow around the boat's hull at sea level. Due to the water basin, the airflow cannot interfere with the 6 degrees of freedom dynamometer (DOF) and it can be duplicated as real conditions of the sea in wind tunnel. In the wind tunnel tests, 20 and 28 degrees of apparent wind angles were used to obtain experimental data. The turntable is shown in Figure 4.2.

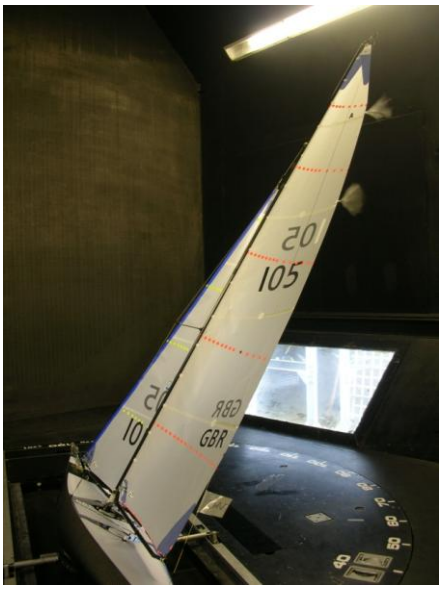

Figure 4.2 : Turntable in the wind tunnel.

4.2.3 Fitting

Fitting apparatuses were used to adjust heel angle and study the effects of heel angle on the performance of sailing boat. They were slightly useful devices to adjust the heel angle of sailing boat. However, on the other hand, it might be tough to change the heel angle regularly because of screws and the water basin under the boat. The screws must be tightened enough so that the rig stands stable during flowing wind. And also changing the heel angle regularly makes you to interfere with water unknowingly spilled on the ground. It could be sometimes dangerous to work in wind tunnel unless it is paid attention on sliding effects. The fitting apparatuses which were used to mount the sailing boat can be seen in Figure 4.3.

Figure 4.3 : Fitting apparatuses in the wind tunnel.

In this study, the heeling angle was fixed to 30°, and it was no need to change the angle whilst running the tests. There were no need of changing of the heel angles, and any serious sliding hazards did not happen. In addition to these precautions mentioned above, the accuracy of fitting devices should be checked before relying on them. That is why; the spirit level provided by the wind tunnel staff was used to approve the accuracy of fitting devices.

4.2.4 Data acquisition software

Data acquisition is the process of sampling signals that measures real world physical conditions like moments and forces, and converting the samples into digital environment. In the digital environment, the samples can be manipulated by a computer.

TurboAD is data acquisition software developed by the Wolfson Unit was used to collect the physical conditions of sailing boat. The data acquisition software has been used several years by the University of Southampton's staff and its students, and it has proved itself well that collects the forces and moments from the 6 components dynamometer. The forces and moments were transferred from the dynamometer to the acquisition software in every 30 seconds and saved in text format file.

There is one very significant step that zero-acquired data has to be taken before running each test. According to some careful observations, the dynamometer did not go to initial zero conditions. To solve this inevitable problem, initial non-zero data were collected before each run. It was an extra time spending in the wind tunnel, however when it comes to analyse raw data, it helps to obtain much more accurate results. These initial zero-acquired data can be subtracted from each real running data in due course. An example of data collection way is presented below in Table 4.1.

Table 4.1 : An example of initial data collection way.

	Wind Speed	Twist Angle (deg.)		Sheeting Angle (deg.)	
Run No	m/s	Main Sail	Jib Sail	Main	Jib
130	ZERO	7	9	4	10
131	3	7	9	4	10
132	5	7	9	4	10
133	7	7	9	4	10

4.3 Corrections in Wind Tunnel

4.3.1 Transformation of axes

To calculate lift and dag coefficients from the wind tunnel raw data, heeling and driving forces have to be converted from the dynamometer axis to the boat axis called transformation of the axes. The equations **(4.1)** and **(4.2)** indicate the transformation of axes [9].

$$Drag = \frac{H_F}{cos\phi} sin\beta_A - D_F\, cos\beta_A \tag{4.1}$$

$$Lift = \frac{H_F}{cos\phi} cos\beta_A - D_F\, sin\beta_A \tag{4.2}$$

A schematic view of the axes transformation is presented in Figure 4.4 [9].

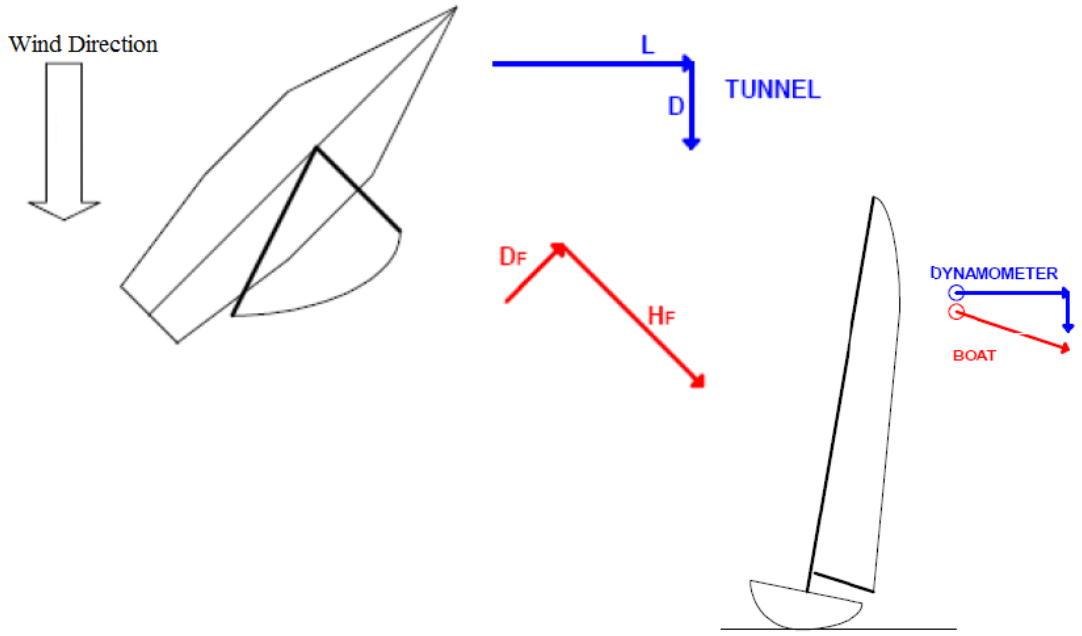

Figure 4.4 : Transformation of the axes [9].

Hence, lift and drag coefficients in equations **(4.3)** and **(4.4)** are transformed from wind tunnel raw data;

$$C_D = \left[\frac{H_F}{cos\phi} sin\beta_A - D_F\, cos\beta_A\right] . (scale^2/\mathrm{A}\ \rho_{(air)}\ g\ q) \tag{4.3}$$

$$C_L = \left[\frac{H_F}{cos\phi} cos\beta_A - D_F\, sin\beta_A\right] . (scale^2/A\ \rho_{(air)}\ g\ q) \tag{4.4}$$

By using the equations (4.3) and (4.4), heeling and driving forces can be transferred to lift and drag coefficients. In addition to this, there are some more corrections for the forces to be analysed before using them in any scientific study [9]. These corrections basically are due to wind tunnel effects on the solid part (sails) and airflow during running the experiment. In forthcoming sections, these corrections will be comprehensively mentioned.

4.3.2 Wind tunnel corrections

4.3.2.1 Downwash correction

In the beginning of the last century, engineers found wind tunnel results quite pessimistic. Minimum drag and change of drag versus lift were too high. On the other hand, the lift curve's slope was quite small. The experiments showed that the slope of lift curve and the changing rate of drag were affected by wind tunnel walls. Closed boundaries of wind tunnel make the drag too small and lift too high. C_D and β corrections are done due to confines of wind tunnel altering streamlines [9,20]. These boundary effects were calculated mathematically and are presented in equations **(4.5)** and **(4.6)**.

$$C_D' = C_D + (\delta \,.\, A \,.\, C_L^2)/(C \,.\, scale^2) \quad \textbf{(4.5)}$$

$$\beta' = \beta + (\delta \,.\, A \,.\, C_L^2)/(C \,.\, scale^2) \quad \textbf{(4.6)}$$

Where downwash boundary correction factor (δ) is typically between 0.09 and 0.14, and wind tunnel's cross sectional area is 14.6 m2. Downwash correction factor is taken 0.09 in this study.

4.3.2.2 Wake blockage

For several years, experimenters believed that wake blockage corrections based on the single theory of simulating the wake satisfied themselves. However, Maskell's method has changed the thoughts says that there is a need of understanding of the momentum effects outside the wake during starting flow separation [20]. In Figure 4.5, it clearly shows the components of drag coefficient versus the square of lift coefficient.

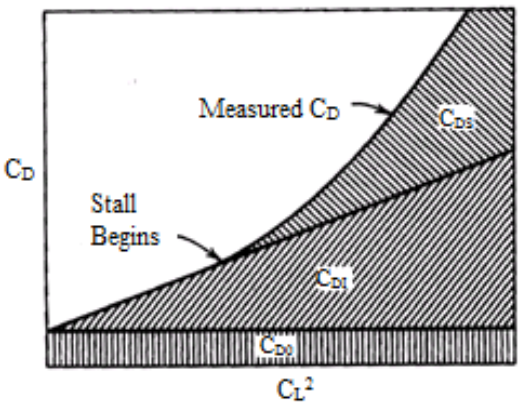

Figure 4.5 : Drag analysis for a lifting body [27].

Lateral constraint therefore has to be removed from the flow pattern around the wake **(4.7)**. This lateral constraint effect increases with the size of the wake, and makes the drag increased **(4.8)** [9,20].

$$C_{DS} = C_D - C_{DI} - C_{D0} \quad \textbf{(4.7)}$$

$$C_{DI} = (C_L^2 \,.\, A)/(\pi \,.\, H_E^2) \quad \textbf{(4.8)}$$

Where,

Zero-lift drag coefficient (C_{DI}) is assumed to be zero, and wake blockage factor (ε_{WB}) is typically 2.5. A Class full size boat is used in the wind tunnel testing, thus there is no need to scale the sailing boat (Scale=1) **(4.9)**.

$$Blockage = max(1 + C_{DS} \,.\, ((\varepsilon_{WB}\, A)/(C\ scale^2)),1) \quad \textbf{(4.9)}$$

Final corrected drag and lift coefficients are in equations **(4.10)** and **(4.11)**:

$$C_D = C_D/Blockage \quad \textbf{(4.10)}$$

$$C_L = C_L/Blockage \quad \textbf{(4.11)}$$

4.3.2.3 Solid blockage

Solid blockage occurs due to lateral constrains on the flow around a sailing boat. This problem typically is the result of the closed circuit system of wind tunnel. The blockage makes all the moments and forces increased, produced by sail boat. However, the effectiveness of the solid blockage mainly depends on tested volume of the sail boat that is usually neglected in open test sections [9,20].

4.4 Analysis of the Wind Tunnel Results

Wind tunnel experiments were mainly based on the performance of the A Class boat by changing various twist and sheeting angles for both main and jib sails. In addition to twist and sheeting angles, another main parameter was wind speed which was varied from 3 to 7 m/s in an increment of 2 m/s. The work flow of raw data analysis is demonstrated in Figure 4.6. In this study, there is no need of scaling the sailing boat.

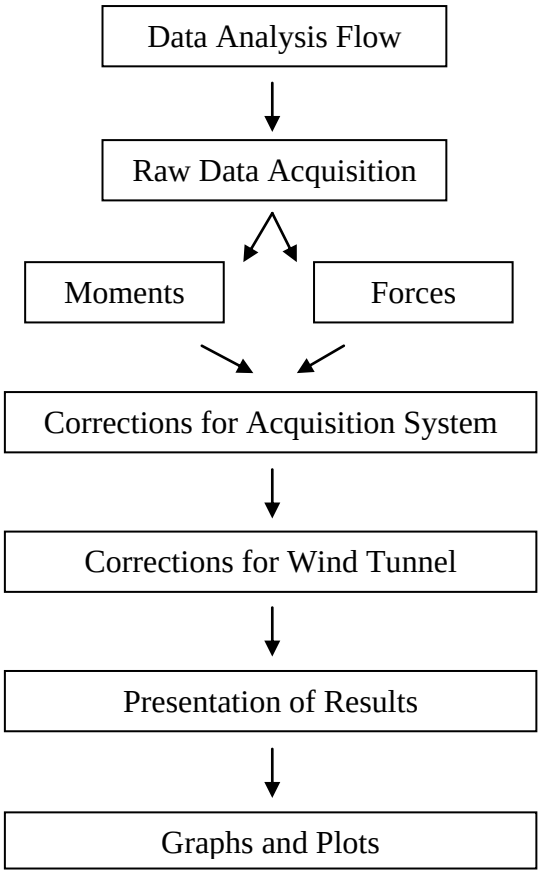

Figure 4.6 : Complete work flow for wind tunnel raw data analysis.

During experimental tests, three different twist and sheeting angles, which are described in Table 4.2, have been measured for both main and jib sails. Different wind speeds and apparent wind angles (AWA) are described in Table 4.3.

Table 4.2 : Various twist and sheeting angles for experimental test.

	Main Sail	Jib Sail	
Twist Angle	7	9	degree
	10	13	
	12	18	
Sheeting Angle	4	10	degree
	6	12	
	8	14	

All the twist and sheeting configurations including different wind speeds were run for 20 degree (AWA). However, due to having some spare time after all runs for 20 degree, some twist and sheeting configurations were run for 28 degree of apparent wind angle as the time allowed. All wind tunnel raw and corrected data is added in Appendix A.2.

Table 4.3 : Different wind speeds and apparent wind angles for testing.

Wind Speed	AWA (deg.)
3 m/s	20°
5 m/s	28°
7 m/s	

The order of changing parameters is simply demonstrated in following Figure 4.7. First of all, the boat was set up in wind tunnel, and apparent wind angle was adjusted.

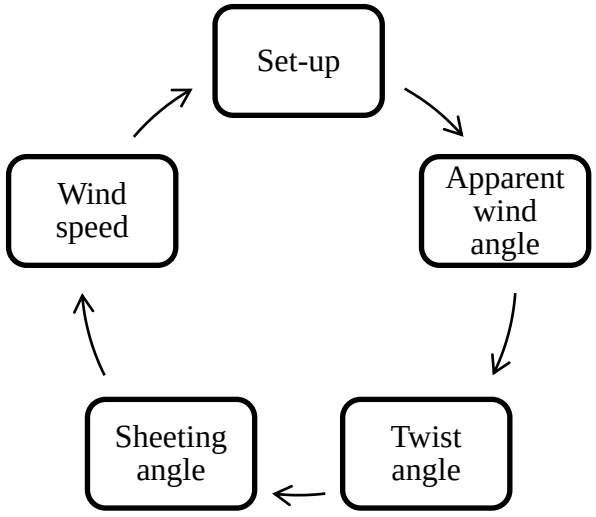

Figure 4.7 : The order of changing parameters during experimental test.

Wind speed was last parameter to change due to its easily changeable feature. Wind speed was changed by wind tunnel staff after all the variations were set up.

Moreover, twist and sheeting angles were changed by entering into the wind tunnel after wind speed of 3, 5 and 7 m/s run. This was quite stressful and tiring work. One of these adjustments is shown on the following Figure 4.8.

Figure 4.8 : Adjusting twist angle of jib sail in the wind tunnel.

To analyse all the configurations easily, they have been diminished into the different case configuration. Twist and sheeting cases will be used to analyse the results.

4.4.1 Twist configurations

One of the main measuring parameters is to adjust the sail trim by changing twist angles of both main and jib sails. There have been 9 twist cases used for the analysis of the experimental results. In analysing part of twist configurations, sheeting angles of the sails are kept unchanged; sheeting angle for the mainsail is fixed to 4° for mainsail and 10° for jib sail. These twist cases are detailed in Table 4.4. Each case represents different twist angles for the sails.

Table 4.4 : The cases of twist configuration.

Twist Cases			
	Main Sail	Jib Sail	
T. Case 1	7	9	deg.
T. Case 2	7	13	deg.
T. Case 3	7	18	deg.
T. Case 4	10	9	deg.
T. Case 5	10	13	deg.
T. Case 6	10	18	deg.
T. Case 7	12	9	deg.
T. Case 8	12	13	deg.
T. Case 9	12	18	deg.

Figure 4.9 shows the square of lift coefficients against drag coefficients with wind speed of 3 m/s. As the twist angle of mainsail increases, drag coefficient increases, and the square of lift coefficient simultaneously decreases.

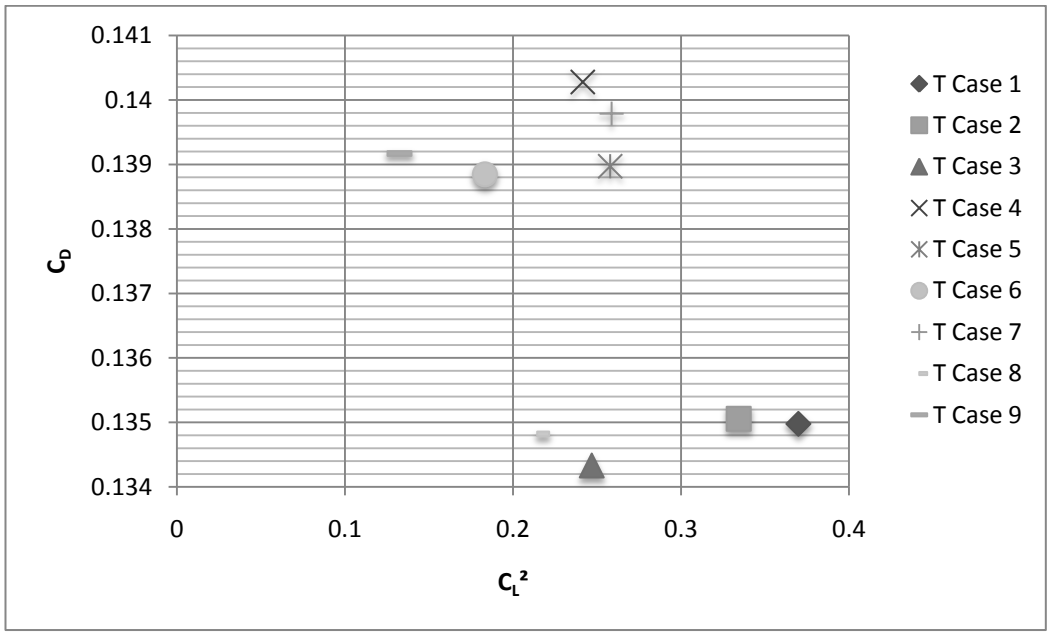

Figure 4.9 : Twist AWA 20° – C_L^2 versus C_D with 3 m/s wind speed.

However, surprisingly there is one exception of these changes. Case 8 has low drag amount when it is compared to the cases numbered 4, 5, 6, 7 and 9.

It might be said that case 1 which consists of the twist angle of 7° for mainsail and of 9° for jib sail is the optimum one for twist configuration with the wind speed of 3 m/s. When wind speed is increased from 3 to 5 m/s shown in Figure 4.10, drag coefficient value of the case 1 for 5 m/s is lower than the drag value of 3 m/s wind speed.

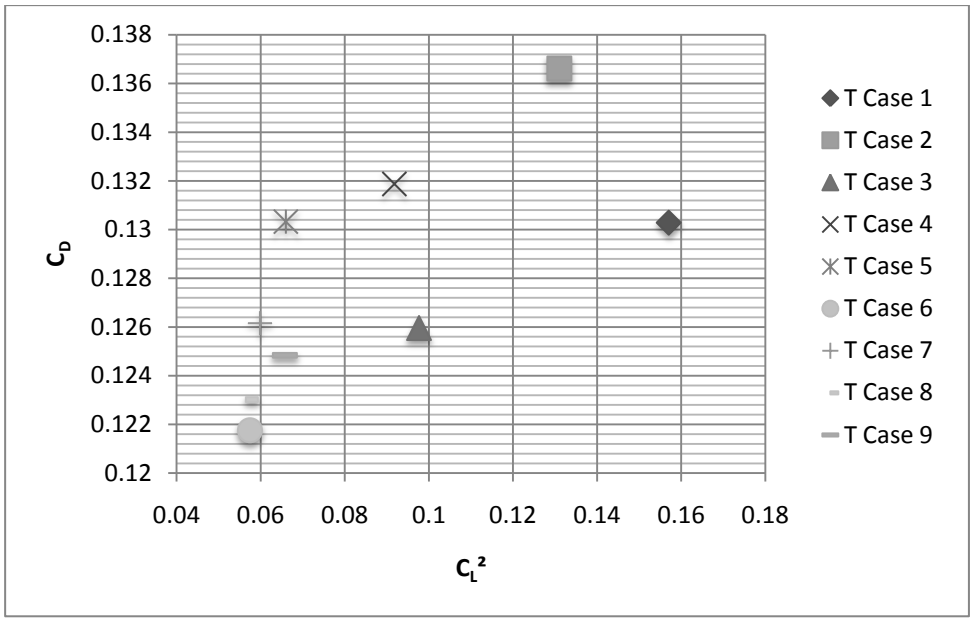

Figure 4.10 : Twist AWA 20° – C_L^2 versus C_D with 5 m/s wind speed.

However, the square of lift coefficient loses more than drag coefficient lost. In plot 3, C_L^2 versus C_D with 7 m/s wind speed. During experiments running, it was clearly observed that wind speed of 7 m/s was too strong for the current apparent wind angle which was 20°. The sails were apparently oscillating with this wind speed, and results of wind speed of 7 m/s are not reliable results. The effects of fully oscillation can be seen in Figure 4.11, produced lift is too small anymore and drag is basically in the same range but it is quite large when compared to the amount of lift production.

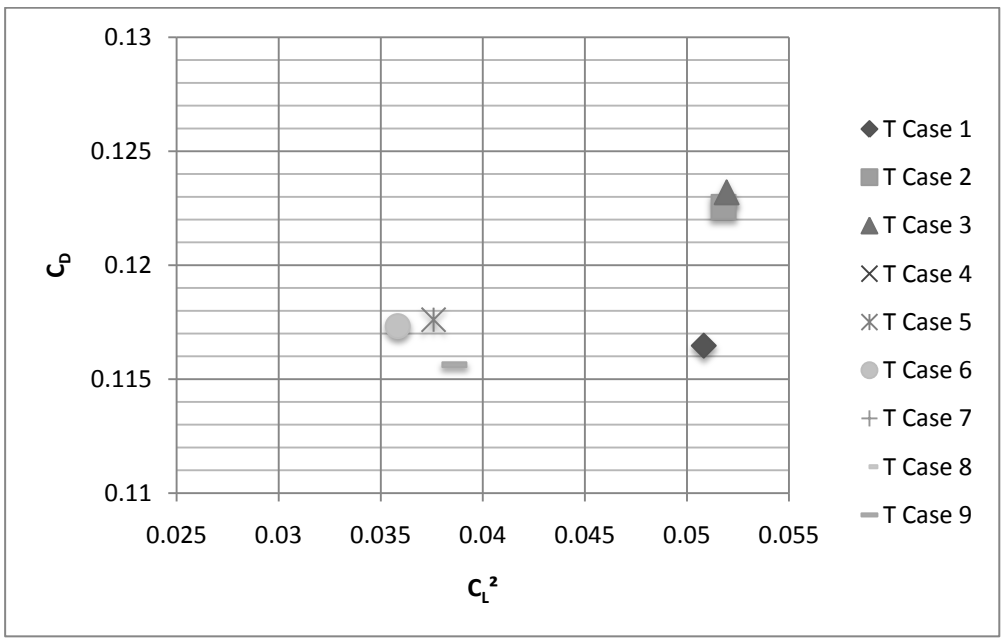

Figure 4.11 : Twist AWA 20° – C_L^2 versus C_D with 7 m/s wind speed.

In Figure 4.12, it is plotted heeling forces versus driving forces for nine cases with different wind speeds.

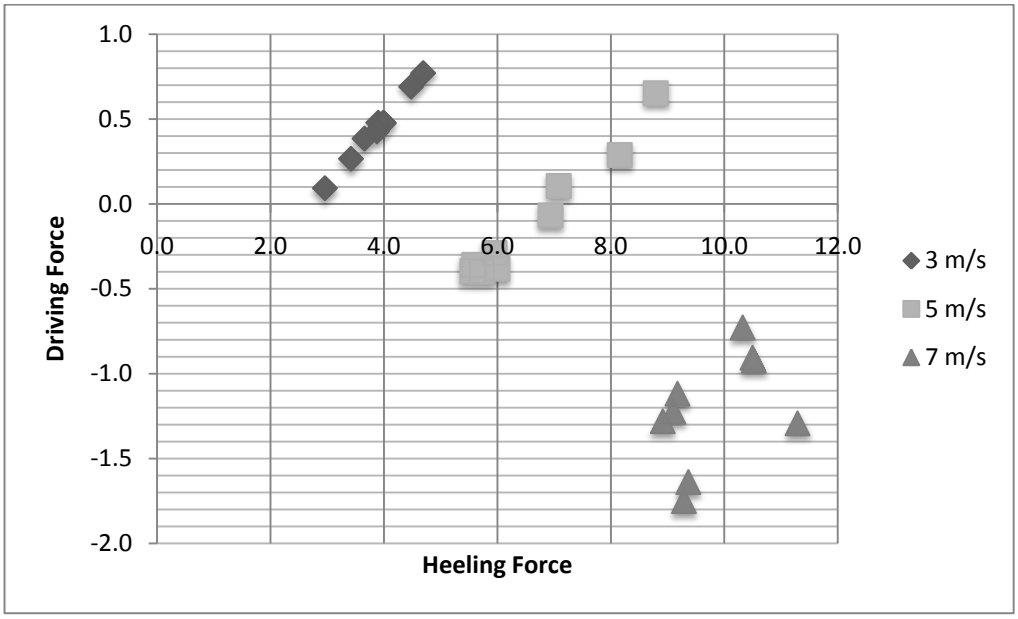

Figure 4.12 : Twist effects on corrected driving and heeling forces.

Due to high oscillation rates with 7 m/s wind speed, all of the driving force values are negative for the wind speed of 7 m/s. This means for 7 m/s that does not produce positive driving forces to power the sails. In part of 3 m/s, it is understood that the flow is smooth and it produces a large amount of driving forces. For AWA 28°, not all twist and sheeting configurations were run. These runs were done due to having extra time in wind tunnel. For example, some of those runs are represented in Figure 4.13 where only difference between Figures 4.9 and 4.13 is apparent wind angle. AWA is 20° in Figure 4.9 and 28° in Figure 4.13. It is so clear that when increasing AWA to 28° under the same conditions, lift increases largely.

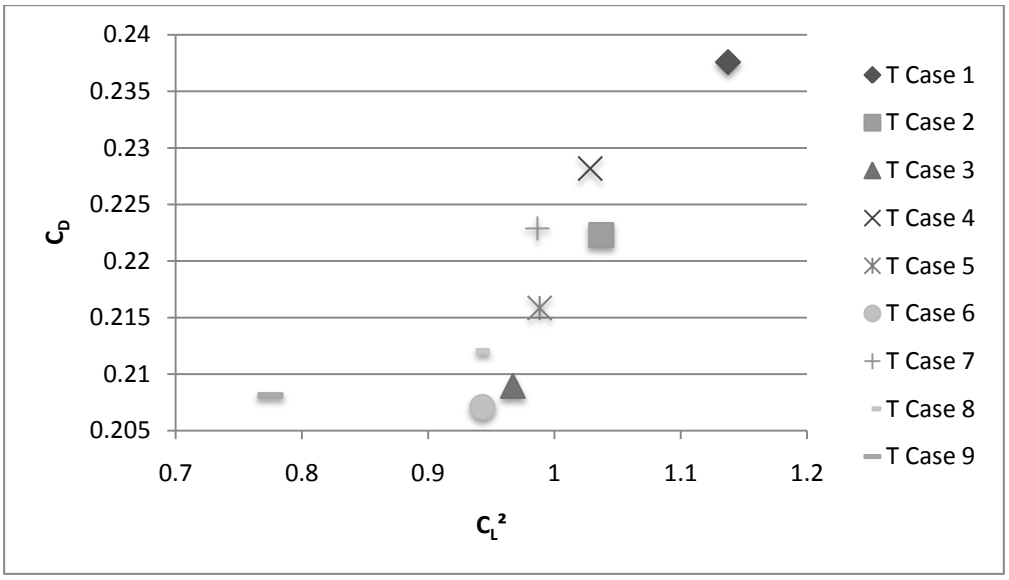

Figure 4.13 : Twist AWA 28° – C_L^2 versus C_D with 3 m/s wind speed.

On the other hand, drag also increases, but its increase rate is not as same as lift's increase rate. To show it more clearly, there is a need of comparing the ratio of square of lift and drag coefficients. C_L^2/C_D ratio of T case 1 roughly for 20° is 2.7 and for 28° it is 4.8. It proves AWA 28° is better wind angle than 20° in sail performance, producing more lift and less drag when comparing C_L^2/C_D ratios.

4.4.2 Sheeting configurations

The other main measuring parameter is sheeting angle that has large influence on the appropriate sail trim. Similar to twist cases, 9 sheeting cases have been examined to analyse the results, and twist angles for the sheeting cases are fixed; twist angle for the mainsail is fixed 7° and for the jib sail twist angle is 9°. The sheeting cases (9 cases) are specified in Table 4.5.

Table 4.5 : The cases of sheeting configuration.

Sheeting Cases			
	Main Sail	Jib Sail	
S. Case 1	4	10	deg.
S. Case 2	4	12	deg.
S. Case 3	4	14	deg.
S. Case 4	6	10	deg.
S. Case 5	6	12	deg.
S. Case 6	6	14	deg.
S. Case 7	8	10	deg.
S. Case 8	8	12	deg.
S. Case 9	8	14	deg.

In Figure 4.14, the square of lift coefficients versus drag coefficients are shown for AWA 20° with 3 m/s wind speed. Sheeting case 4 has quite low drag value compared to other sheeting cases.

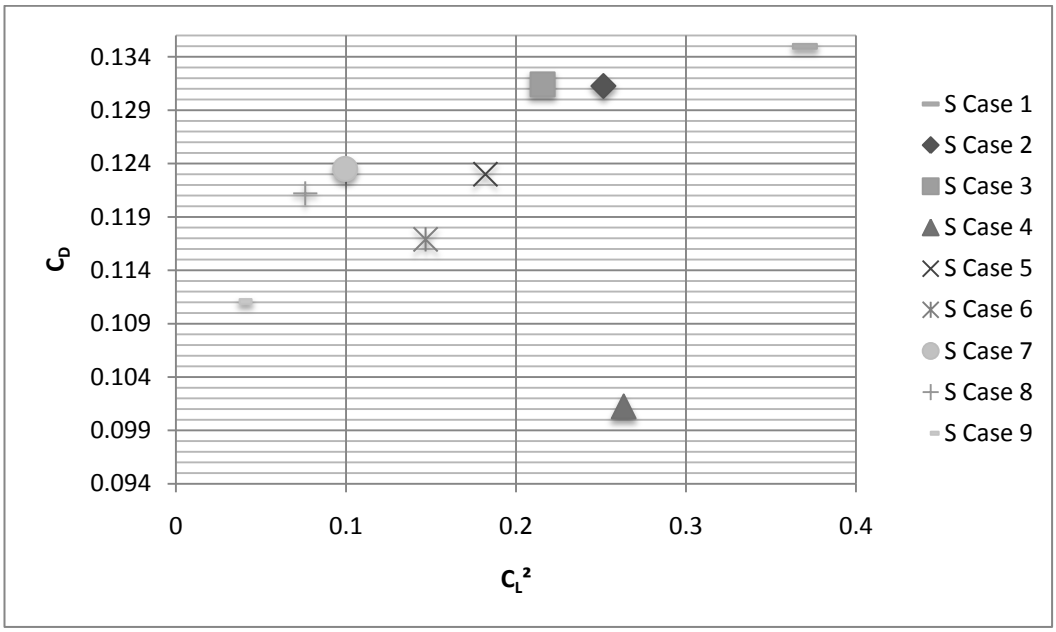

Figure 4.14 : Sheeting AWA 20° – C_L^2 versus C_D with 3 m/s wind speed.

If it is looked at sheeting case 1, it has the biggest lift value apart from the fact that it has the biggest drag value. Lift can be generated in most cases; however decreasing drag values is the most key point. That is why; sheeting case 1 is not a good sheeting configuration although it develops high lift forces. Sheeting case 4 seems the most appropriate sheeting configuration for 3 m/s wind speed as well as with AWA 20°.

Whilst the sheeting angle for jib sail increases from 10° to 12° (from case 2 to case 3), the square of lift coefficient shows a decrease from 0.25 to 0.2. This decrease in lift side proves that the sheeting angle of jib sail should be no more than 12°. In Figures of 4.15 and 4.16, it can be seen clearly large amounts of decreasing lift coefficient, especially in Figure 4.16 which represents 7 m/s wind speed. With 3 m/s, average value for the square of lift coefficient is around 2. With 5 and 7 m/s speeds, these average lift coefficient values are 0.05 and 0.03, respectively. This is very large decrease in terms of lift coefficient. On the other hand, there are no big changes in drag side, and it shows a slow decrease in drag coefficient.

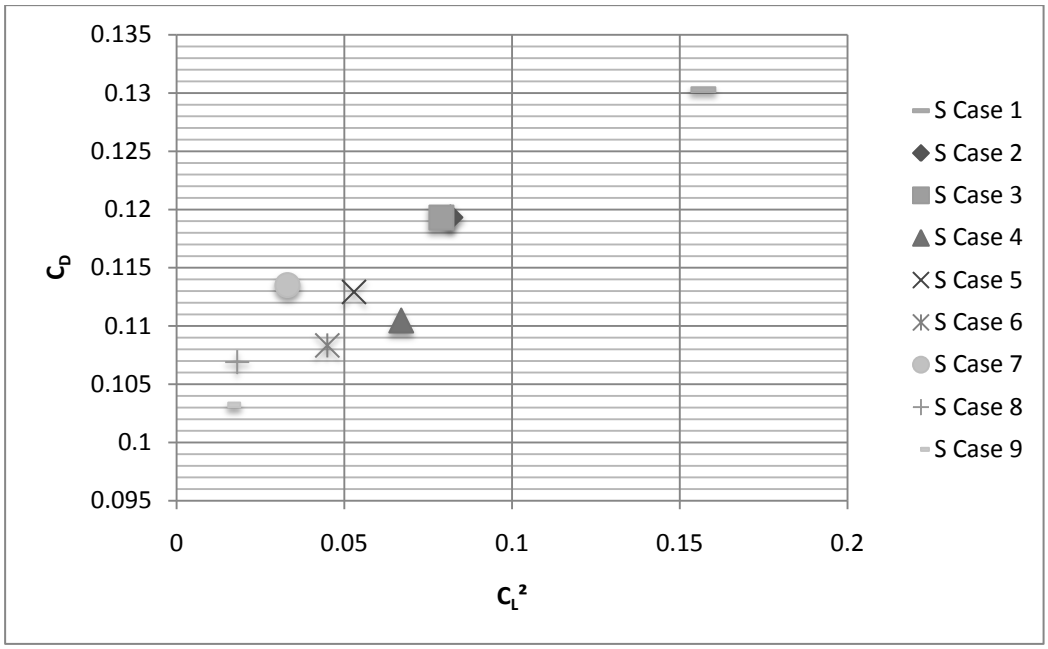

Figure 4.15 : Sheeting AWA 20° – C_L^2 versus C_D with 5 m/s wind speed.

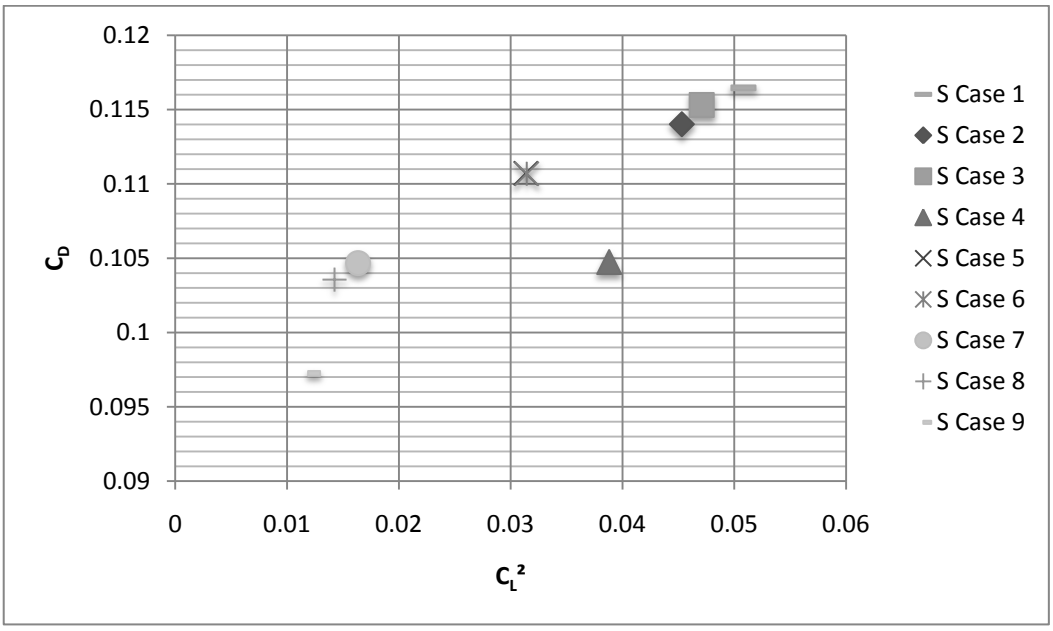

Figure 4.16 : Sheeting AWA 20° – C_L^2 versus C_D with 7 m/s wind speed.

Expect for sheeting case 1 with 5 m/s wind speed in Figure 4.15, all the other 8 cases show a downward in lift and drag coefficient. It is mainly due to insufficient apparent wind angle (20°) at which the sails cannot receive appropriate wind in terms of wind angle. Therefore, cases for 28° (AWA) were run to study 20° wind angle's results more accurately.

So far, effects of wind speed are separately discussed for all cases. Figure 4.17 demonstrates how different wind speeds play an important role on producing driving and heeling force. As it is mentioned in the twist configuration part, it must be again noted that 7 m/s wind speed is too strong for the sailing boat to keep the sails well-trimmed and cause the oscillation problem. Driving forces of the cases under 7 m/s (partially 5 m/s) wind speed are negative as well.

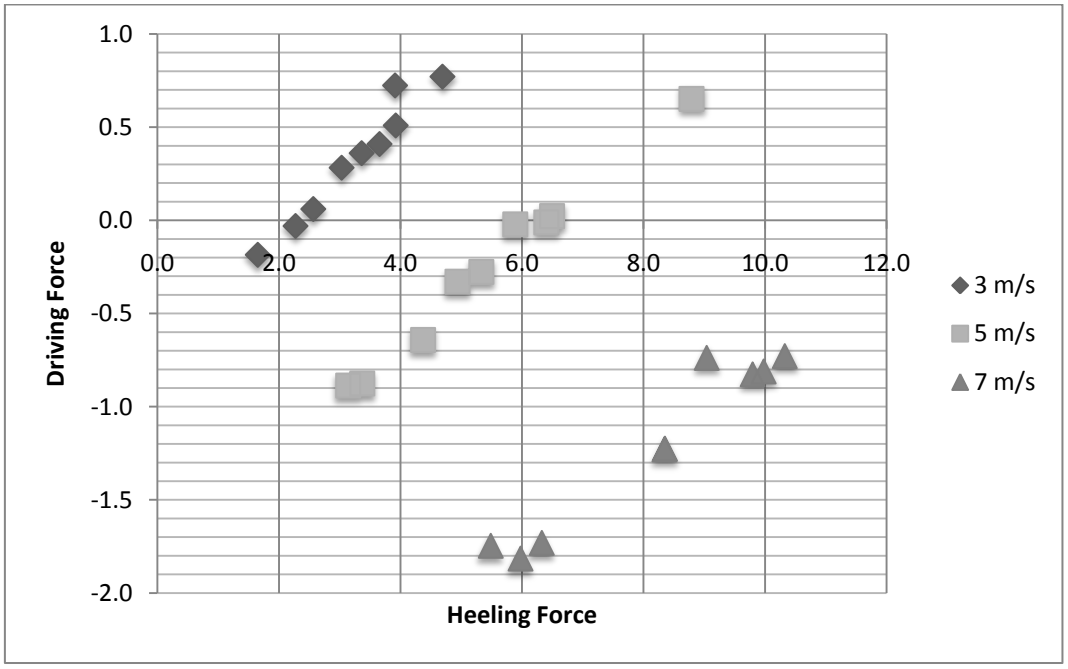

Figure 4.17 : Sheeting effects on corrected driving and heeling forces.

Keeping all conditions same except for AWA with Figure 4.14, these new conditions are represented in Figure 4.18. Results show nearly a linear reduction when increasing sheeting angles for both main and jib sails. Sheeting cases are same as twist cases for 28° showing that sails' performance is better with 28° AWA under these conditions.

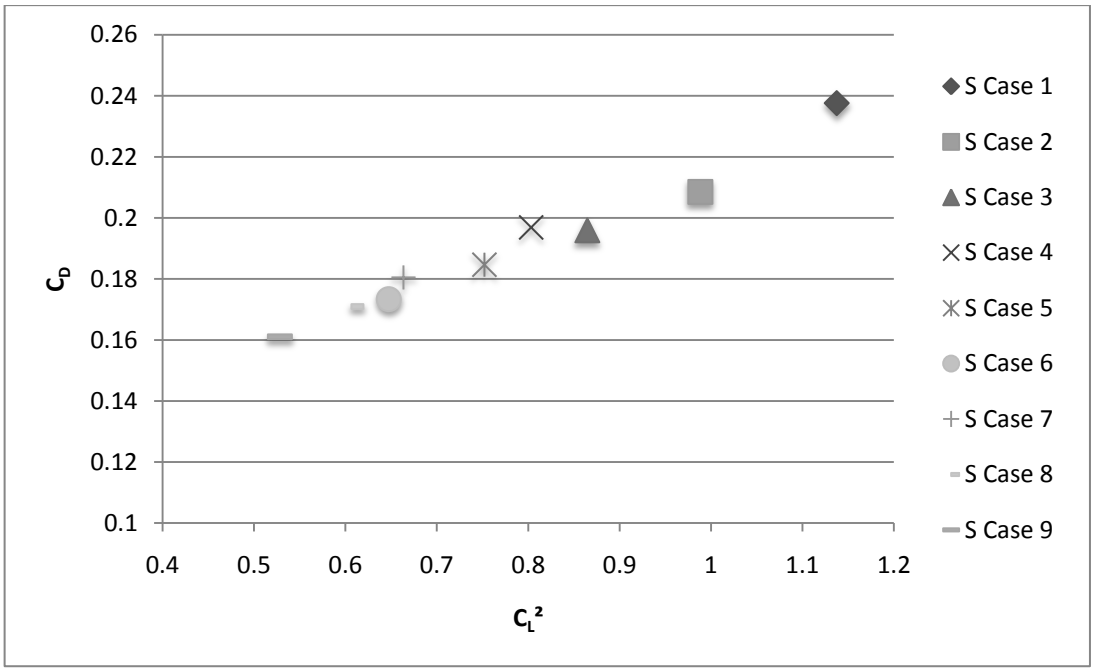

Figure 4.18 : Sheeting AWA 28° – C_L^2 versus C_D with 3 m/s wind speed.

5. COMPUTATIONAL FLUID DYNAMICS (CFD)

5.1 Introduction to CFD

The importance of computational fluid dynamics (CFD) is getting well-known in the marine design environments, and it is indeed widely applied to different topics such as sail and ship hull designs. It must be mentioned full scale and wind tunnel testing systems before setting up a proper introduction to CFD. Full scale testing can obtain very accurate solutions for sailing boat design. However, even though it provides very clear and accurate results, it is very expensive to build full scale model and also time consuming [21]. It also must be noted that there is uncertainty of building full scale model at which the design might have some fundamental problems, and there is no way to go back after building it. At this point, wind tunnel measurements can play an important role to reduce building costs and calculate the performance of given any sail configurations. Comparing wind tunnel testing with full scale testing, wind tunnel testing is less expensive than full scale. The problem with wind tunnel testing is difficult to scale model performance in wind tunnel to real life sail performance. To reduce time consumption and costs, CFD can be very useful tool to simulate flow conditions in digital environment where time and money consumptions are apparently in the lowest level. CFD calculations achieve a more detailed acknowledge of the flow characteristics than either wind tunnel testing or full scale testing, and can therefore assist in a better understanding of the optimization problem [21]. CFD calculations have been successfully applied to the optimization problems of applications in the aerospace industry for several years [22].

One of the major advantages of using CFD in sail design field is that flow solvers integrated in modern CFD software can determine quickly optimized sail shapes. One of the most popular methods which many CFD software use is the Reynolds Averaged Navier-Stokes (RANS) which brings a better understanding of the famous and difficult Navier-Stokes equations. In addition to Reynolds Averaged Navier-Stokes method, other methods are namely direct numerical simulation method

(DNS), vortex lattice method and panel method. A direct solution numerically solves the Navier-Stokes equations without using any turbulence model [23]. Figure 5.1 illustrates CFD work flow stages [24].

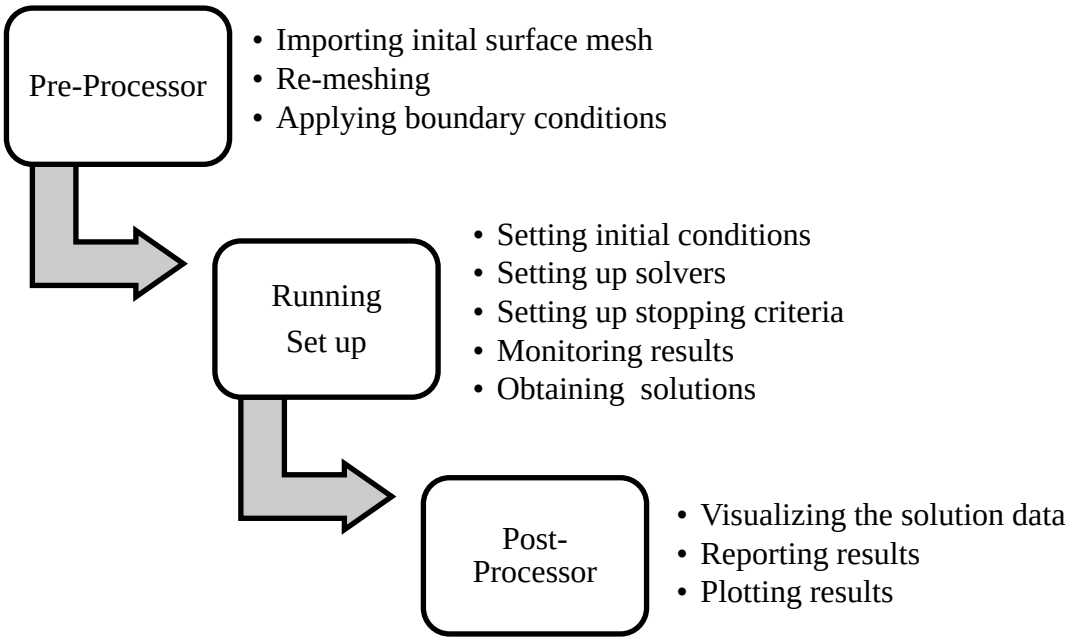

Figure 5.1 : Schematic view of CFD work flow.

Another important advantage of CFD is that it enables the users to create several numbers of simulations. It is possible to reduce the number of simulations to a few; therefore well estimated performance of these designs can be manufactured and tested in either wind tunnel or full scale testing. This makes wind tunnel testing much cheaper than the testing without CFD. A question arises at this point that why direct CFD simulations cannot be applied to industrial manufacturing processes? One of the most significant disadvantages of CFD is that is widely assumed a “Giant black hole” until now due to its complexity. Thus, CFD and experimental methods such as wind tunnel or towing tank testing are still used together to provide a better solution of the flow behaviours. Applying CFD codes on any shape configurations without a deep knowledge of the fluid dynamics might cause completely unrelated solutions. In the following sections of this study, CFD calculations will be provided and there will be a comparison between CFD simulations and wind tunnel testing data.

5.2 STAR-CCM+ Version 5.04.008

STAR-CCM+ is chosen for this study due to its simple user interface and friendly tutorials. It is a commercial CFD code, and it is quite expensive to use it in your studies. The University of Southampton has more than a hundred licenses for STAR-CCM+, this facility enables us to work using this strong commercial CFD code. Why STAR-CCM+ and other commercial CFD codes are getting so popular in many different industries? One of the first reasons is their user friendly and powerful pre and post-processing graphical user interfaces (GUI). In addition to first reason, they have powerful mesh generators to deal with complex geometries, and also they allow the users to write codes for necessary adjustments by plugging in CFD software [25]. STAR-CCM+ is a unique environment that combines the user interface and simulations [24]. This combination of interface and simulation makes STAR-CCM+ very efficient CFD software. STAR-CCM+ is a three dimensional meshing tool that enables the users to import geometries or develop and generate unstructured or structured geometries. In addition to these, STAR-CCM+ includes Reynolds Average Navier-Stokes models, and it makes extremely powerful solver. Moreover, simulation tree in STAR-CCM+ makes the users to control simulation easily, and it is simple and well-organized to understand in the beginning.

The unique environment in STAR-CCM+ is based on parameters as [24]:

- Having graphical user interface
- User-defined boundary conditions
- Pre-processing and post-processing functions
- Database for simulations
- Programming options for users
- Being worked on Linux, Windows and Unix operation systems

There are some numeric solutions available in STAR-CCM+, and they are detailed on the following list [24]:

- Discretization methods based on cells
- Coupled implicit, coupled explicit and segregated implicit solvers
- Algebraic multi-grid linear equation solver
- Criteria functions for converging

5.3 3D Sail Geometry Definition

5.3.1 3D Accumeasure software

AccuMeasure is a software package developed by UK Sailmakers to read a sail's sectional shape from digital photographs. To read a sail's shape from photos, they should be shot looking up from the middle of the foot of the sail [26]. It is important to note that camera must be as close as possible to the sail surface to gain sectional lines properly. Figure 5.2 demonstrates a screen shot of how to obtain draft stripes from photos. To obtain as much as possible of the longest draft stripe, there is a need of rotating of camera for running the longest stripe across the frame [26]. Additionally, AccuMeasure enables the users to determine the position of the measurement tool of the picture edge. There is one more significant point is to zoom out with the camera as far as to obtain as much of the sail as possible in the photos. Sheeting angles of a sail can be found accurately with the way of estimating twist angles by AccuMeasure software.

AccuMeasure determines the characteristics of sail section. These characteristics are listed as:

- Maximum camber
- Draft position
- 15% Camber
- 75% Camber
- Twist

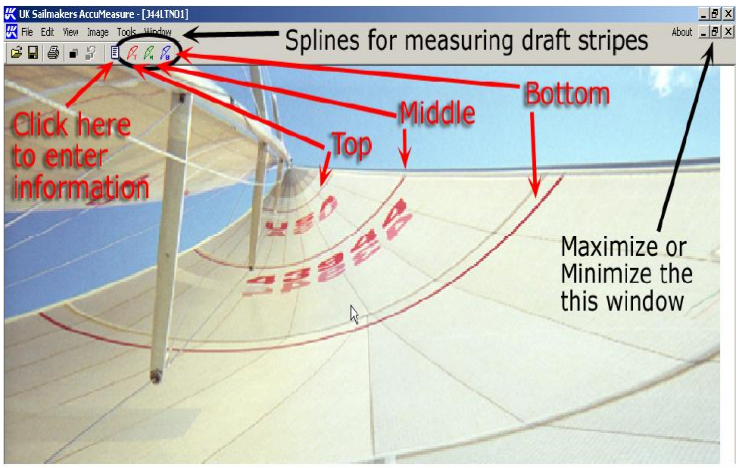

Figure 5.2 : A screen shot of AccuMeasure showing splines for draft stripes [26].

5.3.2 Excel software

After obtaining the sail's sectional characteristics, Microsoft's Excel software was used to calculate the coordinates of sail geometry in terms of x, y and z directions. In addition to these calculations, there is a need of correction the data collected from AccuMeasure software [27]. This correction basically depends on two following parameters as:

- Distance from camera lens to sail gooseneck part
- Distance from camera lens to top of mast

As AccuMeasure software determines only the first estimations of the sail's sectional shape, there are some inputs to enter in Excel. These inputs are heel and apparent wind angles, and they are based on case conditions. Any heel and apparent wind angles can be set up and their geometries can be designed. In this study, 30° heeling angle and 28° apparent wind angle are used to validate the wind tunnel results by CFD calculations.

5.3.3 Rhinoceros software

To compare and validate wind tunnel results with CFD results, 3D geometry in digital environment has to be created. Rhinoceros 3D is computational aided design software (CAD) and it was used to create final 3D sail geometries for meshing in STAR-CCM+. Rhino enables the users to import several data forms from other software. Once created sail sectional stripes in Excel, these stripes in terms of x, y and z directions can be exported to Rhinoceros in text file like pointsfile.txt. In Rhinoceros, it can be meshed for the sail surface. This is initial and base mesh for the CFD meshing structure. The mesh created in Rhino then can be exported in stereo lithography (.stl) format for STAR-CCM+, and it will be re-meshed in STAR-CCM+. Figure 5.3 shows a screen shot from Rhino for the final geometry of the sails. The sail shape characteristics are given in Appendix A.3.

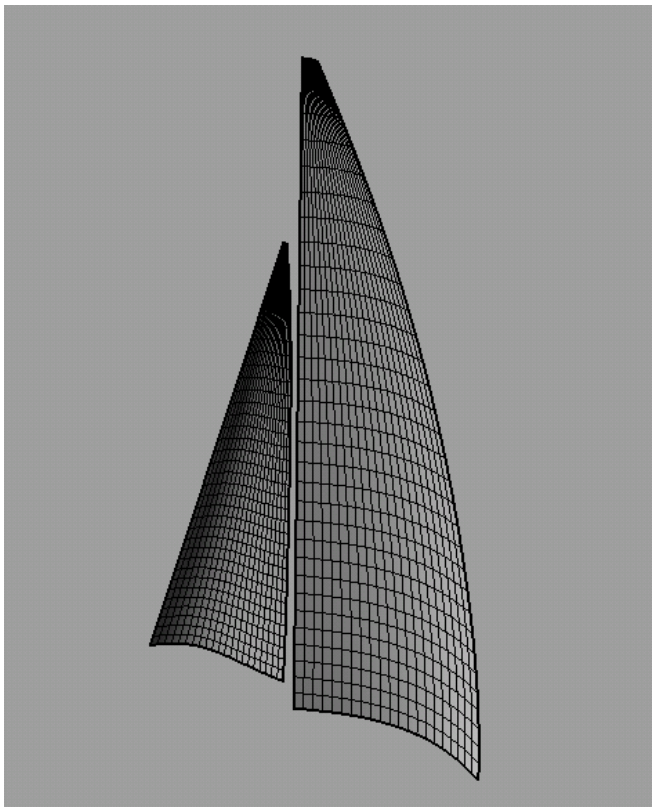

Figure 5.3 : A screen shot of main and jib sails from Rhinoceros.

5.4 Mesh Generation

Before surface and volume meshing in STAR-CCM+, the geometry of flying shapes needs to be modelled in Rhino using the three dimensional coordinates obtained from AccuMeasure and Excel. In the previous sections, these steps were mentioned and detailed. Now, it is time to re-mesh the sail shapes as this mesh is final one before setting up running conditions such as initial, physical and solver conditions in STAR-CCM+.

5.4.1 Mesh types

STAR-CCM+ uses like other major CFD software automatic unstructured mesh generator that makes it an unstructured solver. Any kind of mesh actually can be loaded into STAR-CCM+. However, there is a need to convert the mesh into one of the supported formats, and then STAR-CCM+ treats all the meshes as unstructured mesh or in other words face based mesh.

5.4.1.1 Structure grids

A structured grid of quadrilateral consists of a set of coordinates and connectivity that naturally map into elements of a matrix [25]. A structured grid is organized in columns and rows of cells for two dimensions so that any program CFD code which sweeps over the mesh can address the neighbouring elements to determine differencing expressions. Furthermore, there is a relationship between location of an element (cell) in its column and row and location of the CFD code array systems where are used to store physical variable related to elements. For example, a 3D array x (i, j, k), y (i, j, k) and z (i, j, k) enables to store the x, y and z coordinates of the points in a 3D grid.

Figure 5.4 shows a hybrid mesh where consists of mixing structured and unstructured grids. The grids in white colour (left side of the figure) are a structured mesh that is generally used when simple geometries are being examined. Structured grids need fewer grid points, and they are more accurate and efficient.

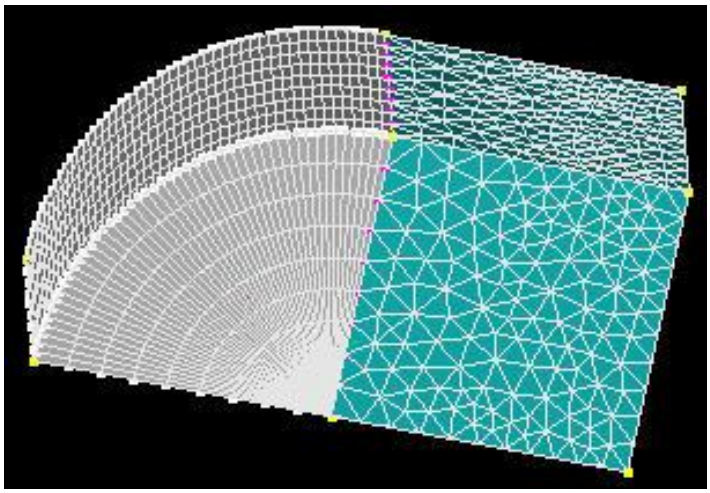

Figure 5.4 : A mixing structured and unstructured 3D grids.

5.4.1.2 Unstructured grids

An unstructured mesh has no direct relationship between neighbouring elements and the location of their data in the data structure. Hence the location of the data and the location of the element must be connected using indirect addressing. This means that there are no ordering points (i, j, k) like in structured mesh to generate the mesh. For this, more data information is needed in unstructured mesh. For any particular point, the connection with other points must be defined explicitly in the connectivity matrix [25]. Figure 5.4 also shows an example of 3D unstructured mesh (the grids in dark

turquoise colours). One of the most important advantages of the unstructured mesh is that does not have any ordering points which possess to global data structure, and therefore it enables the users to delete and add cells or any other cell parameters in any cases. This feature of unstructured mesh gives a huge flexibility to mesh complex geometries. That is why; the vast majority of the commercial CFD codes use unstructured mesh to handle with very complex geometries being used in different industries such as aerospace and marine industries. It is because of complex nature of the sail's geometries, an unstructured mesh was chosen for this study. An unstructured mesh gives much more flexibility in surface and volume meshing steps.

5.4.1.3 Surface meshing

In the generation of unstructured mesh, the first step is to create a surface mesh. Volume mesh is based on the surface mesh, and it therefore cannot be done without an existing surface mesh. The starting point in the surface mesh generation is the import of surface data from CAD programmes in the form of either a mesh or some kind of geometric data.There are three different types of surface data that can be imported into STAR-CCM+ [24]:

- Surface meshes
- Neutral format data
- Native CAD data

The surface mesh is a discrete representation of the geometry so that is used for the generation of the volume mesh. It is made up of vertices and faces [24]. Moreover, it depends on the pre-processing software used to create the surface, feature curves may be included. In this study, native CAD data from Rhinoceros programme will be used to import the initial surface to create the surface mesh. On importing native CAD data into STAR-CCM+, it is automatically discretized into faces (triangular) which are based on a supplied tessellation density [24].

5.4.1.4 Volume meshing

When a surface mesh is generated, then a volume mesh can be created depending on the surface mesh. STAR-CCM+ has three major different meshing models that can be used to generate a volume mesh starting from previously created a surface mesh.

These three meshing models namely are:

- Tetrahedral mesh
- Polyhedral mesh
- Trimmed mesh

The models will be detailed shortly to have a better understanding of meshing tools.

Tetrahedral mesh:

Tetrahedral meshes provide a simple and efficient solution for complex geometries of shapes. When it is compared to other meshing models in STAR-CCM+, the tetrahedral is the fastest meshing model, and it uses the least memory. The final mesh will mainly base on the triangulation of the surface. Hence the starting quality of the surface must be good enough to create very good quality of the volume meshes [24].

Polyhedral mesh:

Polyhedral meshes enable the users to obtain a balanced solution for complex geometries. Out of the three meshing models, they are efficient and easy to create any needed meshes, and it also does not require a lot of meshing preparations like in the tetrahedral meshing. Additionally, they also consist of fewer (five times) cells than an equivalent tetrahedral mesh [24].

Trimmed mesh:

Trimmed meshing model in STAR-CCM+ is a very efficient meshing so that can be applied to either of simple and complex geometries. "It combines a number of highly desirable meshing attributes in a single meshing platform [24]" which is described on the following list:

- Using hexahedral grids with minimal skewness angles for the cells;
- Performing automatically for both curvature and proximity cell refinement
- Options independently for the generation of surface quality
- Enabling the users to specify a needed coordinate system

In addition to these information above about trimmed meshing, trimmed and polyhedral meshing gives better accuracy whilst using a comparison to tetrahedral in given number of cells. In this study, trimmed mesh will be used for the generation of the volume mesh.

5.4.2 2D Meshing

The aim of performing the two dimensional meshing and running is to have a decisive understanding before the three dimensional model is created. Hence, a 2D mesh will be created and then that mesh will be used for running of the simulation. For this case, a horizontal line was cut at the height of 700 mm from the mainsail's foot using the three dimensional sail geometry to study 2D sail geometry. Figure 5.5 shows a screen shot for the lines of 2D sail section. STAR-CCM+ does not support 2D problems. First thing is to create 3D mesh and then convert it to a 2D mesh. There are special requirements in STAR-CCM+ for 3D meshes that will be converted to 2D, and these are [24]:

- The grid needs to be aligned with the x-y plane.
- The grid has to have a boundary plane at the z = 0 direction.

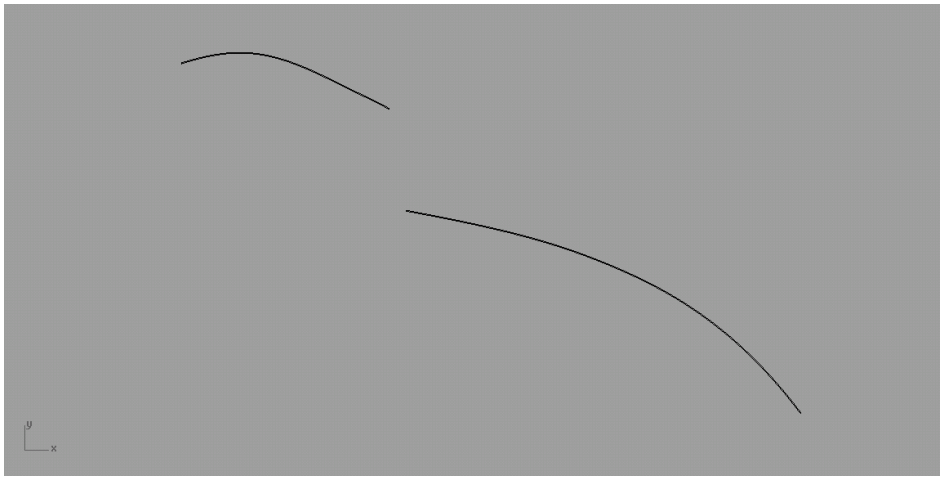

Figure 5.5 : 2D Sections of jib and main sails.

The 2D meshing process starts with importing the surface mesh:

- Launch STAR-CCM+ and start a new simulation as normal
- Select File > Import Surface Mesh
- Change units to be in mm in the create new region dialog

And then visualizing the surface mesh follows these steps:

- Select the Scenes > Geometry Scene 1 > Displayers > Geometry 1 node
- In the Properties panel turn on the mesh display option to show initially created surface mesh

The triangle definition is relatively poor in STL format (format from native CAD program for this study), and therefore the quality of the surface has to be improved to be used as a basis of re-meshing process. Hence feature curves and the boundaries have to be defined.

- Select the Regions > Region 1> Boundaries > SAIL 2D node
- Right click and select split by angle... from the pop-up menu
- Setting the angle value to 89° (presenting 90°)

If the angle of 89° is not enough to split some boundaries, then it can be decreased some for specific boundary. However, on the other hand, some of the boundaries might need to be re-combined in order to simplify the setting up process.

Applying boundary type properties to the created boundaries is shown in Table 5.1:

Table 5.1 : Boundary types for the boundaries.

Boundary Name	Boundary Type
Main Sail	Wall
Jib Sail	Wall
Inlet	Velocity Inlet
Outlet	Flow-split Outlet
Port Side	Wall
Starboard Side	Wall
Top Side	Wall
Bottom Side	Wall

In spite of setting ‘Wall Type’ up for port, starboard, top and bottom sides, ‘Slip’ wall condition (shear stress specification) will be applied to these sides. Additionally, when the 3D mesh is converted to the 2D mesh, top and bottom sides will be removed from the domain. In STAR-CCM+, there is an option to define feature curves which are used to maintain sharp edges of the boundaries. This feature is a very useful when meshing any desired sharp edge in a better way of meshing. Now, it is time to select meshing models and global mesh reference values shown in Table 5.2 for both the surface and volume mesh:

- Selecting the surface re-mesher model for the surface mesh
- Selecting the trimmed mesher for the volume mesh
- Selecting the prism layer mesher for the prism layer

Table 5.2 : 2D Global mesh reference values for the sails.

Main Sail	
Reference Node	Value
Base Size	0.08 m
Thickness of Near Wall Prism Layers	0.0000973 m
Prism Layer Thickness	0.01 m
Number of Prism Layers	20

Jib Sail	
Reference Node	Value
Base Size	0.08 m
Thickness of Near Wall Prism Layers	0.0000897 m
Prism Layer Thickness	0.01 m
Number of Prism Layers	20

Where thickness of near wall prism layers represents the first node height and it was calculated separately for the main and jib sails due to their changing Reynolds numbers which are shown in Table 5.3.

Table 5.3 : 2D Reynolds numbers for the sails.

Reynolds Numbers	
Main Sail	1.0423E-05
Jib Sail	0.5038E-05

2D mesh properties are described in Table 5.4.

Table 5.4 : 2D Mesh properties.

2D Mesh Properties	
Cells	36271
Interior Faces	73086
Vertices	37628

Figure 5.6 shows two screen shots demonstrating the final mesh before setting up the solver parameters. To make mesh in STAR-CCM+, there has to be given a thickness for sails where 1 mm sail thickness was given for the sails. 1 mm thickness does not effect on the results so much when comparing with whole domain and sail. dimensions.

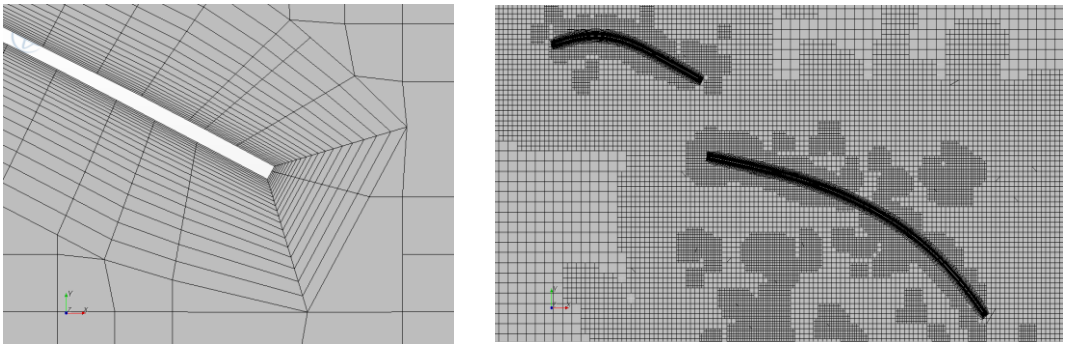

Figure 5.6 : 2D Final mesh.

5.4.3 3D Meshing

Once the three dimensional geometry is created, then it can be imported into the CFD code. The 3D native geometry is imported in a same way which was mentioned in the section of the 2D meshing. Simulated configuration model is detailed in Table 5.5. Due to time limitation, other wind tunnel configurations could not be simulated in CFD.

Table 5.5 : Sail model's characteristics for CFD simulation.

	Twist (°)	Sheeting (°)	Heeling (°)	AWA (°)	Wind Speed (m/s)
Main Sail	7	4	30	28	3
Jib Sail	9	10	30	28	3

All the meshing process of the 2D until Table 5.2 is same with the meshing process for the 3D meshing except for one step is that there is no converting step in the 3D meshing. To compare wind tunnel testing with computational fluid dynamics simulations, wind tunnel testing conditions are needed to be simulated in CFD platform. Therefore, the domain is created in CFD which is shown in Figure 5.7.

The computational domain dimensions are:

Height: 3.7 m

Wide: 4.6 m

Long: 10.0 m

In wind tunnel, long distance is 3.7 m and this distance is very short for computational domain so that was extend to 10.0 m to examine flow characteristics.

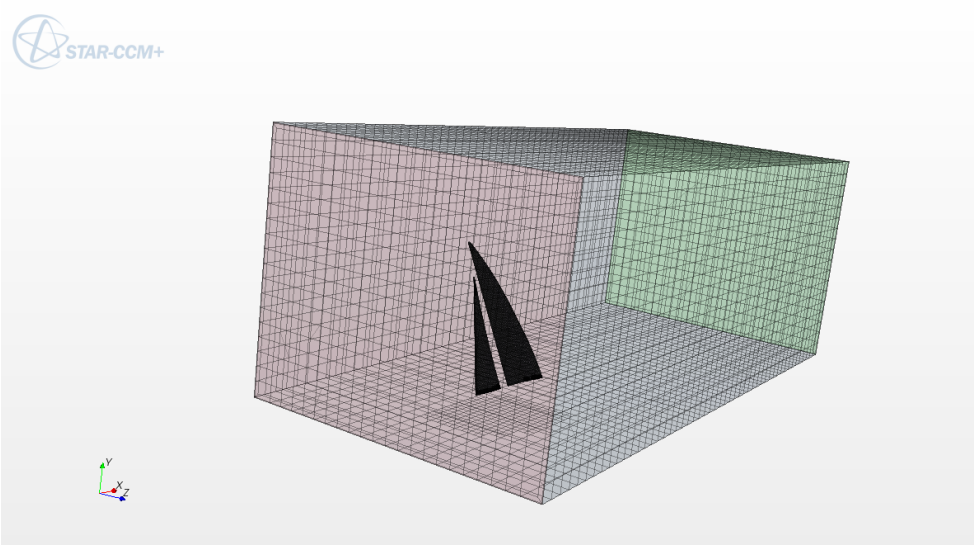

Figure 5.7 : Created wind tunnel domain in CFD.

Reynolds numbers for the 3D simulation are shown in Table 5.6.

Table 5.6 : 3D Reynolds numbers for the sails.

Reynolds Numbers	
Main Sail	0.6019E-05
Jib Sail	0.4384E-05

In order to achieve y+ values around 1, the thickness of near wall prism layer (first wall node distance) was calculated for mainsail 0.0000915 m and for jib sail 0.0000882 m. Global mesh reference values for the 3D simulations are shown in Table 5.7.

Table 5.7 : 3D Global mesh reference values for the sails.

Main Sail	
Reference Node	Value
Base Size	0.2 m
Thickness of Near Wall Prism Layers	0.0000915 m
Prism Layer Thickness	0.006 m
Number of Prism Layers	15

Jib Sail	
Reference Node	Value
Base Size	0.2 m
Thickness of Near Wall Prism Layers	0.0000882 m
Prism Layer Thickness	0.005 m
Number of Prism Layers	15

Additionally, 3D mesh properties are shown in Table 5.8.

Table 5.8 : 3D Mesh properties.

3D Volume Mesh Properties	
Cells	606838
Interior Faces	1753118
Vertices	562794

To check mesh quality, there are some parameters in STAR-CCM+, such as skewness angle and cell quality. “This skewness measure is designed to reflect whether the cells on either side of a face are formed in such a way as to permit diffusion of quantities without these quantities becoming unbounded [24]”. Skewness angles of 90° or greater than it can cause some problems during meshing due to fact that skewness angle occurs in concave cells. Therefore, skewness angles in a mesh should be less than 90° to avoid any problems. Figure 5.8 shows the skewness angles of the sails, and they are mainly less than 1°. Although skewness angles naturally increase on the sharp edges, they are around 85° and less, and this makes the mess in acceptable levels.

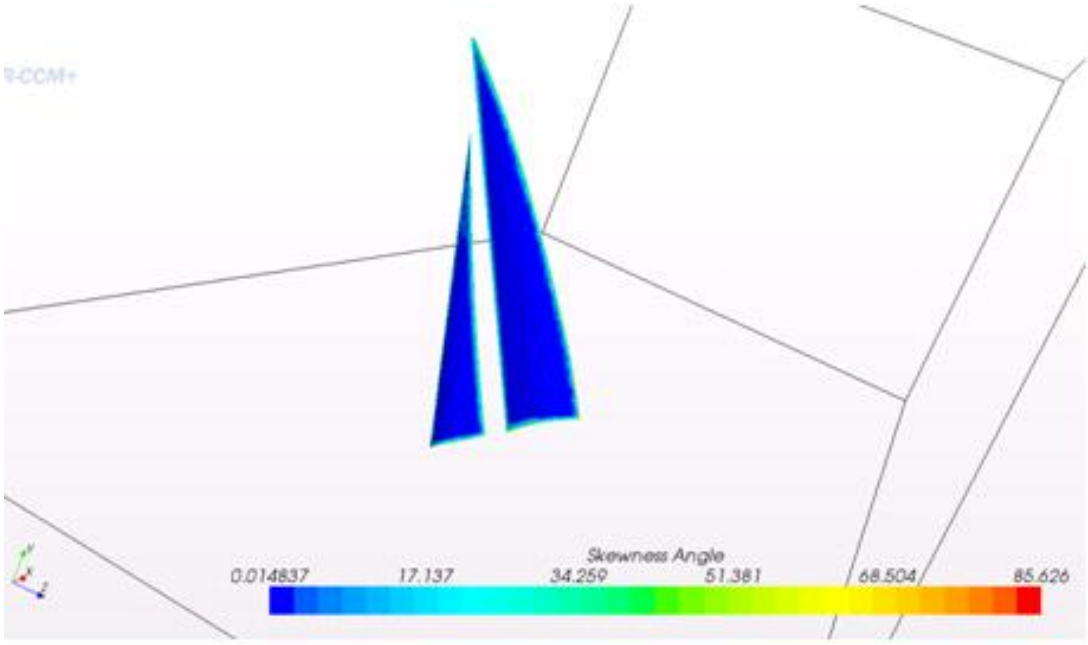

Figure 5.8 : Skewness angles for the sails.

Figure 5.9 illustrates a screen shot from the final 3D mesh.

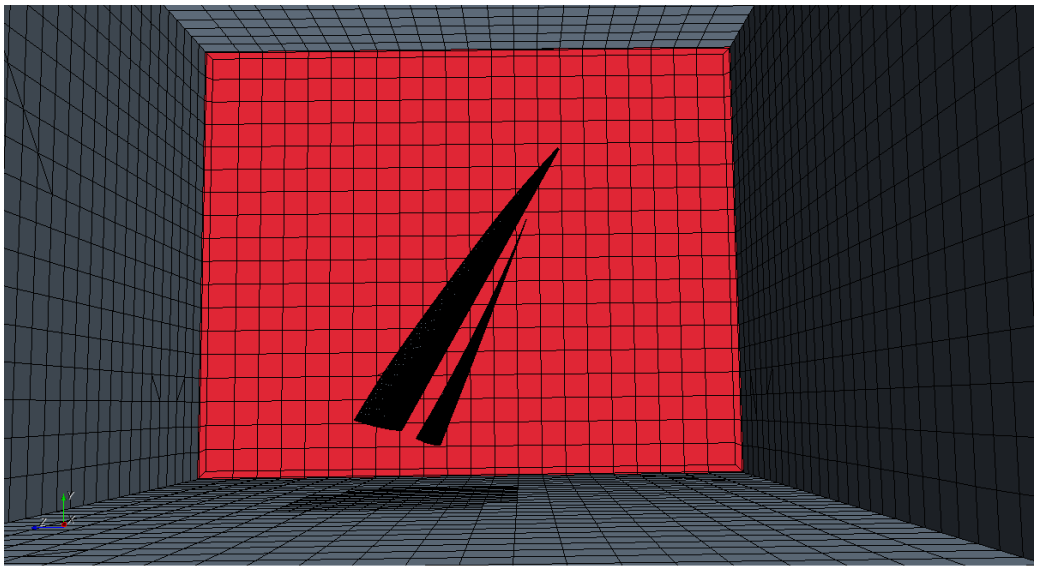

Figure 5.9 : 3D Final mesh.

5.5 Solutuion Procedure

The flow around the sails was calculated using STAR-CCM+, and its incompressible Reynolds Averaged Navier-Stokes (RANS) solver for the unstructured grids. As the unstructured grid's features were mentioned in mesh types section, additionally they are able to handle more complex and dynamic geometric shapes. The sails which were tested in wind tunnel have very complex geometries, and the flow around the sails have high Reynolds numbers which makes turbulence modelling is a must.

In the following section, some information about turbulence modelling will be mentioned.

5.5.1 Turbulence models and wall treatment

In this part, wall treatment and the turbulence models available in STAR-CCM+ will be described and their suitability for the particular problem will be assessed.

5.5.1.1 Wall treatment

One of the most important points about the wall treatment is wall distance node, which is called y^+. It equals to the distance from the wall multiplied by the ratios of frictional velocity and free stream velocity [24]. Y^+ enables the user to control over wall treatment processes.

Wall treatment models in STAR-CCM+:

Y^+ values vary for different turbulence models used in STAR-CCM+. There are three types of wall treatment [24]:

1. The high y^+ wall treatment
2. The low y^+ wall treatment is suitable only for low Reynolds number
3. The all y^+ wall treatment is a mixed one combining the low y^+ and high y^+

In these simulations, the all y^+ wall treatment was used due to its suitability to the problem.

5.5.1.2 Turbulence modelling

It is significant to select an appropriate turbulence model for the case when studying the behaviour of boundary layers. There are four major types of turbulence models in STAR-CCM+. These turbulence models namely are Spalart-Allmaras, K-Epsilon, K-Omega and Reynolds stress transport models [24].

- Spalart-Allmaras models are used when boundary layers are largely attached. It is widely used in the aerospace industry. The Spalart-Allmaras turbulence models are assumed to be less effective for RANS equations when the flow is dominated by free shear stress.
- K-Epsilon turbulence models are popularly used for complex industrial applications, and it has demonstrated excellent performance for many industrial applications. It enables the users to have a good compromise between time, accuracy and robustness. However, even though it has good performance at high Reynolds numbers, it fails to provide good estimations at low Reynolds numbers.
- In K-Omega models, two transport equations are solved similar to K-Epsilon models. But difference is the variable used to choose second transport equation. Additionally, there are some modifications in K-Omega models to eliminate low Reynolds number effects. This model is able to predict free shear stress, and is applicable to wall bounded flows and free shear flows [25]. In this project, SST (Menter) K-Omega model was selected.
- Reynolds stress transport models are the most advance and complex as well as computationally expensive models in STAR-CCM+. They are used for the situations when turbulence is strongly anisotropic [24].

5.5.2 2D Solution

5.5.2.1 Setting up the models

Models include the solution methods and the physical properties of the flow [24]. In this 2D simulation, the flow was compressible, unsteady and turbulent. SST K-Omega turbulence model was chosen and also ideal gas model was active. Figure 5.10 shows a screen shot from 2D simulation presenting which physical models were selected.

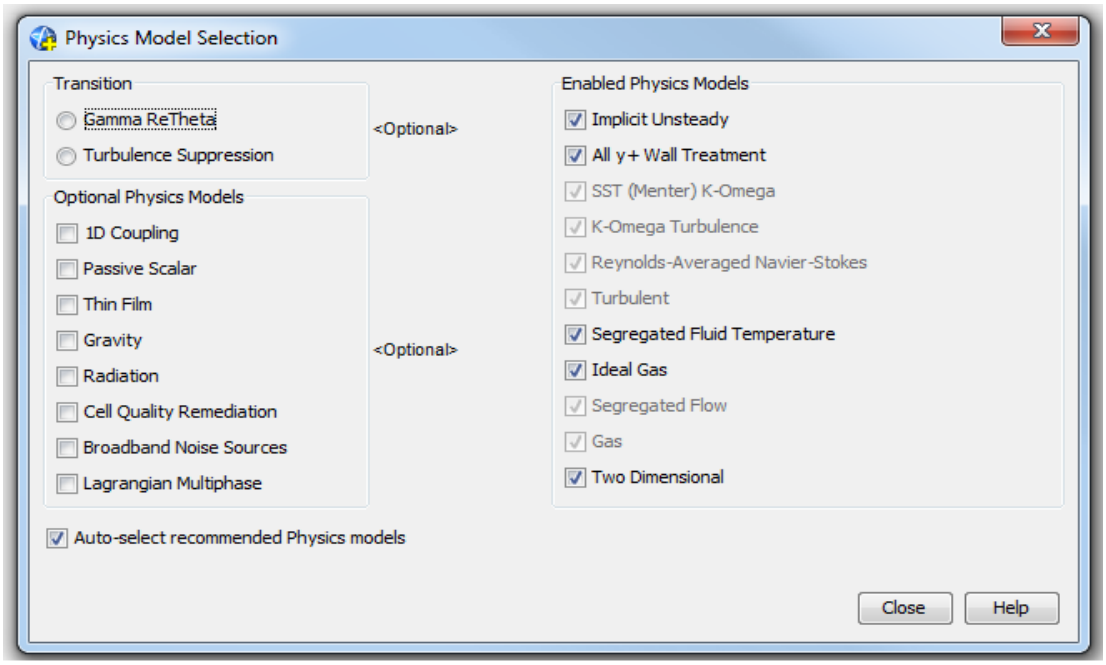

Figure 5.10 : 2D Physical model selections.

5.5.2.2 Setting initial conditions

One of the initial conditions is velocity that has to be defined before running the simulation, and 3 m/s was set up for the simulation.

- Selecting the velocity > Constant node
- In the properties window, setting the value to [3.0, 0.0, 0.0] m/s

5.5.2.3 Setting solver parameters

One of the advantages of 2D simulation is less time consuming. Due to using unsteady solver, 0.001 second time-step was calculated with values of maximum inner iterations and maximum physical time, respectively 10 numbers and 2 seconds.

These values were used to calculate total number of iterations demonstrated in equation **(5.1)**.

$$Total\ number\ of\ iterations = \frac{Max.\ inner\ iterations\ x\ Max.\ physical\ time}{Time\ step} \quad \textbf{(5.1)}$$

When this formulation was applied to those numbers, the total number of iterations was calculated 20000. This means 2D simulation was run until reaching to 20000 iterations. It must be noted that chosen appropriate time step is very significant to obtain good estimations of the turbulent flow behaviours. It therefore was selected very small time step to provide essential sensitiveness needed for the simulation.

5.5.2.4 Running the solution and visualizing the results

STAR-CCM+ enables the users to display easily any desired plot history in one platform. Figures 5.11 and 5.12 represent lift and drag coefficients convergence history from the two dimensional simulation.

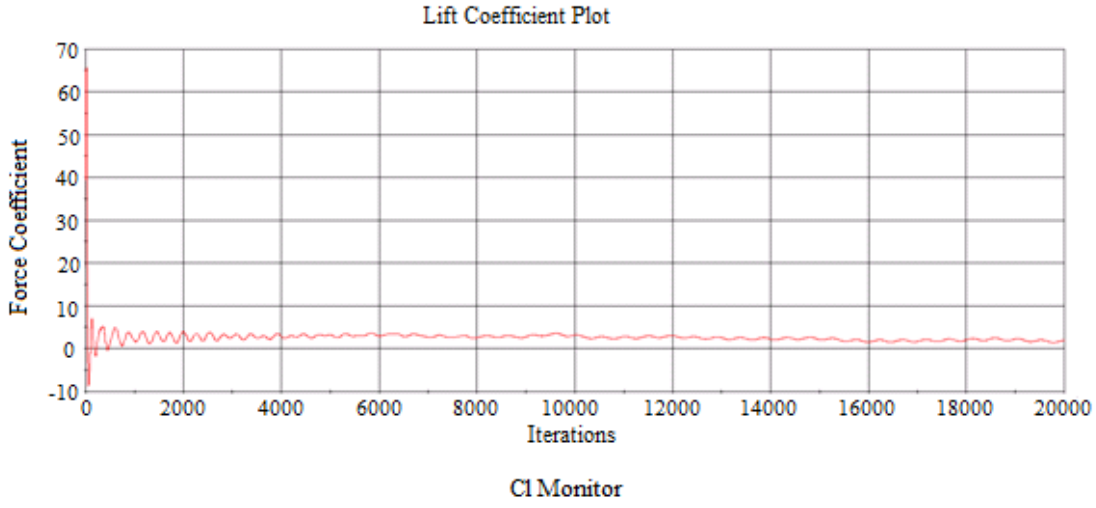

Figure 5.11 : 2D Lift coefficient convergence history.

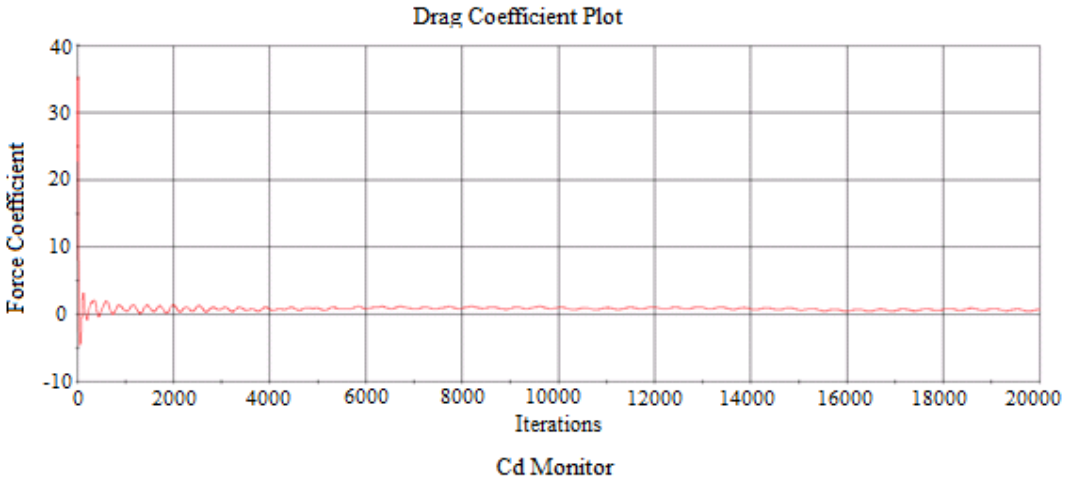

Figure 5.12 : 2D Drag coefficient convergence history.

Table 5.9 illustrates the results of the lift and drag coefficients. These values prove that selected time step was appropriate for this simulation, even though they could be better estimated by selecting lower time steps. However, doing this requires much more computational time to be spent on it.

Table 5.9 : Drag and lift coefficient investigation for 2D simulation.

Two Dimensional CFD Investigation	
Drag Coefficient (C_D)	Lift Coefficient (C_L)
0.298788	1.137874

Figures 5.13 and 5.14 show 2D velocity function and absolute total pressure function, respectively.

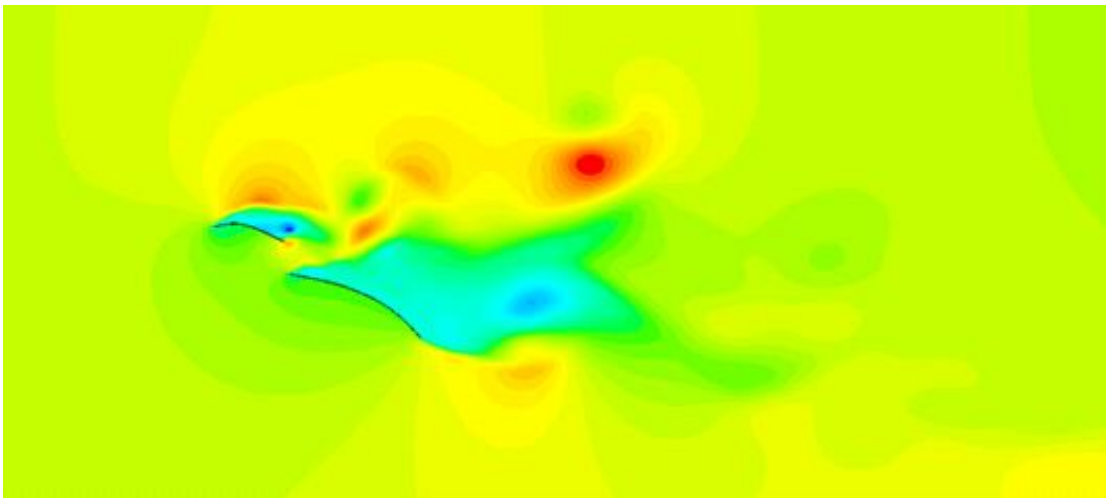

Figure 5.13 : 2D Velocity funtion.

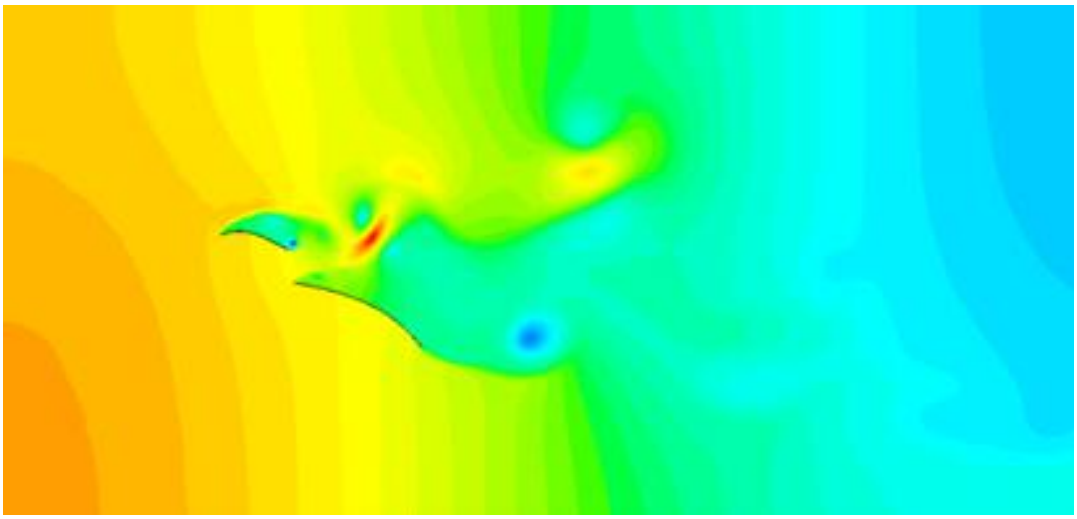

Figure 5.14 : 2D Absolute total pressure function.

5.5.3 3D Solution

5.5.3.1 Setting up the models

Models define the primary variables of the 3D simulation, including velocity, temperature and pressure. In this simulation, the flow is compressible and turbulent, and the segregated flow model will be used together with SST (Menter) K-Omega turbulence model. Table 5.10 provides detailed models selection (including physical models) for the three dimensional simulation.

Table 5.10 : Models selection for the dimensional simulation.

Flow	Segregated flow
Time	Implicit unsteady
Turbulent Model	SST (Menter) K-Omega
Fluid type	Ideal gas (Air)
Temperature	25 °C
Velocity magnitude	2.5 m/s (x-direction)
Time step	0.001s
Wall treatment	All y+ wall treatment
Reference pressure	101325 Pa

5.5.3.2 Setting solver parameter and stopping criteria

For this unsteady flow case, there is a need of setting up a time step in order to heal convergence history. The simulation will be run for 2.0 s with a time step of 0.001 s. The formulation for calculating the total number of iterations was mentioned in equation **(5.1)**.

To define the step size:

- Selecting the solvers > Implicit unsteady node
- In the properties window, changing the time step value to 0.001 s.

To specify run time:

- Selecting the stopping criteria node > Maximum physical node
- Setting the maximum physical time value to 2.0 s.

In STAR-CCM+, the number of inner iterations is 20 by default. For this study, this number is reduced to 10 due to not necessary for the case.

To change the value:

- Selecting the maximum inner iterations node
- In the properties window, changing the maximum inner iterations value to 10

As a result of these changes, the total number of iterations is calculated 20000.

Running the solution and visualizing the results:

Due to using unsteady flow, the important point is to look at which parameters are examined on the convergence issue. The aim of this is to study C_L and C_D coefficients, and Figures 5.15 and 5.16 show the convergence history for the coefficients.

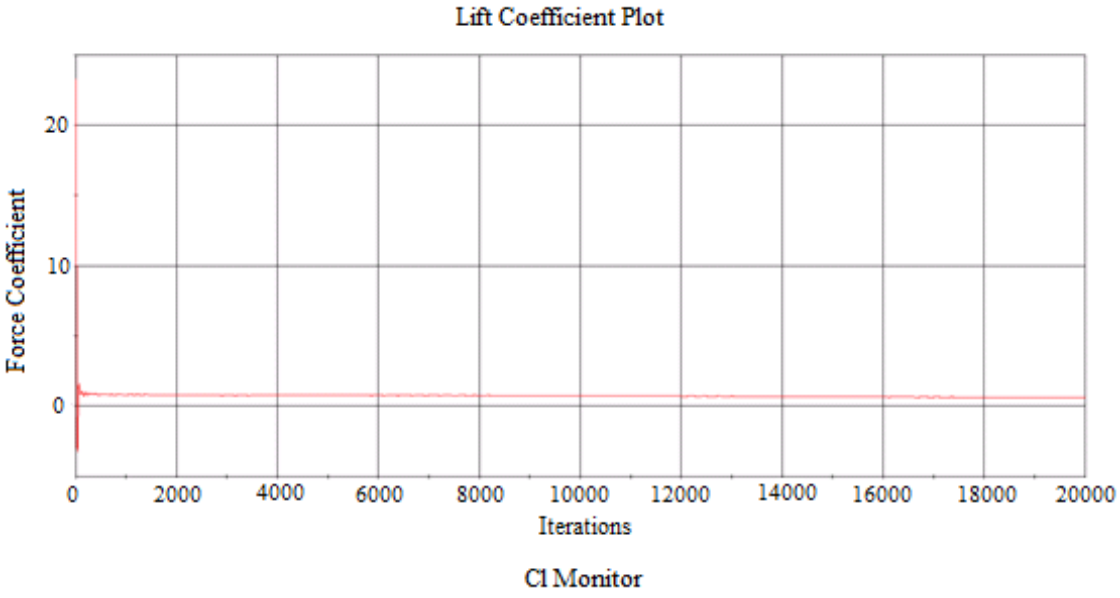

Figure 5.15 : Lift coefficient convergence history for 3D.

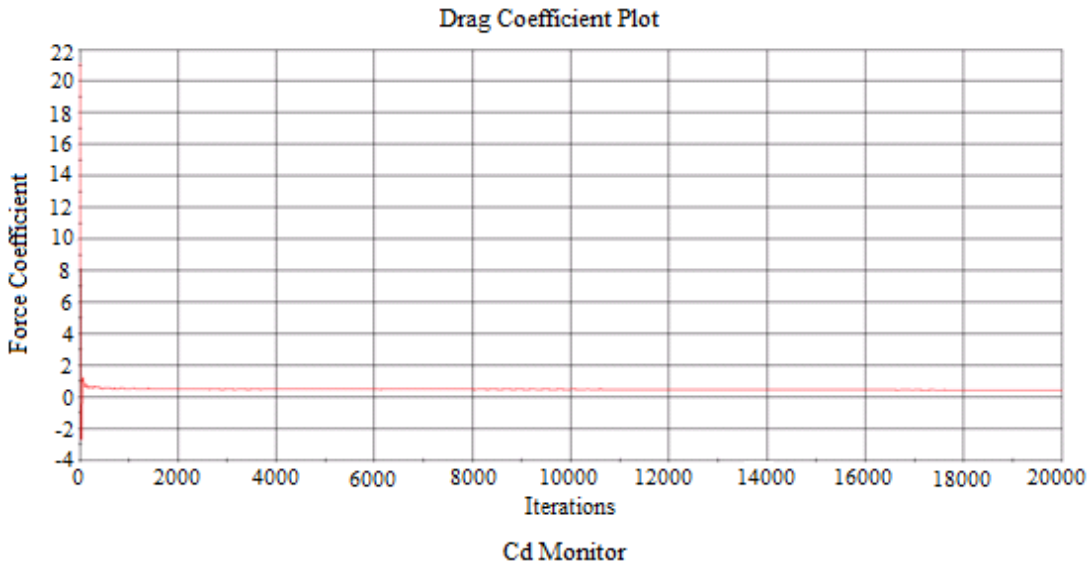

Figure 5.16 : Drag coefficient convergence history for 3D.

Table 5.11 shows the comparison of wind tunnel and CFD data. Twist case 1 is used for this comparison. In twist case 1 consists of 7° for main twist and 9° for jib twist. In addition to twist degrees, 4° for main sheeting and 10° for jib sheeting. AWA is 28° and heeling angle is 30° (fixed value for all cases).

Table 5.11 : 3D Comparison of C_D and C_L.

	CFD		Wind Tunnel		Error (%)	
	C_D	C_L	C_D	C_L	C_D	C_L
3D	0.21856	1.00061	0.2375	1.0665	7.97	6.18
2D	0.29879	1.13787				

The heeled model is compared with the wind tunnel results. There is no correction needed due to same wind tunnel conditions were simulated in the CFD. Lift and drag coefficients are compared to achieve to the aim of the project. SST K-Omega showed a good performance for the simulation provided by STAR-CCM+. The results are not perfectly similar due to fact that there are many different factors which have to be taken into account. The study with 6/8 % errors has showed that is not perfect solution and it could be better. However, as being one part of this study, it is acceptable in limits.

To success better solution, there are some ways of the solution troubleshooting:

- Checking initial or boundary conditions which might be incorrect
- Usually problems due to poor mesh quality

- Wrong numerical scheme
- Using inappropriate turbulence model
- Re-checking wall model
- Using wrong Reynolds numbers
- Scale effects

Due to time limitation, it could not be re-simulated under these troubleshooting ways. To visualize the CFD results, these pictures shown in Figures 5.17 and 5.18 are taken from STAR-CCM+. Figure 5.17 demonstrates pressure effects on the main and jib sails.

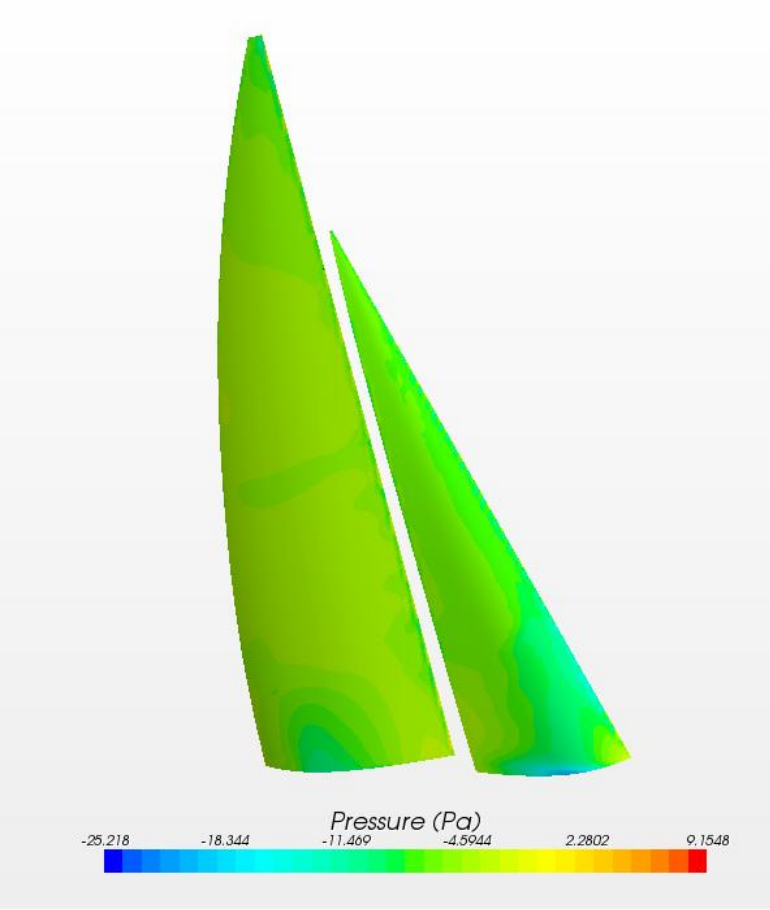

Figure 5.17 : Pressure function for the three dimensional simulation.

Figure 5.18 shows the flow behaviours, and drawing streamlines is very effective way to visualize the flow pattern.

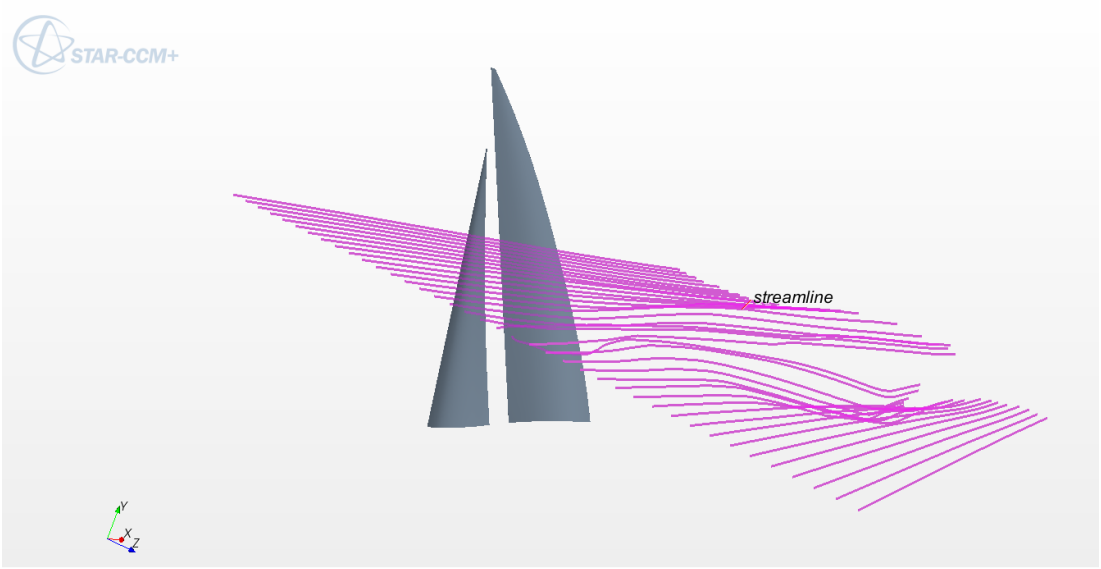

Figure 5.18 : Streamlines for both main and jib sails.

6. CONCLUSION

The aim of the project which is to carry out wind tunnel testing using a set of flying sails and validation of CFD calculations has been conducted. A number of changing twist and sheeting configurations were tested in the wind tunnel, and it has showed that the sails having too much twist and sheeting cause of a reduction in the performance of the sails. It also must be pointed out that 28° apparent wind angle compared to 20° has a better performance in terms of lift and drag forces. In this study, only one heel angle (30°) was tested, and it could be possible to test different heel angles and study their effects on the performance of the upwind sailing conditions unless there were some constraints of the project time. In addition to these, it has been observed in the wind tunnel throughout the experiments and checked by analysis results so that 7 m/s wind speed was too strong for those tested sail configurations. 3 m/s wind speed was therefore chosen for CFD simulations.

A lot of time was spent on learning how to simulate desired models in the STAR-CCM+ software, and also on studying backgrounds of the sail aerodynamics and CFD. Due to this, the limitation of the project time was considerably a significant parameter for more correct CFD simulations to be carried out; most probably less than 8% error could be succeeded. Additionally, there is a need of much developed 3D model creating method. The first high resolution camera was perfectly placed to capture sail trim details; however because of lack of wide angle lens, another wide angle lens camera with low resolution had to be used. Pictures with high quality and appropriate angle will enable the designers to create much more accurate geometries, and then CFD calculations will be closer to real flow behaviours. Even though CFD calculations need to be validated, they have proved that CFD is able to estimate the forces developed by the sails. Furthermore, CFD enables the users to visualize the flow behaviours around the sails, although it is very difficult to demonstrate visually the flow behaviours in the wind tunnel. To perform this in the wind tunnel, it should be attached some sensors on the sail surfaces, and thus a new problem will arise by doing this due to fluid-structure interactions.

REFERENCES

[1] **Claughton, A. R., Wellicome, J. F., and Shenoi, R. A.** (2006). Sailing Yacht Design: Theory. *University of Southampton Press*, United Kingdom.

[2] **Larsson, L., and Eliasson, R. E.** (2000). Principles of Yacht Design. *Adlard Coles Nautical*, London, United Kingdom.

[3] **Gilbert, L.** (2011). In *One Metre Radio Sailing*.

Url-1 <*http://www.onemetre.net*>, date retrieved 10.03.2011.

[4] **Acree, D.** (2005). *Model Yachting Resource News*.

Url-1 <*http://www.myrc.org*>, date retrieved 20.03.2011.

[5] **Gentry, A.** (1973). Another Look at Slot Effect: *Sail Magazine*. United States.

[6] **Marchaj, C. A.** (2003). *Sail Performance: Techniques to Maximize Sail Power (revised edition)*. International Marine and McGraw Hill, London, UK.

[7] **WB-Sails Ltd.** (1998). *Note on the Effect of Side Bend.* Finland.

Url-1 <*http://www.wb-sails.fi*>, date retrieved 11.04.2011.

[8] **Blake, J. I. R.** (2010). *High Performance Craft: Lecture Notes*. University of Southampton, Southampton, UK.

[9] **Campbell, I.** (2010). *Yacht Experimental Techniques: Lecture notes*. University of Southampton, Southampton, UK.

[10] **Kay, H. F.** (1971). *The Science of Yachts: Wind and Water*. John de Graff Inc., New York, USA.

[11] **Spens, P. G.** (1960). *Sailboat Test Technique together with Note on 'Preliminary Estimation of Sail Coefficients from Yeoman Sailing Trials'*: Note no 509: Stevens Institute of Technology, USA.

[12] **Gentry, A.** (1971). The aerodynamics of Sail Interaction: *Proceedings of the Third AIAA Symposium on the Aero/Hydronautics of Sailing*, USA.

[13] **Bar-Meir, G.** (2011). *Basic of Fluid Mechanics version 0.3.0.4*. Chicago, USA.

[14] **Batchelor, G.K.** (1967). An Introduction to Fluid Dynamics. *Cambridge University Press*, **ISBN 0-521-09817-3**, UK.

[15] **Desktop Aeronautics Inc.** (2007). *Applied Aerodynamics: A Digital Textbook version 5.0*: Stanford, CA, USA. Date retrieved 15.04.2011, adress: http://www.desktop.aero/appliedaero/preface/welcome.html

[16] **Anderson, J. D.** (2005). Ludwig Prandtl's Boundary Layer. *American Institute of Physics*, **S-0031-9228-0512-020-1**, USA.

[17] **Clancy, L. J.** (1975). Aerodynamics. *Pitman Publishing*, **ISBN0273011200**, London, United Kingdom.

[18] **Recktenwald, G.** (2002). Conservation of Mass, Momentum, and Energy: *Lecture Notes*. Portland State University, USA.

[19] **Tro, N. J.** (2008). *Chemistry: A Molecular Approach*. Upper Saddle River N.J. Pearson/Prentice Hall, **ISBN9780131000650**, USA.

[20] **Barlow, J. B., Rae, W. H. and Pope, A.** (1999). *Low Speed Wind Tunnel Testing: Third edition*. John Wiley and Sons, USA.

[21] **Doyle, T., Gerritsen, M. and Iaccarino, G**. (2002). Towards Sail-Shape Optimization of a Modern Clipper Ship. *Centre for Turbulence Research Annual Research Briefs*, USA.

[22] **Reuther, J., Jameson, A., Farmer, J., Martinelli, L. and Saunders, D.** (1996). *Aerodynamic Shape Optimization of complex aircraft configurations via an ad-joint formulation.* AIAA Paper 96-0094.

[23] **Orszag, S. A.** (1970). Analytical Theories of Turbulence. *Journal of Fluid Mechanics 41*, **363–386**, USA.

[24] **CD-Adapco, Inc.** (2010). *STAR-CCM+ User Guide Version 5.04.006*.

[25] **Xie, Z.** (2010). Applications of CFD: *Lecture notes*. University of Southampton, Southampton, UK.

[26] **UK Sailmakers,** (2003). *AccuMeasure: Quick Start Manual*.

Url-1 <*http://www.ukhalsey.com*>, date retrieved 10.05.2011.

[27] **Diequez, G. R.** (2008). *Measurements Using a Heeled Yacht Fitting in the Low Speed Section of the 7 by 5 Wind Tunnel and CFD Comparison.* University of Southampton, Southampton, UK.

APPENDICES

APPENDIX A.1 : Gantt chart

APPENDIX A.2 : Raw and corrected wind tunnel data for 20° and 28° AWA

APPENDIX A.3 : Geometric coordinates of main and jib sails

APPENDIX A.1

Table A.1 : Gantt chart.

GANTT CHART	February	March	April	May	June	July	August	September
Research for background of aerodynamics								
Creating 2D and 3D sail geometries								
Understanding study of CFD - Meshing								
Understanding study of CFD - Solver set up								
Submitting interim report								
Understanding study of CFD - Obtaining results								
Wind tunnel tests and raw data collection								
Oral presentation								
Creating final 2D and 3D sail geometries								
Meshing for 2D and 3D sail geometries								
Solver set up for 2D and 3D sail geometries								
Writing report								
Submitting report								

APPENDIX A.2

Table A.2.1: Raw and corrected wind tunnel data for 20° AWA.

AWA 20	ZERO-ACQUIRED DATA				RAW WIND TUNNEL DATA				CORRECTED RAW DATA					VELOCITY
Run No	DF0 [N]	HF0 [N]	HM0 [Nm]	YM0 [Nm]	DF [N]	HF [N]	HM [Nm]	YM [Nm]	DFcorr.	HFcorr.	DF/HF	HMcorr.	YMcorr.	V (m/s)
131	1.35694	0.60456	-3.88283	3.04132	2.12825	5.29600	-0.01917	3.23616	0.77131	4.69144	0.16441	3.86366	0.19484	3
132	1.35694	0.60456	-3.88283	3.04132	2.00895	9.39509	1.84011	3.58906	0.65201	8.79053	0.07417	5.72294	0.54774	5
133	1.35694	0.60456	-3.88283	3.04132	0.62870	10.92935	0.75352	3.44626	-0.72824	10.32479	-0.07053	4.63635	0.40494	7
136	1.4007	-0.78132	-3.62251	1.55008	1.91005	3.13908	-0.371	1.50808	0.50935	3.92040	0.12992	3.25151	-0.04200	3
137	1.4007	-0.78132	-3.62251	1.55008	1.42437	5.71443	0.17797	1.51937	0.02367	6.49575	0.00364	3.80048	-0.03071	5
138	1.4007	-0.78132	-3.62251	1.55008	0.57482	9.01446	0.93611	1.91509	-0.82588	9.79578	-0.08431	4.55862	0.36501	7
140	1.26814	-1.65405	-3.39665	0.79075	1.67772	2.0023	-0.45485	0.7065	0.40958	3.65635	0.11202	2.94180	-0.08425	3
141	1.26814	-1.65405	-3.39665	0.79075	1.25726	4.74703	0.22454	0.90067	-0.01088	6.40108	-0.00170	3.62119	0.10992	5
142	1.26814	-1.65405	-3.39665	0.79075	0.45757	8.32278	1.06783	1.41095	-0.81057	9.97683	-0.08125	4.46448	0.62020	7
148	1.25371	-2.62493	-3.09282	-0.17347	1.97775	1.28668	-0.39508	0.08944	0.72404	3.91161	0.18510	2.69774	0.26291	3
149	1.25371	-2.62493	-3.09282	-0.17347	1.23256	3.26457	-0.80106	0.30303	-0.02115	5.88950	-0.00359	2.29176	0.47650	5
150	1.25371	-2.62493	-3.09282	-0.17347	0.51628	6.41522	0.51189	0.74853	-0.73743	9.04015	-0.08157	3.60471	0.92200	7
152	1.47531	-3.05237	-3.12919	-0.65854	1.83625	0.30844	-0.63492	-0.51435	0.36094	3.36081	0.10740	2.49427	0.14419	3
153	1.47531	-3.05237	-3.12919	-0.65854	1.19899	2.27918	-0.85512	-0.23157	-0.27632	5.33155	-0.05183	2.27407	0.42697	5
154	1.47531	-3.05237	-3.12919	-0.65854	0.24592	5.29111	0.21573	0.13771	-1.22939	8.34348	-0.14735	3.34492	0.79625	7
156	1.43759	-3.35651	-3.02395	-1.09041	1.72071	-0.32454	-0.80987	-1.02143	0.28312	3.03197	0.09338	2.21408	0.06898	3
157	1.43759	-3.35651	-3.02395	-1.09041	1.10876	1.58107	-0.83443	-0.68141	-0.32883	4.93758	-0.06660	2.18952	0.40900	5
158	1.43759	-3.35651	-3.02395	-1.09041	0.21264	4.99556	0.37662	-0.21617	-1.22495	8.35207	-0.14666	3.40057	0.87424	7
164	1.49774	-4.0472	-2.85162	-1.65035	1.55926	-1.4831	-1.32272	-1.24075	0.06152	2.56410	0.02399	1.52890	0.40960	3
165	1.49774	-4.0472	-2.85162	-1.65035	0.85599	0.32368	-1.29404	-0.71261	-0.64175	4.37088	-0.14682	1.55758	0.93774	5
166	1.49774	-4.0472	-2.85162	-1.65035	-0.23278	2.27961	-0.52979	-0.21843	-1.73052	6.32681	-0.27352	2.32183	1.43192	7
168	1.47644	-4.31936	-2.79198	-1.95231	1.4469	-2.04709	-1.45901	-1.67592	-0.02954	2.27227	-0.01300	1.33297	0.27639	3
169	1.47644	-4.31936	-2.79198	-1.95231	0.60159	-0.94734	-2.02524	-1.26161	-0.87485	3.37202	-0.25944	0.76674	0.69070	5
170	1.47644	-4.31936	-2.79198	-1.95231	-0.33839	1.65747	-0.57072	-0.78398	-1.81483	5.97683	-0.30364	2.22126	1.16833	7

Table A.2.1 (continued): Raw and corrected wind tunnel data for 20° AWA.

AWA 20	BODY AXIS						WIND TUNNEL CORRECTIONS								VELOCITY
Run No	LIFT [N]	Cl	DRAG [N]	Cd	L/D	D/L²	Cd	β'	Cdi	Cds	BLOCKAGE	Cl	Cl²	Cd	V (m/s)
131	4.04634	0.62064	-0.879772666	0.13494	-4.59931	-0.05373	0.1377385	20.0045	0.0362471	0.1014914	1.020458984	**0.6082014**	0.3699089	**0.134977**	3
132	7.34684	0.40568	-2.393849345	0.13218	-3.06905	-0.04435	0.1333785	20.0029	0.0154865	0.117892	1.023765071	**0.3962624**	0.1570239	**0.1302824**	5
133	8.18659	0.23064	-4.21560791	0.11876	-1.94197	-0.06290	0.1191506	20.0017	0.0050055	0.1141451	1.023009753	**0.225450**	0.0508276	**0.1164706**	7
136	3.34128	0.51250	-0.862223333	0.13225	-3.87519	-0.07723	0.1341574	20.0037	0.0247157	0.1094417	1.022061622	**0.5014367**	0.2514388	**0.1312616**	3
137	5.29324	0.29228	-2.199434822	0.12145	-2.40664	-0.07850	0.1220689	20.0021	0.0080389	0.1140301	1.022986562	**0.2857157**	0.0816335	**0.119326**	5
138	7.72716	0.21769	-4.126427421	0.11625	-1.87260	-0.06911	0.116596	20.0016	0.0044594	0.1121366	1.022604871	**0.2128818**	0.0453187	**0.1140186**	7
140	3.09685	0.47501	-0.865666047	0.13278	-3.57741	-0.09026	0.1344168	20.0034	0.0212318	0.113185	1.022816211	**0.4644107**	0.2156773	**0.1314183**	3
141	5.20596	0.28746	-2.199522155	0.12145	-2.36686	-0.08116	0.1220535	20.0021	0.007776	0.1142775	1.023036444	**0.2809911**	0.078956	**0.1193051**	5
142	7.87903	0.22197	-4.173963474	0.11759	-1.88766	-0.06724	0.1179489	20.0016	0.0046365	0.1133124	1.022841902	**0.2170156**	0.0470958	**0.1153149**	7
148	3.39772	0.52116	-0.657474368	0.10085	-5.16783	-0.05695	0.1028171	20.0038	0.0255577	0.0772594	1.015574208	**0.5131637**	0.263337	**0.101240**	3
149	4.78660	0.26431	-2.034202133	0.11233	-2.35306	-0.08879	0.1128321	20.0019	0.0065736	0.1062584	1.02141993	**0.2587648**	0.0669592	**0.1104659**	5
150	7.13843	0.20111	-3.784870928	0.10663	-1.88604	-0.07428	0.1069231	20.0015	0.0038058	0.1031173	1.020786731	**0.1970127**	0.038814	**0.1047458**	7
152	2.84193	0.43591	-0.810292063	0.12429	-3.50729	-0.10033	0.1256648	20.0032	0.0178803	0.1077846	1.021727574	**0.4266368**	0.182019	**0.1229925**	3
153	4.25696	0.23506	-2.08315336	0.11503	-2.04352	-0.11495	0.1154291	20.0017	0.0051994	0.1102297	1.022220475	**0.2299521**	0.052878	**0.1129199**	5
154	6.42576	0.18103	-4.008886937	0.11294	-1.60288	-0.09709	0.1131785	20.0013	0.0030838	0.1100947	1.022193259	**0.177100**	0.0313644	**0.1107213**	7
156	2.55127	0.39132	-0.770949039	0.11825	-3.30926	-0.11844	0.1193626	20.0028	0.0144099	0.1049527	1.021156721	**0.3832165**	0.1468549	**0.1168896**	3
157	3.92079	0.21650	-1.997750944	0.11031	-1.96260	-0.12996	0.1106525	20.0016	0.0044106	0.1062419	1.021416591	**0.211960**	0.044927	**0.1083324**	5
158	6.43407	0.18126	-4.007652654	0.11291	-1.60545	-0.09681	0.1131444	20.0013	0.0030918	0.1100526	1.022184765	**0.177330**	0.031446	**0.1106888**	7
164	2.10488	0.32286	-0.819163959	0.12565	-2.56955	-0.18489	0.1264031	20.0023	0.0098085	0.1165946	1.023503538	**0.3154412**	0.0995031	**0.12350**	3
165	3.36693	0.18592	-2.097976743	0.11585	-1.60484	-0.18507	0.1160975	20.0013	0.0032525	0.1128449	1.022747663	**0.1817808**	0.0330442	**0.1135153**	5
166	4.63617	0.13061	-3.790053337	0.10678	-1.22325	-0.17633	0.1068994	20.0009	0.0016053	0.1052941	1.021225535	**0.1278981**	0.0163579	**0.1046776**	7
168	1.84042	0.28229	-0.804920631	0.12346	-2.28646	-0.23764	0.1240403	20.0020	0.0074986	0.1165417	1.023492864	**0.2758112**	0.0760718	**0.1211931**	3
169	2.48501	0.13722	-1.975388853	0.10908	-1.25799	-0.31989	0.1092142	20.0010	0.0017718	0.1074424	1.021658599	**0.1343092**	0.0180389	**0.1068989**	5
170	4.32638	0.12189	-3.749578612	0.10564	-1.15383	-0.20032	0.1057431	20.0009	0.0013979	0.1043452	1.021034251	**0.1193744**	0.0142502	**0.1035647**	7

Table A.2.1 (continued): Raw and corrected wind tunnel data for 20° AWA.

AWA 20	ZERO-ACQUIRED DATA				RAW WIND TUNNEL DATA				CORRECTED RAW DATA					VELOCITY
Run No	DF0 [N]	HF0 [N]	HM0 [Nm]	YM0 [Nm]	DF [N]	HF [N]	HM [Nm]	YM [Nm]	DFcorr.	HFcorr.	DF/HF	HMcorr.	YMcorr.	V (m/s)
172	1.4195	-4.60407	-2.73345	-2.24659	1.23461	-2.95313	-1.79649	-2.17325	-0.18489	1.65094	-0.11199	0.93696	0.07334	3
173	1.4195	-4.60407	-2.73345	-2.24659	0.53328	-1.46501	-1.75475	-1.67231	-0.88622	3.13906	-0.28232	0.97870	0.57428	5
174	1.4195	-4.60407	-2.73345	-2.24659	-0.32706	0.88074	-0.1896	-1.37098	-1.74656	5.48481	-0.31844	2.54385	0.87561	7
196	0.18767	2.72742	-4.12112	4.25921	0.87863	7.20656	-0.70236	4.57435	0.69096	4.47914	0.15426	3.41876	0.31514	3
197	0.18767	2.72742	-4.12112	4.25921	0.47531	10.88386	0.07768	5.23285	0.28764	8.15644	0.03527	4.19880	0.97364	5
198	0.18767	2.72742	-4.12112	4.25921	-0.71853	13.22493	-0.58763	5.75702	-0.90620	10.49751	-0.08633	3.53349	1.49781	7
200	0.39898	2.57325	-4.10861	4.26411	0.97056	6.6599	-1.02346	4.43528	0.57158	4.08665	0.13987	3.08515	0.17117	3
201	0.39898	2.57325	-4.10861	4.26411	0.38248	9.3756	-1.03262	4.78376	-0.01650	6.80235	-0.00243	3.07599	0.51965	5
202	0.39898	2.57325	-4.10861	4.26411	-0.34468	12.95619	0.15949	5.41678	-0.74366	10.38294	-0.07162	4.26810	1.15267	7
204	0.3682	2.38026	-4.05924	4.08878	0.77867	6.06608	-1.28303	4.09844	0.41047	3.68582	0.11136	2.77621	0.00966	3
205	0.3682	2.38026	-4.05924	4.08878	0.2385	8.55279	-1.24952	4.42424	-0.12970	6.17253	-0.02101	2.80972	0.33546	5
206	0.3682	2.38026	-4.05924	4.08878	-0.64141	12.36881	-0.12725	5.09002	-1.00961	9.98855	-0.10108	3.93199	1.00124	7
212	0.40216	2.0848	-4.01069	3.81477	0.96918	6.19331	-1.00703	4.17857	0.56702	4.10851	0.13801	3.00366	0.36380	3
213	0.40216	2.0848	-4.01069	3.81477	0.40957	9.34037	-0.67113	4.84049	0.00741	7.25557	0.00102	3.33956	1.02572	5
214	0.40216	2.0848	-4.01069	3.81477	-0.84134	11.6734	-1.2419	5.30787	-1.24350	9.58860	-0.12969	2.76879	1.49310	7
216	0.39947	1.97594	-3.97348	3.69136	0.84093	5.62966	-1.29896	3.85865	0.44146	3.65372	0.12082	2.67452	0.16729	3
217	0.39947	1.97594	-3.97348	3.69136	0.17419	7.94119	-1.63665	4.26242	-0.22528	5.96525	-0.03777	2.33683	0.57106	5
218	0.39947	1.97594	-3.97348	3.69136	-0.77056	11.40057	-0.4563	4.82834	-1.17003	9.42463	-0.12415	3.51718	1.13698	7
220	0.44911	1.83336	-3.9638	3.60184	0.70591	4.88115	-1.75672	3.51626	0.25680	3.04779	0.08426	2.20708	-0.08558	3
221	0.44911	1.83336	-3.9638	3.60184	0.09478	7.09804	-1.90542	3.95121	-0.35433	5.26468	-0.06730	2.05838	0.34937	5
222	0.44911	1.83336	-3.9638	3.60184	-0.96315	10.77152	-0.66251	4.57242	-1.41226	8.93816	-0.15800	3.30129	0.97058	7
228	0.55274	1.56195	-3.92386	3.42225	0.83189	4.74056	-1.74373	3.6777	0.27915	3.17861	0.08782	2.18013	0.25545	3
229	0.55274	1.56195	-3.92386	3.42225	-0.0765	6.34339	-2.72369	4.13808	-0.62924	4.78144	-0.13160	1.20017	0.71583	5
230	0.55274	1.56195	-3.92386	3.42225	-0.96339	9.58706	-1.03439	4.77478	-1.51613	8.02511	-0.18892	2.88947	1.35253	7
232	0.58857	1.44211	-3.8943	3.32195	0.75511	4.31547	-1.93956	3.45651	0.16654	2.87336	0.05796	1.95474	0.13456	3
233	0.58857	1.44211	-3.8943	3.32195	-0.01168	5.91385	-2.69179	3.91685	-0.60025	4.47174	-0.13423	1.20251	0.59490	5
234	0.58857	1.44211	-3.8943	3.32195	-1.1812	9.13972	-1.25918	4.53922	-1.76977	7.69761	-0.22991	2.63512	1.21727	7
236	0.53623	1.34307	-3.88127	3.13582	0.45277	3.39478	-2.73848	3.09426	-0.08346	2.05171	-0.04068	1.14279	-0.04156	3

Table A.2.1 (continued): Raw and corrected wind tunnel data for 20° AWA.

AWA 20	BODY AXIS						WIND TUNNEL CORRECTIONS								VELOCITY
Run No	LIFT [N]	Cl	DRAG [N]	Cd	L/D	D/L²	Cd	β'	Cdi	Cds	BLOCKAGE	Cl	Cl²	Cd	V (m/s)
172	1.28877	0.19768	-0.738394504	0.11326	-1.74536	-0.44457	0.1135415	20.0014	0.003677	0.1098645	1.022146854	**0.1933933**	0.037401	**0.1110814**	3
173	2.29206	0.12656	-1.906396146	0.10527	-1.20230	-0.36288	0.1053841	20.0009	0.0015073	0.1038768	1.020939835	**0.1239679**	0.015368	**0.1032227**	5
174	3.94620	0.11117	-3.517145046	0.09909	-1.12199	-0.22586	0.0991767	20.0008	0.001163	0.0980137	1.019757931	**0.1090206**	0.0118855	**0.0972552**	7
196	3.84977	0.59049	-0.882666092	0.13539	-4.36153	-0.05956	0.1379173	20.0043	0.0328109	0.1051064	1.021187704	**0.5782424**	0.3343643	**0.1350558**	3
197	6.72289	0.37123	-2.519373592	0.13912	-2.66848	-0.05574	0.1401155	20.0027	0.0129677	0.1271478	1.025630873	**0.3619492**	0.1310072	**0.136614**	5
198	8.27443	0.23311	-4.441909328	0.12514	-1.86281	-0.06488	0.1255344	20.0017	0.0051135	0.1204209	1.024274855	**0.2275875**	0.0517961	**0.1225593**	7
200	3.49501	0.53608	-0.860607111	0.13200	-4.06109	-0.07045	0.1340889	20.0039	0.0270423	0.1070466	1.021578821	**0.5247548**	0.2753676	**0.1312566**	3
201	5.53085	0.30540	-2.34204565	0.12932	-2.36155	-0.07656	0.1300006	20.0022	0.0087768	0.1212238	1.024436693	**0.2981188**	0.0888748	**0.126900**	5
202	8.22934	0.23184	-4.249986441	0.11973	-1.93632	-0.06276	0.1201232	20.0017	0.0050579	0.1150653	1.023195241	**0.2265861**	0.0513413	**0.117400**	7
204	3.12109	0.47873	-0.874909055	0.13420	-3.56733	-0.08982	0.1358602	20.0035	0.0215655	0.1142947	1.023039909	**0.4679444**	0.2189719	**0.1328005**	3
205	4.98477	0.27525	-2.233007728	0.12330	-2.23231	-0.08987	0.1238526	20.0020	0.0071292	0.1167234	1.02352949	**0.2689229**	0.0723195	**0.1210054**	5
206	7.82961	0.22058	-4.365008369	0.12297	-1.79372	-0.07120	0.1233266	20.0016	0.0045785	0.1187482	1.023937656	**0.2154237**	0.0464074	**0.1204435**	7
212	3.51145	0.53860	-0.872368669	0.13381	-4.02519	-0.07075	0.1359126	20.0039	0.0272973	0.1086153	1.021895047	**0.5270598**	0.2777921	**0.1330006**	3
213	5.90676	0.32616	-2.474587969	0.13664	-2.38697	-0.07093	0.1374144	20.0024	0.0100104	0.1274041	1.025682538	**0.3179942**	0.1011203	**0.1339737**	5
214	7.43486	0.20946	-4.44800212	0.12531	-1.67151	-0.08047	0.1256301	20.0015	0.0041284	0.1215017	1.024492712	**0.2044516**	0.0418004	**0.1226266**	7
216	3.10415	0.47613	-0.834809134	0.12805	-3.71839	-0.08664	0.1296915	20.0035	0.021332	0.1083595	1.021843475	**0.4659489**	0.2171084	**0.1269192**	3
217	4.78778	0.26437	-2.251929614	0.12435	-2.12608	-0.09824	0.1248548	20.0019	0.0065769	0.118278	1.023842868	**0.2582162**	0.0666756	**0.1219473**	5
218	7.32318	0.20631	-4.32288186	0.12179	-1.69405	-0.08061	0.1220956	20.0015	0.0040053	0.1180903	1.023805038	**0.2015158**	0.0406086	**0.1192567**	7
220	2.55635	0.39210	-0.801092508	0.12287	-3.19108	-0.12259	0.1239905	20.0028	0.0144673	0.1095232	1.022078065	**0.3836332**	0.1471744	**0.1213122**	3
221	4.17943	0.23078	-2.133587894	0.11781	-1.95888	-0.12215	0.1181995	20.0017	0.0050117	0.1131878	1.022816776	**0.2256328**	0.0509101	**0.1155627**	5
222	6.85555	0.19314	-4.384121065	0.12351	-1.56372	-0.09328	0.1237827	20.0014	0.0035101	0.1202726	1.02424495	**0.1885666**	0.0355574	**0.1208526**	7
228	2.66943	0.40945	-0.824833453	0.12652	-3.23633	-0.11575	0.1277329	20.0030	0.0157755	0.1119574	1.022568745	**0.4004111**	0.160329	**0.1249138**	3
229	3.70475	0.20457	-2.226640979	0.12295	-1.66383	-0.16223	0.1232549	20.0015	0.0039379	0.119317	1.024052321	**0.1997648**	0.039906	**0.12036**	5
230	6.08174	0.17134	-4.169445446	0.11746	-1.45865	-0.11273	0.1176771	20.0012	0.0027625	0.1149146	1.023164876	**0.1674592**	0.0280426	**0.1150128**	7
232	2.38766	0.36623	-0.82625059	0.12673	-2.88976	-0.14493	0.127707	20.0027	0.012621	0.115086	1.023199427	**0.3579257**	0.1281108	**0.1248114**	3
233	3.46130	0.19113	-2.093475651	0.11560	-1.65337	-0.17474	0.1158632	20.0014	0.0034374	0.1124258	1.022663165	**0.1868913**	0.0349284	**0.1132955**	5
234	5.74009	0.16171	-4.295777485	0.12102	-1.33622	-0.13038	0.1212129	20.0012	0.0024608	0.1187521	1.023938449	**0.1579326**	0.0249427	**0.1183791**	7
236	1.64496	0.25231	-0.780152894	0.11966	-2.10850	-0.28832	0.120125	20.0018	0.0059904	0.1141346	1.023007635	**0.2466355**	0.0608291	**0.1174234**	3

Table A.2.1 (continued): Raw and corrected wind tunnel data for 20° AWA.

AWA 20	ZERO-ACQUIRED DATA				RAW WIND TUNNEL DATA				CORRECTED RAW DATA					VELOCITY
Run No	DF0 [N]	HF0 [N]	HM0 [Nm]	YM0 [Nm]	DF [N]	HF [N]	HM [Nm]	YM [Nm]	DFcorr.	HFcorr.	DF/HF	HMcorr.	YMcorr.	V (m/s)
238	0.53623	1.34307	-3.88127	3.13582	-1.36126	9.01074	-1.24008	4.40443	-1.89749	7.66767	-0.24747	2.64119	1.26861	7
260	0.40849	0.90132	-3.8485	2.50964	0.88677	4.79864	-0.82633	2.50755	0.47828	3.89732	0.12272	3.02217	-0.00209	3
261	0.40849	0.90132	-3.8485	2.50964	0.51473	7.98365	-0.36594	2.89071	0.10624	7.08233	0.01500	3.48256	0.38107	5
262	0.40849	0.90132	-3.8485	2.50964	-0.51492	11.421	0.26351	3.74891	-0.92341	10.51968	-0.08778	4.11201	1.23927	7
264	0.57352	0.77403	-3.77586	2.52016	1.0465	4.52742	-0.88788	2.45885	0.47298	3.75339	0.12601	2.88798	-0.06131	3
265	0.57352	0.77403	-3.77586	2.52016	0.63603	7.60211	-0.49238	2.78783	0.06251	6.82808	0.00915	3.28348	0.26767	5
266	0.57352	0.77403	-3.77586	2.52016	-0.53669	11.20389	0.26066	3.60396	-1.11021	10.42986	-0.10645	4.03652	1.08380	7
268	0.45767	0.63996	-3.75614	2.33021	0.83266	4.05715	-1.03462	2.20249	0.37499	3.41719	0.10974	2.72152	-0.12772	3
269	0.45767	0.63996	-3.75614	2.33021	0.35056	7.04613	-0.76695	2.58856	-0.10711	6.40617	-0.01672	2.98919	0.25835	5
270	0.45767	0.63996	-3.75614	2.33021	-0.86087	10.87393	0.28138	3.37313	-1.31854	10.23397	-0.12884	4.03752	1.04292	7
276	0.51021	0.49953	-3.71229	2.22473	0.72761	3.42395	-1.71178	2.30569	0.21740	2.92442	0.07434	2.00051	0.08096	3
277	0.51021	0.49953	-3.71229	2.22473	-0.03389	5.30019	-2.35399	2.86422	-0.54410	4.80066	-0.11334	1.35830	0.63949	5
278	0.51021	0.49953	-3.71229	2.22473	-1.34803	8.68689	-1.03312	3.62179	-1.85824	8.18736	-0.22696	2.67917	1.39706	7
280	0.54943	0.4554	-3.70358	2.18755	0.73636	3.21065	-1.73329	2.1662	0.18693	2.75525	0.06785	1.97029	-0.02135	3
281	0.54943	0.4554	-3.70358	2.18755	-0.10465	4.85587	-2.51428	2.71785	-0.65408	4.40047	-0.14864	1.18930	0.53030	5
282	0.54943	0.4554	-3.70358	2.18755	-1.48949	8.30487	-1.07418	3.37813	-2.03892	7.84947	-0.25975	2.62940	1.19058	7
284	0.48503	0.36293	-3.69254	2.04125	0.62826	2.98093	-1.79163	1.98808	0.14323	2.61800	0.05471	1.90091	-0.05317	3
285	0.48503	0.36293	-3.69254	2.04125	-0.22987	4.6881	-2.45101	2.58357	-0.71490	4.32517	-0.16529	1.24153	0.54232	5
286	0.48503	0.36293	-3.69254	2.04125	-1.80453	8.1923	-1.02981	3.32511	-2.28956	7.82937	-0.29243	2.66273	1.28386	7
292	0.47367	0.27049	-3.68057	1.94493	0.63955	3.01213	-1.82673	2.03614	0.16588	2.74164	0.06050	1.85384	0.09121	3
293	0.47367	0.27049	-3.68057	1.94493	-0.21804	4.58037	-2.6596	2.59721	-0.69171	4.30988	-0.16049	1.02097	0.65228	5
294	0.47367	0.27049	-3.68057	1.94493	-1.66496	7.95056	-1.25271	3.40638	-2.13863	7.68007	-0.27846	2.42786	1.46145	7
296	0.53959	0.18966	-3.65826	1.92947	0.6643	2.75046	-1.87409	1.88709	0.12471	2.56080	0.04870	1.78417	-0.04238	3
297	0.53959	0.18966	-3.65826	1.92947	-0.21202	4.31223	-2.62422	2.55212	-0.75161	4.12257	-0.18232	1.03404	0.62265	5
298	0.53959	0.18966	-3.65826	1.92947	-1.74577	7.50402	-1.29442	3.24979	-2.28536	7.31436	-0.31245	2.36384	1.32032	7
300	0.47803	0.14013	-3.65863	1.79267	0.57192	2.57196	-1.93836	1.77011	0.09389	2.43183	0.03861	1.72027	-0.02256	3
301	0.47803	0.14013	-3.65863	1.79267	-0.31565	4.30245	-2.54464	2.44468	-0.79368	4.16232	-0.19068	1.11399	0.65201	5
302	0.47803	0.14013	-3.65863	1.79267	-1.7428	7.31036	-1.25509	3.15575	-2.22083	7.17023	-0.30973	2.40354	1.36308	7

Table A.2.1 (continued): Raw and corrected wind tunnel data for 20° AWA.

AWA 20	BODY AXIS						WIND TUNNEL CORRECTIONS								VELOCITY
Run No	LIFT [N]	Cl	DRAG [N]	Cd	L/D	D/L²	Cd	β'	Cdi	Cds	BLOCKAGE	Cl	Cl²	Cd	V (m/s)
238	5.67790	0.15996	-4.405554943	0.12412	-1.28880	-0.13665	0.1243015	20.0012	0.0024078	0.1218938	1.024571756	**0.1561248**	0.024375	**0.121320**	7
260	3.31330	0.50821	-0.883525758	0.13552	-3.75008	-0.08048	0.1373931	20.0037	0.0243034	0.1130896	1.022796986	**0.4968794**	0.2468891	**0.1343307**	3
261	5.79505	0.31999	-2.322466578	0.12824	-2.49521	-0.06916	0.1289856	20.0023	0.0096353	0.1193503	1.024059036	**0.3124748**	0.0976405	**0.1259553**	5
262	8.28738	0.23348	-4.465664024	0.12581	-1.85580	-0.06502	0.1262049	20.0017	0.0051295	0.1210754	1.024406782	**0.2279142**	0.0519449	**0.123198**	7
264	3.19460	0.49000	-0.83927917	0.12873	-3.80636	-0.08224	0.1304744	20.0036	0.0225933	0.1078812	1.02174705	**0.4795708**	0.2299882	**0.1276974**	3
265	5.57519	0.30785	-2.276600715	0.12571	-2.44891	-0.07324	0.1263977	20.0022	0.0089181	0.1174796	1.023681934	**0.3007305**	0.0904388	**0.1234736**	5
266	8.15895	0.22986	-4.610478357	0.12989	-1.76965	-0.06926	0.1302725	20.0017	0.0049717	0.1253008	1.025258547	**0.2241959**	0.0502638	**0.1270631**	7
268	2.89197	0.44358	-0.816372478	0.12522	-3.54247	-0.09761	0.1266464	20.0032	0.0185155	0.1081309	1.021797398	**0.4341198**	0.18846	**0.1239448**	3
269	5.18160	0.28612	-2.291689658	0.12654	-2.26104	-0.08535	0.1271372	20.0021	0.0077034	0.1194338	1.024075875	**0.2793923**	0.0780601	**0.1241482**	5
270	7.93783	0.22363	-4.739246194	0.13352	-1.67491	-0.07522	0.1338797	20.0016	0.0047059	0.1291738	1.02603929	**0.2179539**	0.0475039	**0.1304821**	7
276	2.44428	0.37491	-0.795921372	0.12208	-3.07101	-0.13322	0.1231017	20.0027	0.0132266	0.1098751	1.022148985	**0.3667895**	0.1345345	**0.1204342**	3
277	3.74560	0.20683	-2.153209176	0.11890	-1.73955	-0.15348	0.1192069	20.0015	0.0040253	0.1151816	1.023218697	**0.2021325**	0.0408576	**0.1165019**	5
278	6.11245	0.17220	-4.546416456	0.12808	-1.34445	-0.12169	0.1282995	20.0012	0.0027904	0.1255091	1.025300538	**0.1679541**	0.0282086	**0.1251335**	7
280	2.29758	0.35241	-0.766694258	0.11760	-2.99674	-0.14524	0.1185	20.0026	0.0116867	0.1068133	1.021531784	**0.3449847**	0.1190144	**0.1160022**	3
281	3.38736	0.18704	-2.11968353	0.11705	-1.59805	-0.18474	0.1172991	20.0014	0.0032921	0.114007	1.022981918	**0.1828418**	0.0334311	**0.1146639**	5
282	5.78396	0.16295	-4.600634933	0.12961	-1.25721	-0.13752	0.1298045	20.0012	0.0024986	0.1273059	1.025662749	**0.1588719**	0.0252403	**0.1265567**	7
284	2.17295	0.33330	-0.760816561	0.11670	-2.85607	-0.16113	0.1175033	20.0024	0.0104531	0.1070502	1.021579533	**0.326255**	0.1064423	**0.1150212**	3
285	3.30806	0.18267	-2.151081518	0.11878	-1.53786	-0.19657	0.1190211	20.0013	0.0031398	0.1158813	1.02335975	**0.1784958**	0.0318607	**0.1163043**	5
286	5.69336	0.16040	-4.829284886	0.13605	-1.17892	-0.14899	0.1362401	20.0012	0.0024209	0.1338192	1.026975728	**0.1561835**	0.0243933	**0.1326615**	7
292	2.28027	0.34976	-0.781819894	0.11992	-2.91662	-0.15036	0.1208065	20.0025	0.0115112	0.1092952	1.022032102	**0.3422178**	0.117113	**0.1182022**	3
293	3.30249	0.18236	-2.124060558	0.11729	-1.55480	-0.19475	0.1175283	20.0013	0.0031292	0.114399	1.023060944	**0.178247**	0.031772	**0.114879**	5
294	5.61656	0.15823	-4.636393472	0.13062	-1.21141	-0.14697	0.1308009	20.0011	0.002356	0.1284448	1.025892342	**0.1542395**	0.0237898	**0.1274996**	7
296	2.12091	0.32531	-0.758656116	0.11637	-2.79562	-0.16866	0.1171338	20.0024	0.0099585	0.1071753	1.021604754	**0.3184344**	0.1014005	**0.1146566**	3
297	3.13231	0.17296	-2.116284353	0.11686	-1.48010	-0.21570	0.1170746	20.0013	0.002815	0.1142596	1.023032836	**0.1690668**	0.0285836	**0.1144388**	5
298	5.27549	0.14862	-4.649194383	0.13098	-1.13471	-0.16705	0.1311401	20.0011	0.0020786	0.1290615	1.026016658	**0.1448555**	0.0209831	**0.1278148**	7
300	2.00683	0.30782	-0.743507105	0.11404	-2.69914	-0.18461	0.1147297	20.0022	0.0089159	0.1058138	1.0213303	**0.3013867**	0.0908339	**0.1123336**	3
301	3.15220	0.17406	-2.169412522	0.11979	-1.45302	-0.21833	0.120011	20.0013	0.0028509	0.1171602	1.023617539	**0.170043**	0.0289146	**0.1172421**	5
302	5.17731	0.14586	-4.539260655	0.12788	-1.14056	-0.16935	0.1280371	20.0011	0.0020019	0.1260352	1.025406589	**0.1422443**	0.0202334	**0.1248647**	7

Table A.2.1 (continued): Raw and corrected wind tunnel data for 20° AWA.

AWA 20	ZERO-ACQUIRED DATA				RAW WIND TUNNEL DATA				CORRECTED RAW DATA					VELOCITY
Run No	DF0 [N]	HF0 [N]	HM0 [Nm]	YM0 [Nm]	DF [N]	HF [N]	HM [Nm]	YM [Nm]	DFcorr.	HFcorr.	DF/HF	HMcorr.	YMcorr.	V (m/s)
304	0.56503	0.23093	-3.69126	1.97125	0.99217	4.10799	-0.88496	2.07305	0.42714	3.87706	0.11017	2.80630	0.10180	3
305	0.56503	0.23093	-3.69126	1.97125	0.49765	7.16883	-0.75467	2.56679	-0.06738	6.93790	-0.00971	2.93659	0.59554	5
306	0.56503	0.23093	-3.69126	1.97125	-0.72747	11.52168	0.60203	3.45101	-1.29250	11.29075	-0.11447	4.29329	1.47976	7
308	0.5229	0.20121	-3.67497	1.91541	0.89625	3.89733	-1.00722	1.90318	0.37335	3.69612	0.10101	2.66775	-0.01223	3
309	0.5229	0.20121	-3.67497	1.91541	0.45751	6.94622	-0.80942	2.42329	-0.06539	6.74501	-0.00969	2.86555	0.50788	5
310	0.5229	0.20121	-3.67497	1.91541	-0.85428	11.33744	0.62765	3.28743	-1.37718	11.13623	-0.12367	4.30262	1.37202	7
312	0.55062	0.16178	-3.67245	1.88508	0.84181	3.61892	-1.16004	1.72371	0.29119	3.45714	0.08423	2.51241	-0.16137	3
313	0.55062	0.16178	-3.67245	1.88508	0.26561	6.74685	-0.89134	2.41144	-0.28501	6.58507	-0.04328	2.78111	0.52636	5
314	0.55062	0.16178	-3.67245	1.88508	-0.8866	10.70883	0.47778	3.07461	-1.43722	10.54705	-0.13627	4.15023	1.18953	7
316	0.36054	0.19413	-3.66575	1.77677	0.58647	3.44598	-1.47878	1.86069	0.22593	3.25185	0.06948	2.18697	0.08392	3
317	0.36054	0.19413	-3.66575	1.77677	-0.11878	5.62362	-1.92835	2.51004	-0.47932	5.42949	-0.08828	1.73740	0.73327	5
318	0.36054	0.19413	-3.66575	1.77677	-1.47291	9.66939	-0.38686	3.40569	-1.83345	9.47526	-0.19350	3.27889	1.62892	7
320	0.37193	0.25325	-3.66627	1.7832	0.56355	3.23435	-1.64731	1.73978	0.19162	2.98110	0.06428	2.01896	-0.04342	3
321	0.37193	0.25325	-3.66627	1.7832	-0.17936	5.57493	-1.91011	2.50619	-0.55129	5.32168	-0.10359	1.75616	0.72299	5
322	0.37193	0.25325	-3.66627	1.7832	-1.69427	9.42649	-0.46429	3.14852	-2.06620	9.17324	-0.22524	3.20198	1.36532	7
324	0.38584	0.21488	-3.65816	1.76592	0.52807	3.11393	-1.66327	1.66571	0.14223	2.89905	0.04906	1.99489	-0.10021	3
325	0.38584	0.21488	-3.65816	1.76592	-0.10745	5.62726	-1.96338	2.52271	-0.49329	5.41238	-0.09114	1.69478	0.75679	5
326	0.38584	0.21488	-3.65816	1.76592	-1.60965	9.09589	-0.4706	3.09189	-1.99549	8.88101	-0.22469	3.18756	1.32597	7
328	0.39629	0.23501	-3.65511	1.83684	0.32157	2.45685	-2.3853	1.89029	-0.07472	2.22184	-0.03363	1.26981	0.05345	3
329	0.39629	0.23501	-3.65511	1.83684	-0.43264	4.56917	-2.23825	2.7045	-0.82893	4.33416	-0.19126	1.41686	0.86766	5
330	0.39629	0.23501	-3.65511	1.83684	-2.07615	7.33428	-1.31633	3.57241	-2.47244	7.09927	-0.34827	2.33878	1.73557	7
332	0.33711	0.2208	-3.64037	1.7492	0.0803	2.03538	-3.11628	1.89735	-0.25681	1.81458	-0.14153	0.52409	0.14815	3
333	0.33711	0.2208	-3.64037	1.7492	-0.62577	4.29116	-2.34116	2.62617	-0.96288	4.07036	-0.23656	1.29921	0.87697	5
334	0.33711	0.2208	-3.64037	1.7492	-2.09625	7.0826	-1.36716	3.42223	-2.43336	6.86180	-0.35462	2.27321	1.67303	7
336	0.35319	0.19252	-3.63765	1.73928	0.04941	1.85606	-3.17736	1.75007	-0.30378	1.66354	-0.18261	0.46029	0.01079	3
337	0.35319	0.19252	-3.63765	1.73928	-0.66176	4.09133	-2.51001	2.54472	-1.01495	3.89881	-0.26032	1.12764	0.80544	5
340	-0.04619	0.97242	-3.83765	2.35007	0.4326	4.96197	-1.14519	2.74804	0.47879	3.98955	0.12001	2.69246	0.39797	3
341	-0.04619	0.97242	-3.83765	2.35007	-0.42812	6.97401	-1.75943	3.26342	-0.38193	6.00159	-0.06364	2.07822	0.91335	5

Table A.2.1 (continued): Raw and corrected wind tunnel data for 20° AWA.

AWA 20	BODY AXIS						WIND TUNNEL CORRECTIONS								VELOCITY
Run No	LIFT [N]	Cl	DRAG [N]	Cd	L/D	D/L^2	Cd	β'	Cdi	Cds	BLOCKAGE	Cl	Cl^2	Cd	V (m/s)
304	3.28166	0.50335	-0.924652311	0.14183	-3.54908	-0.08586	0.1436656	20.0037	0.0238416	0.119824	1.024154532	**0.4914829**	0.2415554	**0.1402773**	3
305	5.62609	0.31066	-2.436218041	0.13452	-2.30935	-0.07697	0.1352241	20.0023	0.0090817	0.1261424	1.025428217	**0.3029591**	0.0917842	**0.1318709**	5
306	8.80555	0.24808	-5.076216646	0.14301	-1.73467	-0.06547	0.1434567	20.0018	0.005791	0.1376657	1.027751122	**0.2413766**	0.0582627	**0.1395831**	7
308	3.11848	0.47833	-0.913313252	0.14009	-3.41447	-0.09391	0.1417481	20.0035	0.0215295	0.1202186	1.024234069	**0.4670075**	0.218096	**0.1383942**	3
309	5.46971	0.30203	-2.368375787	0.13078	-2.30948	-0.07916	0.1314396	20.0022	0.0085838	0.1228558	1.024765678	**0.2947284**	0.0868649	**0.1282631**	5
310	8.65472	0.24383	-5.102940864	0.14376	-1.69603	-0.06813	0.1441945	20.0018	0.0055943	0.1386001	1.027939483	**0.2371986**	0.0562632	**0.1402752**	7
312	2.89966	0.44476	-0.908782424	0.13939	-3.19071	-0.10808	0.1408283	20.0032	0.0186141	0.1222142	1.024636341	**0.4340681**	0.1884151	**0.1374422**	3
313	5.27450	0.29125	-2.520048379	0.13915	-2.09301	-0.09058	0.1397683	20.0021	0.007982	0.1317862	1.026565909	**0.2837114**	0.0804922	**0.1361513**	5
314	8.15746	0.22982	-4.957848581	0.13968	-1.64536	-0.07450	0.1400587	20.0017	0.0049699	0.1350887	1.027231643	**0.2237244**	0.0500526	**0.1363458**	7
316	2.71327	0.41617	-0.899893449	0.13803	-3.01510	-0.12224	0.1392862	20.0030	0.0162979	0.1229883	1.024792389	**0.4061038**	0.1649203	**0.1359165**	3
317	4.27653	0.23614	-2.307408415	0.12741	-1.85339	-0.12617	0.1278158	20.0017	0.0052473	0.1225685	1.02470776	**0.2304488**	0.0531067	**0.1247339**	5
318	7.16788	0.20194	-4.963609219	0.13984	-1.44409	-0.09661	0.1401336	20.0015	0.0038373	0.1362964	1.027475077	**0.1965378**	0.0386271	**0.1363864**	7
320	2.48277	0.38082	-0.839532349	0.12877	-2.95732	-0.13620	0.1298233	20.0028	0.0136465	0.1161768	1.023419316	**0.3721029**	0.1384606	**0.1268525**	3
321	4.16748	0.23012	-2.338164901	0.12911	-1.78237	-0.13463	0.1294937	20.0017	0.0049831	0.1245106	1.025099265	**0.2244865**	0.0503942	**0.1263231**	5
322	6.85316	0.19307	-5.079025753	0.14309	-1.34931	-0.10814	0.1433598	20.0014	0.0035077	0.1398521	1.028191854	**0.1877773**	0.0352603	**0.139429**	7
324	2.40137	0.36833	-0.857881015	0.13159	-2.79919	-0.14877	0.1325698	20.0027	0.0127663	0.1198035	1.024150396	**0.359646**	0.1293453	**0.1294437**	3
325	4.25847	0.23515	-2.314683956	0.12781	-1.83976	-0.12764	0.1282141	20.0017	0.0052031	0.123011	1.024796974	**0.2294555**	0.0526498	**0.1251117**	5
326	6.63628	0.18696	-4.912631541	0.13840	-1.35086	-0.11155	0.1386552	20.0014	0.0032892	0.135366	1.027287529	**0.1819951**	0.0331222	**0.1349721**	7
328	1.78600	0.27394	-0.830127868	0.12733	-2.15147	-0.26025	0.127873	20.0020	0.0070617	0.1208113	1.024353546	**0.2674305**	0.0715191	**0.1248329**	3
329	3.28160	0.18120	-2.261309429	0.12487	-1.45120	-0.20998	0.1251039	20.0013	0.0030898	0.1220141	1.024596012	**0.1768544**	0.0312775	**0.1221007**	5
330	5.04504	0.14213	-4.751426966	0.13386	-1.06179	-0.18668	0.1340066	20.0010	0.0019009	0.1321056	1.026630295	**0.1384449**	0.019167	**0.1305305**	7
332	1.40063	0.21483	-0.861945374	0.13221	-1.62497	-0.43937	0.1325436	20.0016	0.0043431	0.1282005	1.025843097	**0.2094228**	0.0438579	**0.1292046**	3
333	3.02725	0.16716	-2.296956341	0.12683	-1.31794	-0.25064	0.1270367	20.0012	0.0026293	0.1244074	1.025078454	**0.1630697**	0.0265917	**0.1239288**	5
334	4.86336	0.13701	-4.633484255	0.13054	-1.04961	-0.19590	0.1306734	20.0010	0.0017665	0.1289069	1.025985496	**0.1335432**	0.0178338	**0.1273638**	7
336	1.26381	0.19385	-0.854424014	0.13106	-1.47913	-0.53495	0.1313277	20.0014	0.003536	0.1277917	1.02576069	**0.1889794**	0.0357132	**0.1280296**	3
337	2.87222	0.15860	-2.28721258	0.12630	-1.25577	-0.27725	0.1264784	20.0012	0.0023669	0.1241115	1.025018814	**0.1547277**	0.0239407	**0.1233913**	5
340	3.38850	0.51974	-0.914591033	0.14028	-3.70494	-0.07965	0.142244	20.0038	0.0254193	0.1168248	1.023549927	**0.5077841**	0.2578447	**0.1389713**	3
341	4.77095	0.26344	-2.411561475	0.13316	-1.97837	-0.10595	0.1336659	20.0019	0.0065307	0.1271351	1.025628329	**0.2568608**	0.0659775	**0.1303258**	5

Table A.2.1 (continued): Raw and corrected wind tunnel data for 20° AWA.

AWA 20	ZERO-ACQUIRED DATA				RAW WIND TUNNEL DATA				CORRECTED RAW DATA					VELOCITY
Run No	DF0 [N]	HF0 [N]	HM0 [Nm]	YM0 [Nm]	DF [N]	HF [N]	HM [Nm]	YM [Nm]	DFcorr.	HFcorr.	DF/HF	HMcorr.	YMcorr.	V (m/s)
344	0.28343	0.97168	-3.82117	2.56856	0.64894	4.55989	-1.39898	2.78266	0.36551	3.58821	0.10186	2.42219	0.21410	3
345	0.28343	0.97168	-3.82117	2.56856	-0.05038	6.63225	-1.75267	3.26728	-0.33381	5.66057	-0.05897	2.06850	0.69872	5
346	0.28343	0.97168	-3.82117	2.56856	-1.09014	9.93417	-0.32287	3.84723	-1.37357	8.96249	-0.15326	3.49830	1.27867	7
348	0.27387	0.93791	-3.81179	2.55948	0.51599	4.23114	-1.77567	2.69124	0.24212	3.29323	0.07352	2.03612	0.13176	3
349	0.27387	0.93791	-3.81179	2.55948	-0.01159	6.53808	-1.61684	3.09129	-0.28546	5.60017	-0.05097	2.19495	0.53181	5
350	0.27387	0.93791	-3.81179	2.55948	-1.40679	10.00247	-0.35466	3.80313	-1.68066	9.06456	-0.18541	3.45713	1.24365	7
352	0.29659	0.93139	-3.81583	2.59143	0.55151	4.24898	-1.87634	3.01956	0.25492	3.31759	0.07684	1.93949	0.42813	3
353	0.29659	0.93139	-3.81583	2.59143	-0.41484	5.74296	-2.69536	3.48668	-0.71143	4.81157	-0.14786	1.12047	0.89525	5
354	0.29659	0.93139	-3.81583	2.59143	-1.1005	9.05662	-0.61157	4.22633	-1.39709	8.12523	-0.17194	3.20426	1.63490	7
356	0.28958	0.93388	-3.80923	2.55758	0.42305	3.89207	-2.15324	2.86556	0.13347	2.95819	0.04512	1.65599	0.30798	3
357	0.28958	0.93388	-3.80923	2.55758	-0.28656	5.809	-2.26468	3.33585	-0.57614	4.87512	-0.11818	1.54455	0.77827	5
358	0.28958	0.93388	-3.80923	2.55758	-1.49522	8.69216	-1.03358	3.95443	-1.78480	7.75828	-0.23005	2.77565	1.39685	7
360	0.28509	0.93403	-3.80726	2.59386	0.30823	3.56933	-2.37719	2.70088	0.02314	2.63530	0.00878	1.43007	0.10702	3
361	0.28509	0.93403	-3.80726	2.59386	-0.21133	5.73868	-2.01408	3.17249	-0.49642	4.80465	-0.10332	1.79318	0.57863	5
362	0.28509	0.93403	-3.80726	2.59386	-1.67275	8.66859	-1.08876	3.91735	-1.95784	7.73456	-0.25313	2.71850	1.32349	7
364	0.2746	0.90877	-3.79110	2.56558	0.38768	3.79151	-2.13695	2.98007	0.11308	2.88274	0.03923	1.65415	0.41449	3
365	0.2746	0.90877	-3.79110	2.56558	-0.57837	5.08268	-2.95478	3.50654	-0.85297	4.17391	-0.20436	0.83632	0.94096	5
366	0.2746	0.90877	-3.79110	2.56558	-1.45659	8.02704	-1.18874	4.24802	-1.73119	7.11827	-0.24320	2.60236	1.68244	7
368	0.33438	0.88365	-3.78857	2.58883	0.28321	3.31456	-2.67443	2.90293	-0.05117	2.43091	-0.02105	1.11414	0.31410	3
369	0.33438	0.88365	-3.78857	2.58883	-0.378	5.16499	-2.37328	3.36617	-0.71238	4.28134	-0.16639	1.41529	0.77734	5
370	0.33438	0.88365	-3.78857	2.58883	-1.77046	7.67816	-1.54412	4.00664	-2.10484	6.79451	-0.30979	2.24445	1.41781	7
372	0.26555	0.87815	-3.78736	2.528	0.10663	2.80919	-3.09769	2.61813	-0.15892	1.93104	-0.08230	0.68967	0.09013	3
373	0.26555	0.87815	-3.78736	2.528	-0.48003	4.90356	-2.45307	3.18891	-0.74558	4.02541	-0.18522	1.33429	0.66091	5
374	0.26555	0.87815	-3.78736	2.528	-2.0395	7.74449	-1.45707	3.99072	-2.30505	6.86634	-0.33570	2.33029	1.46272	7
376	0.09099	0.86595	-3.79967	2.43061	0.35751	4.28451	-1.69456	2.65631	0.26652	3.41856	0.07796	2.10511	0.22570	3
377	0.09099	0.86595	-3.79967	2.43061	-0.26808	6.4581	-1.80812	3.08302	-0.35907	5.59215	-0.06421	1.99155	0.65241	5
378	0.09099	0.86595	-3.79967	2.43061	-1.18949	9.7825	-0.40455	3.85653	-1.28048	8.91655	-0.14361	3.39512	1.42592	7
380	0.22103	0.84166	-3.79192	2.431	0.38076	3.90154	-1.98169	2.49921	0.15973	3.05988	0.05220	1.81023	0.06821	3

Table A.2.1 (continued): Raw and corrected wind tunnel data for 20° AWA.

AWA 20	BODY AXIS						WIND TUNNEL CORRECTIONS								VELOCITY
Run No	LIFT [N]	Cl	DRAG [N]	Cd	L/D	D/L²	Cd	β'	Cdi	Cds	BLOCKAGE	Cl	Cl²	Cd	V (m/s)
344	3.02834	0.46450	-0.883773049	0.13556	-3.42660	-0.09637	0.1371225	20.0034	0.0203028	0.1168196	1.023548893	**0.4538123**	0.2059456	**0.1339677**	3
345	4.50768	0.24891	-2.249707756	0.12422	-2.00368	-0.11072	0.1246745	20.0018	0.0058299	0.1188447	1.023957109	**0.2430829**	0.0590893	**0.1217576**	5
346	6.88680	0.19402	-4.356085707	0.12272	-1.58096	-0.09185	0.1229954	20.0014	0.0035422	0.1194531	1.024079765	**0.189457**	0.0358939	**0.1201033**	7
348	2.75174	0.42207	-0.898832619	0.13787	-3.06146	-0.11870	0.1391594	20.0031	0.0167634	0.122396	1.024673	**0.4119097**	0.1696696	**0.1358086**	3
349	4.47285	0.24698	-2.183615602	0.12058	-2.04837	-0.10915	0.1210181	20.0018	0.0057401	0.115278	1.023238128	**0.2413741**	0.0582614	**0.1182698**	5
350	6.87891	0.19380	-4.67956591	0.13184	-1.46999	-0.09889	0.132108	20.0014	0.0035341	0.1285739	1.025918359	**0.1889006**	0.0356835	**0.1287705**	7
352	2.77535	0.42570	-0.895136164	0.13730	-3.10048	-0.11621	0.1386147	20.0031	0.0170523	0.1215624	1.024504949	**0.4155129**	0.172651	**0.1352992**	3
353	3.70492	0.20458	-2.314179382	0.12778	-1.60097	-0.16859	0.1280887	20.0015	0.0039383	0.1241504	1.025026649	**0.1995843**	0.0398339	**0.1249613**	5
354	6.19848	0.17463	-4.091827493	0.11528	-1.51484	-0.10650	0.1154986	20.0013	0.0028695	0.1126291	1.022704156	**0.1707504**	0.0291557	**0.1129346**	7
356	2.44690	0.37532	-0.886339794	0.13595	-2.76068	-0.14804	0.1369726	20.0027	0.013255	0.1237176	1.024939411	**0.3661833**	0.1340902	**0.1336397**	3
357	3.79671	0.20965	-2.208783748	0.12197	-1.71891	-0.15323	0.1222842	20.0015	0.0041359	0.1181483	1.023816728	**0.2047707**	0.0419311	**0.1194395**	5
358	5.78502	0.16298	-4.330651427	0.12201	-1.33583	-0.12940	0.1221984	20.0012	0.0024995	0.1196989	1.024129309	**0.1591389**	0.0253252	**0.1193193**	7
360	2.15146	0.33000	-0.879581196	0.13491	-2.44600	-0.19003	0.135704	20.0024	0.0102474	0.1254567	1.025289974	**0.3218591**	0.1035933	**0.1323567**	3
361	3.76297	0.20778	-2.109769292	0.11650	-1.78360	-0.14900	0.1168111	20.0015	0.0040627	0.1127484	1.022728203	**0.2031673**	0.0412769	**0.1142152**	5
362	5.71446	0.16099	-4.48514312	0.12636	-1.27409	-0.13735	0.1265461	20.0012	0.0024389	0.1241073	1.02501796	**0.1570617**	0.0246684	**0.1234575**	7
364	2.37946	0.36497	-0.879694706	0.13493	-2.70487	-0.15537	0.1358978	20.0026	0.0125344	0.1233634	1.024868004	**0.3561155**	0.1268183	**0.1326003**	3
365	3.14407	0.17361	-2.229090911	0.12309	-1.41047	-0.22550	0.1233052	20.0013	0.0028362	0.120469	1.024284556	**0.169494**	0.0287282	**0.1203818**	5
366	5.28006	0.14875	-4.061378194	0.11442	-1.30007	-0.14568	0.1145801	20.0011	0.0020822	0.1124979	1.022677707	**0.1454542**	0.0211569	**0.1120393**	7
368	1.96311	0.30111	-0.879504258	0.13490	-2.23207	-0.22822	0.1355599	20.0022	0.0085317	0.1270282	1.025606764	**0.2935922**	0.0861964	**0.1321753**	3
369	3.27314	0.18074	-2.13372275	0.11782	-1.53400	-0.19916	0.1180575	20.0013	0.0030738	0.1149837	1.023178795	**0.1766427**	0.0312026	**0.1153831**	5
370	4.90591	0.13821	-4.3017619	0.12119	-1.14044	-0.17873	0.1213304	20.0010	0.0017975	0.1195328	1.024095828	**0.1349601**	0.0182142	**0.1184756**	7
372	1.52440	0.23382	-0.809790529	0.12421	-1.88247	-0.34848	0.1246057	20.0017	0.0051446	0.1194612	1.024081381	**0.228321**	0.0521305	**0.1216756**	3
373	3.05503	0.16869	-2.077387329	0.11471	-1.47061	-0.22258	0.1149162	20.0012	0.0026778	0.1122384	1.022625393	**0.1649611**	0.0272122	**0.1123737**	5
374	4.90506	0.13819	-4.514465066	0.12718	-1.08652	-0.18764	0.1273227	20.0010	0.0017969	0.1255258	1.025303911	**0.1347778**	0.0181651	**0.1241805**	7
376	2.86096	0.43883	-0.918769504	0.14092	-3.11390	-0.11225	0.1423221	20.0032	0.0181205	0.1242015	1.025036964	**0.428107**	0.1832756	**0.1388458**	3
377	4.44452	0.24542	-2.250043374	0.12424	-1.97531	-0.11390	0.1246806	20.0018	0.0056676	0.1190129	1.023991026	**0.2396689**	0.0574412	**0.1217594**	5
378	6.87699	0.19374	-4.252897316	0.11982	-1.61701	-0.08993	0.1200875	20.0014	0.0035321	0.1165554	1.023495622	**0.189295**	0.0358326	**0.1173307**	7
380	2.53743	0.38920	-0.896443494	0.13750	-2.83056	-0.13923	0.1385994	20.0028	0.014254	0.1243454	1.025065964	**0.3796849**	0.1441606	**0.1352102**	3

Table A.2.1 (continued): Raw and corrected wind tunnel data for 20° AWA.

AWA 20	ZERO-ACQUIRED DATA				RAW WIND TUNNEL DATA				CORRECTED RAW DATA					VELOCITY
Run No	DF0 [N]	HF0 [N]	HM0 [Nm]	YM0 [Nm]	DF [N]	HF [N]	HM [Nm]	YM [Nm]	DFcorr.	HFcorr.	DF/HF	HMcorr.	YMcorr.	V (m/s)
382	0.22103	0.84166	-3.79192	2.431	-1.33808	9.55728	-0.49081	3.66163	-1.55911	8.71562	-0.17889	3.30111	1.23063	7
384	0.196	0.78339	-3.7821	2.40205	0.33500	3.63435	-2.02806	2.36594	0.13900	2.85096	0.04876	1.75404	-0.03611	3
385	0.196	0.78339	-3.7821	2.40205	-0.19749	5.99074	-1.81447	2.89189	-0.39349	5.20735	-0.07556	1.96763	0.48984	5
386	0.196	0.78339	-3.7821	2.40205	-1.61057	9.87704	-0.33898	3.71458	-1.80657	9.09365	-0.19866	3.44312	1.31253	7
388	0.22976	0.82747	-3.7864	2.44132	0.34226	3.6397	-2.05033	2.57591	0.11250	2.81223	0.04000	1.73607	0.13459	3
389	0.22976	0.82747	-3.7864	2.44132	-0.3881	5.43788	-2.38691	3.15072	-0.61786	4.61041	-0.13401	1.39949	0.70940	5
390	0.22976	0.82747	-3.7864	2.44132	-1.76391	8.20259	-1.26392	3.83098	-1.99367	7.37512	-0.27032	2.52248	1.38966	7
392	0.23874	0.78507	-3.76697	2.41887	0.22978	3.16002	-2.54561	2.49835	-0.00896	2.37495	-0.00377	1.22136	0.07948	3
393	0.23874	0.78507	-3.76697	2.41887	-0.36249	5.25823	-2.27008	3.02157	-0.60123	4.47316	-0.13441	1.49689	0.60270	5
394	0.23874	0.78507	-3.76697	2.41887	-1.89493	8.07857	-1.32195	3.75497	-2.13367	7.29350	-0.29254	2.44502	1.33610	7
396	0.25488	0.73735	-3.76541	2.37378	0.23857	3.03018	-2.50214	2.39791	-0.01631	2.29283	-0.00711	1.26327	0.02413	3
397	0.25488	0.73735	-3.76541	2.37378	-0.36216	5.10803	-2.23943	2.95094	-0.61704	4.37068	-0.14118	1.52598	0.57716	5
398	0.25488	0.73735	-3.76541	2.37378	-2.10173	8.45448	-1.06667	3.86893	-2.35661	7.71713	-0.30537	2.69874	1.49515	7
400	0.30568	0.70058	-3.74901	2.38411	0.14942	2.69085	-2.96608	2.58625	-0.15626	1.99027	-0.07851	0.78293	0.20214	3
401	0.30568	0.70058	-3.74901	2.38411	-0.49338	4.61117	-2.46387	3.11402	-0.79906	3.91059	-0.20433	1.28514	0.72991	5
402	0.30568	0.70058	-3.74901	2.38411	-2.245	6.83389	-1.87784	3.92307	-2.55068	6.13331	-0.41587	1.87117	1.53896	7
404	0.26361	0.66897	-3.75041	2.33639	0.05194	2.42465	-3.22369	2.45774	-0.21167	1.75568	-0.12056	0.52672	0.12135	3
405	0.26361	0.66897	-3.75041	2.33639	-0.55241	4.32341	-2.53224	2.9558	-0.81602	3.65444	-0.22330	1.21817	0.61941	5
406	0.26361	0.66897	-3.75041	2.33639	-2.17416	6.76604	-1.87109	3.93487	-2.43777	6.09707	-0.39983	1.87932	1.59848	7
408	0.24302	0.65393	-3.73549	2.28983	0.0009	2.24928	-3.27064	2.39502	-0.24212	1.59535	-0.15177	0.46485	0.10519	3
409	0.24302	0.65393	-3.73549	2.28983	-0.63982	4.21011	-2.63092	2.94921	-0.88284	3.55618	-0.24826	1.10457	0.65938	5
410	0.24302	0.65393	-3.73549	2.28983	-2.41565	6.94205	-1.68827	3.92022	-2.65867	6.28812	-0.42281	2.04722	1.63039	7
412	0.26602	0.6886	-3.79972	2.2801	0.74202	4.68666	-0.98822	2.48374	0.47600	3.99806	0.11906	2.81150	0.20364	3
413	0.26602	0.6886	-3.79972	2.2801	-0.13352	6.41276	-1.91203	2.95055	-0.39954	5.72416	-0.06980	1.88769	0.67045	5
414	0.26602	0.6886	-3.79972	2.2801	-1.37281	10.05476	-0.32057	3.68919	-1.63883	9.36616	-0.17497	3.47915	1.40909	7
416	0.2678	0.68195	-3.75558	2.28932	0.60985	4.29516	-1.17558	2.31307	0.34205	3.61321	0.09467	2.58000	0.02375	3
417	0.2678	0.68195	-3.75558	2.28932	-0.0928	6.27924	-1.7249	2.8252	-0.36060	5.59729	-0.06442	2.03068	0.53588	5
418	0.2678	0.68195	-3.75558	2.28932	-1.53614	9.93197	-0.21164	3.5449	-1.80394	9.25002	-0.19502	3.54394	1.25558	7

Table A.2.1 (continued): Raw and corrected wind tunnel data for 20° AWA.

AWA 20	BODY AXIS						WIND TUNNEL CORRECTIONS								VELOCITY
Run No	LIFT [N]	Cl	DRAG [N]	Cd	L/D	D/L²	Cd	β'	Cdi	Cds	BLOCKAGE	Cl	Cl²	Cd	V (m/s)
382	6.63095	0.18681	-4.446001764	0.12526	-1.49144	-0.10112	0.1255086	20.0014	0.0032839	0.1222247	1.024638465	**0.1823188**	0.0332401	**0.1224906**	7
384	2.36128	0.36218	-0.844468474	0.12953	-2.79617	-0.15146	0.1304799	20.0026	0.0123436	0.1181364	1.023814326	**0.3537576**	0.1251444	**0.1274449**	3
385	4.12118	0.22756	-2.150778243	0.11876	-1.91613	-0.12663	0.119138	20.0017	0.004873	0.1142651	1.023033933	**0.2224406**	0.0494798	**0.1164556**	5
386	6.86529	0.19341	-4.807831974	0.13545	-1.42794	-0.10201	0.1357205	20.0014	0.0035201	0.1322004	1.026649399	**0.1883924**	0.0354917	**0.1321975**	7
388	2.32191	0.35614	-0.856123888	0.13132	-2.71212	-0.15880	0.1322362	20.0026	0.0119354	0.1203008	1.02425064	**0.3477115**	0.1209033	**0.1291053**	3
389	3.56893	0.19707	-2.157451572	0.11913	-1.65424	-0.16938	0.1194126	20.0014	0.0036545	0.1157581	1.023334897	**0.1925765**	0.0370857	**0.1166896**	5
390	5.41133	0.15245	-4.395876587	0.12384	-1.23100	-0.15012	0.1240119	20.0011	0.002187	0.1218249	1.024557863	**0.1487971**	0.0221406	**0.1210394**	7
392	1.93007	0.29604	-0.820700385	0.12588	-2.35174	-0.22031	0.1265184	20.0021	0.008247	0.1182714	1.023841541	**0.289149**	0.0836071	**0.1235722**	3
393	3.46216	0.19117	-2.094882219	0.11568	-1.65268	-0.17477	0.115941	20.0014	0.0034391	0.1125019	1.022678502	**0.1869353**	0.0349448	**0.1133699**	5
394	5.30344	0.14941	-4.49951787	0.12676	-1.17867	-0.15997	0.126925	20.0011	0.0021007	0.1248244	1.025162517	**0.1457444**	0.0212414	**0.1238097**	7
396	1.86107	0.28546	-0.799520432	0.12263	-2.32773	-0.23084	0.123225	20.0021	0.0076678	0.1155572	1.02329441	**0.2789601**	0.0778187	**0.1204199**	3
397	3.37408	0.18631	-2.074688535	0.11456	-1.62631	-0.18224	0.1148126	20.0014	0.0032664	0.1115462	1.022485865	**0.1822138**	0.0332019	**0.1122877**	5
398	5.58216	0.15726	-4.853902936	0.13675	-1.15004	-0.15577	0.1369265	20.0011	0.0023273	0.1345992	1.027132958	**0.1531095**	0.0234425	**0.1333094**	7
400	1.57339	0.24133	-0.8275488	0.12693	-1.90127	-0.33429	0.1273555	20.0018	0.0054805	0.1218749	1.024567958	**0.2355465**	0.0554822	**0.1243016**	3
401	2.94575	0.16266	-2.088371338	0.11532	-1.41055	-0.24067	0.1155082	20.0012	0.0024897	0.1130186	1.02278266	**0.1590359**	0.0252924	**0.1129353**	5
402	4.23577	0.11933	-4.494570739	0.12662	-0.94242	-0.25051	0.126727	20.0009	0.00134	0.125387	1.025275934	**0.1163906**	0.0135468	**0.1236028**	7
404	1.36607	0.20953	-0.799382662	0.12261	-1.70891	-0.42836	0.1229312	20.0015	0.0041314	0.1187998	1.023948062	**0.2046331**	0.0418747	**0.1200561**	3
405	2.73227	0.15087	-2.016700065	0.11136	-1.35482	-0.27014	0.1115239	20.0011	0.0021419	0.1093819	1.022049581	**0.1476164**	0.0217906	**0.1091178**	5
406	4.23972	0.11944	-4.376075235	0.12329	-0.96884	-0.24345	0.1233889	20.0009	0.0013425	0.1220464	1.024602518	**0.1165758**	0.0135899	**0.1204261**	7
408	1.22658	0.18814	-0.773160213	0.11859	-1.58645	-0.51390	0.1188473	20.0014	0.0033307	0.1155166	1.023286226	**0.183856**	0.033803	**0.1161428**	3
409	2.63252	0.14536	-2.045883427	0.11297	-1.28674	-0.29522	0.1131235	20.0011	0.0019884	0.1111351	1.022402989	**0.1421777**	0.0202145	**0.1106447**	5
410	4.32976	0.12198	-4.648996284	0.13097	-0.93133	-0.24799	0.1310822	20.0009	0.0014001	0.1296821	1.026141748	**0.1188731**	0.0141308	**0.1277428**	7
412	3.39460	0.52068	-0.920123367	0.14113	-3.68929	-0.07985	0.1430997	20.0038	0.0255109	0.1175888	1.023703947	**0.5086215**	0.2586958	**0.1397862**	3
413	4.53997	0.25069	-2.333222813	0.12884	-1.94579	-0.11320	0.1292926	20.0018	0.0059137	0.1233789	1.024871132	**0.2446054**	0.0598318	**0.126155**	5
414	7.13674	0.20106	-4.743411843	0.13363	-1.50456	-0.09313	0.1339275	20.0015	0.003804	0.1301235	1.026230738	**0.1959213**	0.0383851	**0.1305043**	7
416	3.04174	0.46655	-0.914368741	0.14025	-3.32660	-0.09883	0.1418292	20.0034	0.0204829	0.1213464	1.024461411	**0.4554138**	0.2074017	**0.1384427**	3
417	4.44825	0.24562	-2.253239087	0.12442	-1.97416	-0.11388	0.1248578	20.0018	0.0056772	0.1191806	1.024024827	**0.2398621**	0.0575338	**0.1219285**	5
418	6.99332	0.19702	-4.858842273	0.13689	-1.43930	-0.09935	0.1371678	20.0014	0.0036526	0.1335152	1.026914439	**0.1918562**	0.0368088	**0.1335728**	7

Table A.2.1 (continued): Raw and corrected wind tunnel data for 20° AWA.

AWA 20	ZERO-ACQUIRED DATA				RAW WIND TUNNEL DATA				CORRECTED RAW DATA					VELOCITY
Run No	DF0 [N]	HF0 [N]	HM0 [Nm]	YM0 [Nm]	DF [N]	HF [N]	HM [Nm]	YM [Nm]	DFcorr.	HFcorr.	DF/HF	HMcorr.	YMcorr.	V (m/s)
421	0.22649	0.63368	-3.7431	2.22558	-0.2428	6.0738	-1.7484	2.73737	-0.46929	5.44012	-0.08626	1.99470	0.51179	5
422	0.22649	0.63368	-3.7431	2.22558	-2.03733	9.98028	-0.0687	3.33995	-2.26382	9.34660	-0.24221	3.67440	1.11437	7
424	-0.07506	0.58283	-3.74	1.9449	0.08293	3.44217	-1.89509	1.97551	0.15799	2.85934	0.05525	1.84491	0.03061	3
425	-0.07506	0.58283	-3.74	1.9449	-0.74175	5.40576	-2.07834	2.71292	-0.66669	4.82293	-0.13823	1.66166	0.76802	5
426	-0.07506	0.58283	-3.74	1.9449	-2.48933	7.94856	-1.32443	3.50096	-2.41427	7.36573	-0.32777	2.41557	1.55606	7
428	-0.13975	0.56458	-3.71363	1.87783	-0.20096	2.8618	-2.61924	1.84169	-0.06121	2.29722	-0.02665	1.09439	-0.03614	3
429	-0.13975	0.56458	-3.71363	1.87783	-0.92143	5.10696	-2.2334	2.65115	-0.78168	4.54238	-0.17209	1.48023	0.77332	5
430	-0.13975	0.56458	-3.71363	1.87783	-2.57591	7.84162	-1.23177	3.36543	-2.43616	7.27704	-0.33477	2.48186	1.48760	7
432	-0.10808	0.57592	-3.69417	1.88404	-0.11426	2.86632	-2.52159	1.91632	-0.00618	2.29040	-0.00270	1.17258	0.03228	3
433	-0.10808	0.57592	-3.69417	1.88404	-0.89991	4.8919	-2.36904	2.53378	-0.79183	4.31598	-0.18346	1.32513	0.64974	5
434	-0.10808	0.57592	-3.69417	1.88404	-2.95833	8.16701	-0.95902	3.37029	-2.85025	7.59109	-0.37547	2.73515	1.48625	7
436	-0.97251	4.06089	-4.31893	4.72437	-1.07102	6.26331	-3.419	4.85671	-0.09851	2.20242	-0.04473	0.89993	0.13234	3
437	-0.97251	4.06089	-4.31893	4.72437	-1.83003	8.50997	-2.83239	5.55804	-0.85752	4.44908	-0.19274	1.48654	0.83367	5
438	-0.97251	4.06089	-4.31893	4.72437	-3.56114	10.77111	-2.28118	6.48414	-2.58863	6.71022	-0.38577	2.03775	1.75977	7
440	-1.02934	4.15453	-4.33371	4.66711	-1.15804	6.19383	-3.53074	4.75211	-0.12870	2.03930	-0.06311	0.80297	0.08500	3
441	-1.02934	4.15453	-4.33371	4.66711	-1.98576	8.21214	-3.12601	5.5022	-0.95642	4.05761	-0.23571	1.20770	0.83509	5
442	-1.02934	4.15453	-4.33371	4.66711	-3.68661	10.56455	-2.30685	6.37761	-2.65727	6.41002	-0.41455	2.02686	1.71050	7
444	-1.15117	4.14279	-4.37377	4.6379	-0.76634	7.79951	-1.83112	4.64512	0.38483	3.65672	0.10524	2.54265	0.00722	3
445	-1.15117	4.14279	-4.37377	4.6379	-1.54738	9.70348	-2.52742	5.17098	-0.39621	5.56069	-0.07125	1.84635	0.53308	5
446	-1.15117	4.14279	-4.37377	4.6379	-2.9024	13.43176	-1.02659	6.21358	-1.75123	9.28897	-0.18853	3.34718	1.57568	7
448	-1.05829	4.17597	-4.36174	4.66984	-0.71594	7.60922	-1.87206	4.60249	0.34235	3.43325	0.09972	2.48968	-0.06735	3
449	-1.05829	4.17597	-4.36174	4.66984	-1.58415	9.83158	-2.32515	5.3924	-0.52586	5.65561	-0.09298	2.03659	0.72256	5
450	-1.05829	4.17597	-4.36174	4.66984	-3.12475	13.27786	-0.86668	6.18035	-2.06646	9.10189	-0.22704	3.49506	1.51051	7
452	-1.05778	4.14305	-4.34826	4.6879	-0.81818	7.17442	-2.15108	4.58496	0.23960	3.03137	0.07904	2.19718	-0.10294	3
453	-1.05778	4.14305	-4.34826	4.6879	-1.75727	9.2336	-2.65665	5.35812	-0.69949	5.09055	-0.13741	1.69161	0.67022	5
454	-1.05778	4.14305	-4.34826	4.6879	-3.51729	12.80924	-1.05038	6.40046	-2.45951	8.66619	-0.28381	3.29788	1.71256	7
456	-1.05613	4.14852	-4.33359	4.6881	-0.92842	6.9008	-2.56604	4.72908	0.12771	2.75228	0.04640	1.76755	0.04098	3
457	-1.05613	4.14852	-4.33359	4.6881	-1.81589	8.93938	-2.78528	5.62099	-0.75976	4.79086	-0.15859	1.54831	0.93289	5

Table A.2.1 (continued): Raw and corrected wind tunnel data for 20° AWA.

AWA 20	BODY AXIS						WIND TUNNEL CORRECTIONS								VELOCITY
Run No	LIFT [N]	Cl	DRAG [N]	Cd	L/D	D/L²	Cd	β'	Cdi	Cds	BLOCKAGE	Cl	Cl²	Cd	V (m/s)
421	4.28815	0.23678	-2.301618972	0.12709	-1.86310	-0.12517	0.1274983	20.0017	0.0052759	0.1222224	1.024638005	**0.2310908**	0.053403	**0.1244325**	5
422	6.93570	0.19540	-5.32402042	0.14999	-1.30272	-0.11068	0.1502685	20.0014	0.0035927	0.1466758	1.029567395	**0.1897852**	0.0360184	**0.145953**	7
424	2.37372	0.36409	-0.829489839	0.12723	-2.86166	-0.14721	0.1281925	20.0026	0.012474	0.1157185	1.023326923	**0.3557914**	0.1265875	**0.1252703**	3
425	3.72742	0.20582	-2.276022883	0.12568	-1.63769	-0.16382	0.1259854	20.0015	0.0039863	0.1219992	1.024593001	**0.2008812**	0.0403533	**0.1229615**	5
426	5.27911	0.14873	-4.787899734	0.13489	-1.10259	-0.17180	0.135048	20.0011	0.0020814	0.1329666	1.026803851	**0.1448438**	0.0209797	**0.1315227**	7
428	1.85134	0.28397	-0.843214099	0.12934	-2.19558	-0.24602	0.1299208	20.0021	0.0075879	0.1223329	1.024660276	**0.2771322**	0.0768022	**0.126794**	3
429	3.46505	0.19133	-2.288124386	0.12635	-1.51436	-0.19057	0.1266119	20.0014	0.0034449	0.1231671	1.024828431	**0.1866984**	0.0348563	**0.1235445**	5
430	5.20045	0.14651	-4.778135839	0.13461	-1.08839	-0.17668	0.1347682	20.0011	0.0020199	0.1327483	1.026759854	**0.1426918**	0.0203609	**0.1312558**	7
432	1.86209	0.28562	-0.789170237	0.12105	-2.35956	-0.22760	0.1216381	20.0021	0.0076763	0.1139619	1.022972817	**0.2792011**	0.0779533	**0.1189065**	3
433	3.27780	0.18099	-2.220228906	0.12260	-1.47633	-0.20665	0.1228349	20.0013	0.0030826	0.1197523	1.024140074	**0.176728**	0.0312328	**0.1199396**	5
434	5.33337	0.15025	-5.274664582	0.14860	-1.01113	-0.18543	0.1487648	20.0011	0.0021244	0.1466403	1.029560248	**0.1459408**	0.0212987	**0.1444935**	7
436	1.76315	0.27044	-0.845841124	0.12974	-2.08449	-0.27209	0.1302693	20.0020	0.0068821	0.1233872	1.024872797	**0.2638751**	0.0696301	**0.1271078**	3
437	3.36666	0.18590	-2.327480195	0.12852	-1.44648	-0.20535	0.1287702	20.0013	0.003252	0.1255182	1.025302382	**0.1813132**	0.0328745	**0.1255924**	5
438	4.69401	0.13224	-4.727546915	0.13319	-0.99291	-0.21456	0.1333141	20.0010	0.0016456	0.1316685	1.026542177	**0.1288232**	0.0165954	**0.1298672**	7
440	1.62146	0.24871	-0.818420119	0.12553	-1.98120	-0.31129	0.1259815	20.0018	0.0058205	0.120161	1.024222459	**0.2428238**	0.0589634	**0.1230021**	3
441	3.01878	0.16669	-2.28652517	0.12626	-1.32025	-0.25091	0.1264596	20.0012	0.0026147	0.1238449	1.024965075	**0.1626319**	0.0264491	**0.1233794**	5
442	4.42938	0.12479	-4.68937297	0.13211	-0.94456	-0.23902	0.1322247	20.0009	0.0014653	0.1307594	1.026358929	**0.1215823**	0.0147823	**0.128829**	7
444	3.08982	0.47393	-0.889049987	0.13637	-3.47541	-0.09312	0.1379961	20.0034	0.0211355	0.1168606	1.023557147	**0.4630211**	0.2143885	**0.1348201**	3
445	4.40792	0.24340	-2.274183604	0.12558	-1.93824	-0.11705	0.1260064	20.0018	0.0055747	0.1204317	1.024277028	**0.2376287**	0.0564674	**0.1230198**	5
446	7.04063	0.19835	-4.822632759	0.13587	-1.45991	-0.09729	0.1361515	20.0014	0.0037022	0.1324493	1.026699576	**0.1931945**	0.0373241	**0.1326109**	7
448	2.89537	0.44410	-0.852536888	0.13077	-3.39619	-0.10170	0.1321969	20.0032	0.0185591	0.1136378	1.022907482	**0.4341588**	0.1884938	**0.1292364**	3
449	4.44676	0.24554	-2.428479304	0.13410	-1.83109	-0.12281	0.1345339	20.0018	0.0056734	0.1288606	1.025976147	**0.2393258**	0.0572768	**0.1311277**	5
450	6.79502	0.19143	-5.054866935	0.14241	-1.34425	-0.10948	0.1426746	20.0014	0.0034484	0.1392262	1.028065679	**0.1862071**	0.0346731	**0.1387796**	7
452	2.53789	0.38927	-0.81163925	0.12449	-3.12687	-0.12601	0.1255922	20.0028	0.0142591	0.1113331	1.022442892	**0.3807274**	0.1449533	**0.1228354**	3
453	3.93549	0.21731	-2.398376232	0.13243	-1.64090	-0.15485	0.1327769	20.0016	0.0044438	0.1283331	1.02586982	**0.2118309**	0.0448723	**0.1294286**	5
454	6.32402	0.17816	-5.275194944	0.14862	-1.19882	-0.13190	0.1488462	20.0013	0.0029869	0.1458593	1.029402802	**0.1730752**	0.029955	**0.1445947**	7
456	2.27763	0.34935	-0.821327055	0.12598	-2.77311	-0.15833	0.1268642	20.0025	0.0114845	0.1153797	1.023258619	**0.3414108**	0.1165614	**0.1239805**	3
457	3.67375	0.20286	-2.352511489	0.12990	-1.56163	-0.17431	0.1302002	20.0015	0.0038723	0.1263279	1.025465603	**0.1978205**	0.039133	**0.1269669**	5

Table A.2.1 (continued): Raw and corrected wind tunnel data for 20° AWA.

AWA 20	ZERO-ACQUIRED DATA				RAW WIND TUNNEL DATA				CORRECTED RAW DATA					VELOCITY
Run No	DF0 [N]	HF0 [N]	HM0 [Nm]	YM0 [Nm]	DF [N]	HF [N]	HM [Nm]	YM [Nm]	DFcorr.	HFcorr.	DF/HF	HMcorr.	YMcorr.	V (m/s)
460	-1.04911	4.12834	-4.34337	4.69671	-1.07742	6.66609	-3.15922	4.87499	-0.02831	2.53775	-0.01116	1.18415	0.17828	3
461	-1.04911	4.12834	-4.34337	4.69671	-1.73133	8.84192	-2.58914	5.49678	-0.68222	4.71358	-0.14473	1.75423	0.80007	5
462	-1.04911	4.12834	-4.34337	4.69671	-3.59067	11.2623	-1.97265	6.25612	-2.54156	7.13396	-0.35626	2.37072	1.55941	7
464	-1.00477	4.08192	-4.32334	4.66685	-1.06867	6.25945	-3.31497	4.73046	-0.06390	2.17753	-0.02935	1.00837	0.06361	3
465	-1.00477	4.08192	-4.32334	4.66685	-1.85711	8.36077	-3.05047	5.3941	-0.85234	4.27885	-0.19920	1.27287	0.72725	5
466	-1.00477	4.08192	-4.32334	4.66685	-3.73345	11.50362	-1.73666	6.43053	-2.72868	7.42170	-0.36766	2.58668	1.76368	7
468	-0.97881	4.06411	-4.32171	4.67029	-1.12491	6.10653	-3.59367	4.84768	-0.14610	2.04242	-0.07153	0.72804	0.17739	3
469	-0.97881	4.06411	-4.32171	4.67029	-1.92117	8.16987	-3.13396	5.6011	-0.94236	4.10576	-0.22952	1.18775	0.93081	5
470	-0.97881	4.06411	-4.32171	4.67029	-4.03802	10.68385	-2.1997	6.47268	-3.05921	6.61974	-0.46213	2.12201	1.80239	7
472	-1.05498	4.01605	-4.29407	4.51883	-1.193	6.02768	-3.56374	4.65641	-0.13802	2.01163	-0.06861	0.73033	0.13758	3
473	-1.05498	4.01605	-4.29407	4.51883	-1.99535	7.98359	-3.17951	5.37514	-0.94037	3.96754	-0.23702	1.11456	0.85631	5
474	-1.05498	4.01605	-4.29407	4.51883	-4.14941	10.78562	-1.9878	6.46768	-3.09443	6.76957	-0.45711	2.30627	1.94885	7
476	-1.04777	4.04717	-4.30935	4.63324	-1.1567	6.13927	-3.31483	5.14318	-0.10893	2.09210	-0.05207	0.99452	0.50994	3
477	-1.04777	4.04717	-4.30935	4.63324	-2.0659	7.43064	-3.27757	5.30775	-1.01813	3.38347	-0.30091	1.03178	0.67451	5
478	-1.04777	4.04717	-4.30935	4.63324	-3.29586	9.93438	-2.41061	6.18202	-2.24809	5.88721	-0.38186	1.89874	1.54878	7
480	-0.96825	4.02032	-4.32859	4.65735	-0.87544	6.97822	-2.85394	4.95778	0.09281	2.95790	0.03138	1.47465	0.30043	3
481	-0.96825	4.02032	-4.32859	4.65735	-1.25752	9.97093	-2.04875	5.32474	-0.28927	5.95061	-0.04861	2.27984	0.66739	5
482	-0.96825	4.02032	-4.32859	4.65735	-2.08647	13.19555	-0.78987	6.0692	-1.11822	9.17523	-0.12187	3.53872	1.41185	7
484	-0.92397	4.00091	-4.32736	4.68088	-0.96101	6.47191	-3.23439	4.79489	-0.03704	2.47100	-0.01499	1.09297	0.11401	3
485	-0.92397	4.00091	-4.32736	4.68088	-1.26115	9.45363	-2.18618	5.15783	-0.33718	5.45272	-0.06184	2.14118	0.47695	5
486	-0.92397	4.00091	-4.32736	4.68088	-2.1621	13.09685	-0.69962	5.79268	-1.23813	9.09594	-0.13612	3.62774	1.11180	7
488	-0.96286	3.9221	-4.32481	4.59637	-0.89441	6.62681	-2.83248	4.66917	0.06845	2.70471	0.02531	1.49233	0.07280	3
489	-0.96286	3.9221	-4.32481	4.59637	-1.21759	9.60056	-2.05758	5.07424	-0.25473	5.67846	-0.04486	2.26723	0.47787	5
490	-0.96286	3.9221	-4.32481	4.59637	-2.07671	13.47331	-0.55384	5.6685	-1.11385	9.55121	-0.11662	3.77097	1.07213	7
492	-0.96891	3.8971	-4.3195	4.57699	-1.04015	6.22639	-3.40306	4.84898	-0.07124	2.32929	-0.03058	0.91644	0.27199	3
493	-0.96891	3.8971	-4.3195	4.57699	-1.56242	8.76544	-2.85688	5.25118	-0.59351	4.86834	-0.12191	1.46262	0.67419	5
494	-0.96891	3.8971	-4.3195	4.57699	-2.35505	12.08753	-1.24988	5.90421	-1.38614	8.19043	-0.16924	3.06962	1.32722	7
496	-0.99711	3.82466	-4.29439	4.4909	-1.1165	5.97994	-3.50511	4.6906	-0.11939	2.15528	-0.05539	0.78928	0.19970	3

Table A.2.1 (continued): Raw and corrected wind tunnel data for 20° AWA.

AWA 20	BODY AXIS						WIND TUNNEL CORRECTIONS								VELOCITY
Run No	LIFT [N]	Cl	DRAG [N]	Cd	L/D	D/L²	Cd	β'	Cdi	Cds	BLOCKAGE	Cl	Cl²	Cd	V (m/s)
460	2.05683	0.31548	-0.894564317	0.13721	-2.29925	-0.21145	0.1379342	20.0023	0.0093658	0.1285684	1.025917253	**0.3075149**	0.0945654	**0.1344496**	3
461	3.63383	0.20065	-2.253216407	0.12442	-1.61273	-0.17064	0.1247109	20.0015	0.0037886	0.1209222	1.024375913	**0.1958789**	0.0383686	**0.1217433**	5
462	5.05279	0.14235	-4.828243199	0.13602	-1.04651	-0.18911	0.1361711	20.0010	0.0019068	0.1342643	1.027065456	**0.138599**	0.0192097	**0.1325827**	7
464	1.75314	0.26890	-0.804805481	0.12344	-2.17834	-0.26185	0.1239691	20.0020	0.0068043	0.1171648	1.023618476	**0.2626994**	0.069011	**0.1211087**	3
465	3.22966	0.17834	-2.264390499	0.12504	-1.42628	-0.21709	0.1252665	20.0013	0.0029927	0.1222738	1.024648361	**0.1740461**	0.030292	**0.1222532**	5
466	5.23153	0.14739	-5.102491358	0.14375	-1.02529	-0.18643	0.143908	20.0011	0.0020441	0.1418639	1.028597404	**0.1432881**	0.0205315	**0.139907**	7
468	1.61884	0.24830	-0.835837873	0.12820	-1.93679	-0.31894	0.1286516	20.0018	0.0058017	0.1228499	1.0247645	**0.242304**	0.0587112	**0.1255426**	3
469	3.06213	0.16909	-2.289781362	0.12644	-1.33730	-0.24420	0.1266452	20.0012	0.0026903	0.1239549	1.02498725	**0.1649636**	0.027213	**0.1235578**	5
470	4.48100	0.12624	-5.138801486	0.14477	-0.87199	-0.25592	0.144889	20.0009	0.0014996	0.1433893	1.028904899	**0.1226948**	0.015054	**0.1408186**	7
472	1.59618	0.24483	-0.817714356	0.12542	-1.95200	-0.32095	0.1258593	20.0018	0.0056404	0.1202189	1.024234136	**0.2390355**	0.057138	**0.1228814**	3
473	2.95024	0.16291	-2.240637349	0.12372	-1.31670	-0.25743	0.1239167	20.0012	0.0024973	0.1214194	1.024476133	**0.159015**	0.0252858	**0.1209561**	5
474	4.59250	0.12938	-5.223142338	0.14715	-0.87926	-0.24765	0.1472709	20.0009	0.0015752	0.1456957	1.029369824	**0.1256909**	0.0157982	**0.143069**	7
476	1.67028	0.25619	-0.817901059	0.12545	-2.04216	-0.29317	0.1259293	20.0019	0.0061763	0.119753	1.024140217	**0.2501557**	0.0625779	**0.122961**	3
477	2.45189	0.13539	-2.113944142	0.11673	-1.15987	-0.35163	0.1168613	20.0010	0.0017249	0.1151365	1.023209598	**0.1323181**	0.0175081	**0.1142106**	5
478	4.12512	0.11622	-4.126057992	0.11624	-0.99977	-0.24247	0.1163397	20.0008	0.0012709	0.1150688	1.023195958	**0.1135806**	0.0129006	**0.1137023**	7
480	2.43462	0.37343	-0.92444851	0.14180	-2.63359	-0.15596	0.1428077	20.0027	0.0131223	0.1296853	1.026142408	**0.3639185**	0.1324367	**0.1391694**	3
481	4.75691	0.26267	-2.307053369	0.12739	-2.06190	-0.10195	0.1278922	20.0019	0.0064924	0.1213998	1.024472181	**0.2563938**	0.0657378	**0.1248371**	5
482	7.13557	0.20103	-4.188896562	0.11801	-1.70345	-0.08227	0.1183053	20.0015	0.0038027	0.1145026	1.02308181	**0.1964919**	0.0386091	**0.1156362**	7
484	1.99992	0.30676	-0.879937989	0.13497	-2.27280	-0.22000	0.1356513	20.0022	0.0088547	0.1267966	1.025560092	**0.299111**	0.0894674	**0.1322705**	3
485	4.33754	0.23951	-2.181785634	0.12047	-1.98807	-0.11596	0.1208907	20.0017	0.0053981	0.1154926	1.023281393	**0.2340621**	0.054785	**0.1181402**	5
486	7.03552	0.19821	-4.274456327	0.12042	-1.64595	-0.08636	0.1207076	20.0014	0.0036969	0.1170107	1.023587413	**0.1936413**	0.037497	**0.117926**	7
488	2.22136	0.34072	-0.860743342	0.13202	-2.58075	-0.17444	0.1328668	20.0025	0.0109241	0.1219427	1.024581614	**0.3325469**	0.1105874	**0.1296791**	3
489	4.54567	0.25100	-2.181515604	0.12046	-2.08372	-0.10558	0.1209167	20.0018	0.0059285	0.1149882	1.023179702	**0.2453174**	0.0601806	**0.1181774**	5
490	7.44283	0.20968	-4.313382839	0.12152	-1.72552	-0.07786	0.1218382	20.0015	0.0041373	0.1177009	1.023726544	**0.204824**	0.0419529	**0.1190144**	7
492	1.87447	0.28751	-0.863607802	0.13246	-2.17051	-0.24579	0.1330636	20.0021	0.0077786	0.1252849	1.025255354	**0.2804314**	0.0786417	**0.1297858**	3
493	3.78605	0.20906	-2.222787312	0.12274	-1.70329	-0.15507	0.1230556	20.0015	0.0041127	0.1189429	1.023976918	**0.2041637**	0.0416828	**0.1201742**	5
494	6.25478	0.17621	-4.103837572	0.11562	-1.52413	-0.10490	0.115841	20.0013	0.0029219	0.1129191	1.02276262	**0.1722915**	0.0296844	**0.1132629**	7
496	1.71860	0.26361	-0.849339077	0.13028	-2.02345	-0.28756	0.1307793	20.0019	0.0065388	0.1242406	1.025044832	**0.257165**	0.0661338	**0.127584**	3

Table A.2.1 (continued): Raw and corrected wind tunnel data for 20° AWA.

AWA 20	ZERO-ACQUIRED DATA				RAW WIND TUNNEL DATA				CORRECTED RAW DATA					VELOCITY
Run No	DF0 [N]	HF0 [N]	HM0 [Nm]	YM0 [Nm]	DF [N]	HF [N]	HM [Nm]	YM [Nm]	DFcorr.	HFcorr.	DF/HF	HMcorr.	YMcorr.	V (m/s)
498	-0.99711	3.82466	-4.29439	4.4909	-2.48287	11.80191	-1.3308	5.73939	-1.48576	7.97725	-0.18625	2.96359	1.24849	7
500	-1.11225	3.72543	-4.29303	4.41227	-1.34534	5.47521	-3.71343	4.42875	-0.23309	1.74978	-0.13321	0.57960	0.01648	3
501	-1.11225	3.72543	-4.29303	4.41227	-1.69757	8.19334	-2.73352	4.93072	-0.58532	4.46791	-0.13101	1.55951	0.51845	5
502	-1.11225	3.72543	-4.29303	4.41227	-2.53782	11.60106	-1.34563	5.68738	-1.42557	7.87563	-0.18101	2.94740	1.27511	7
504	-0.93914	3.70109	-4.29456	4.52098	-1.3089	5.12212	-4.22164	4.85462	-0.36976	1.42103	-0.26021	0.07292	0.33364	3
505	-0.93914	3.70109	-4.29456	4.52098	-1.86331	7.36442	-3.29419	5.31535	-0.92417	3.66333	-0.25228	1.00037	0.79437	5
506	-0.93914	3.70109	-4.29456	4.52098	-2.9528	9.94832	-2.2135	5.96497	-2.01366	6.24723	-0.32233	2.08106	1.44399	7
508	-0.99128	3.58741	-4.2795	4.38172	-1.40602	4.81594	-4.31933	4.62205	-0.41474	1.22853	-0.33759	-0.03983	0.24033	3
509	-0.99128	3.58741	-4.2795	4.38172	-1.86984	7.0067	-3.17248	4.98613	-0.87856	3.41929	-0.25694	1.10702	0.60441	5
510	-0.99128	3.58741	-4.2795	4.38172	-2.99231	9.79818	-2.16575	5.81935	-2.00103	6.21077	-0.32219	2.11375	1.43763	7
512	-0.95736	3.53443	-4.27397	4.36717	-1.37959	4.61032	-4.30076	4.56657	-0.42223	1.07589	-0.39245	-0.02679	0.19940	3
513	-0.95736	3.53443	-4.27397	4.36717	-1.87226	6.81464	-3.19515	4.98451	-0.91490	3.28021	-0.27892	1.07882	0.61734	5
514	-0.95736	3.53443	-4.27397	4.36717	-3.08768	9.69831	-2.19398	5.806	-2.13032	6.16388	-0.34561	2.07999	1.43883	7

Table A.2.1 (continued): Raw and corrected wind tunnel data for 20° AWA.

AWA 20	BODY AXIS						WIND TUNNEL CORRECTIONS								VELOCITY
Run No	LIFT [N]	Cl	DRAG [N]	Cd	L/D	D/L²	Cd	β'	Cdi	Cds	BLOCKAGE	Cl	Cl²	Cd	V (m/s)
498	6.05179	0.17049	-4.124537897	0.11620	-1.46726	-0.11262	0.1164098	20.0012	0.0027353	0.1136745	1.02291489	**0.1666752**	0.0277806	**0.1138021**	7
500	1.35493	0.20782	-0.817492959	0.12539	-1.65742	-0.44530	0.1257038	20.0015	0.0040642	0.1216396	1.024520517	**0.2028501**	0.0411481	**0.1226953**	3
501	3.46260	0.19120	-2.078136103	0.11475	-1.66621	-0.17333	0.1150164	20.0014	0.00344	0.1115764	1.022491937	**0.1869931**	0.0349664	**0.1124863**	5
502	5.98692	0.16867	-4.033221711	0.11363	-1.48440	-0.11252	0.1138327	20.0012	0.002677	0.1111557	1.022407145	**0.1649704**	0.0272152	**0.111338**	7
504	1.04691	0.16058	-0.833481628	0.12784	-1.25607	-0.76046	0.1280299	20.0012	0.0024264	0.1256035	1.025319576	**0.1566137**	0.0245279	**0.1248683**	3
505	2.70747	0.14950	-2.121368381	0.11714	-1.27629	-0.28939	0.1173005	20.0011	0.0021032	0.1151973	1.023221853	**0.146109**	0.0213478	**0.1146384**	5
506	4.48754	0.12643	-4.028899943	0.11350	-1.11384	-0.20006	0.1136205	20.0009	0.001504	0.1121165	1.022600815	**0.1236314**	0.0152847	**0.1111093**	7
508	0.87693	0.13451	-0.809910124	0.12423	-1.08275	-1.05319	0.1243586	20.0010	0.0017025	0.1226561	1.024725436	**0.1312615**	0.0172296	**0.121358**	3
509	2.52238	0.13928	-1.995042405	0.11016	-1.26433	-0.31357	0.1103036	20.0010	0.0018255	0.1084781	1.021867376	**0.136301**	0.018578	**0.1079431**	5
510	4.46161	0.12570	-4.004561571	0.11282	-1.11413	-0.20117	0.1129335	20.0009	0.0014867	0.1114468	1.022465819	**0.1229332**	0.0151126	**0.1104521**	7
512	0.75049	0.11511	-0.764742467	0.11730	-0.98137	-1.35776	0.1173955	20.0008	0.0012469	0.1161485	1.023413613	**0.1124801**	0.0126518	**0.1147097**	3
513	2.39844	0.13244	-1.981622673	0.10942	-1.21034	-0.34448	0.109549	20.0010	0.0016505	0.1078986	1.021750556	**0.1296182**	0.0168009	**0.107217**	5
514	4.38515	0.12354	-4.110017105	0.11579	-1.06694	-0.21373	0.1159006	20.0009	0.0014362	0.1144644	1.023074112	**0.1207548**	0.0145817	**0.1132866**	7

Table A.2.2 : Run numbers for 20° AWA.

AWA 20°	Wind Speed	Twist Angle (°)		Sheeting Angle (°)		AWA 20°	Wind Speed	Twist Angle (°)		Sheeting Angle (°)	
Run No	m/s	Main Sail	Jib Sail	Main Sail	Jib Sail	Run No	m/s	Main Sail	Jib Sail	Main Sail	Jib Sail
130	zero	7	9	4	10	163	zero	7	9	8	10
131	3	7	9	4	10	164	3	7	9	8	10
132	5	7	9	4	10	165	5	7	9	8	10
133	7	7	9	4	10	166	7	7	9	8	10
135	zero	7	9	4	12	167	zero	7	9	8	12
136	3	7	9	4	12	168	3	7	9	8	12
137	5	7	9	4	12	169	5	7	9	8	12
138	7	7	9	4	12	170	7	7	9	8	12
139	zero	7	9	4	14	171	zero	7	9	8	14
140	3	7	9	4	14	172	3	7	9	8	14
141	5	7	9	4	14	173	5	7	9	8	14
142	7	7	9	4	14	174	7	7	9	8	14
147	zero	7	9	6	10	195	zero	7	13	4	10
148	3	7	9	6	10	196	3	7	13	4	10
149	5	7	9	6	10	197	5	7	13	4	10
150	7	7	9	6	10	198	7	7	13	4	10
151	zero	7	9	6	12	199	zero	7	13	4	12
152	3	7	9	6	12	200	3	7	13	4	12
153	5	7	9	6	12	201	5	7	13	4	12
154	7	7	9	6	12	202	7	7	13	4	12
155	zero	7	9	6	14	203	zero	7	13	4	14
156	3	7	9	6	14	204	3	7	13	4	14
157	5	7	9	6	14	205	5	7	13	4	14
158	7	7	9	6	14	206	7	7	13	4	14

Table A.2.2 (continued): Run numbers for 20° AWA.

AWA 20°	Wind Speed	Twist Angle (°)		Sheeting Angle (°)		AWA 20°	Wind Speed	Twist Angle (°)		Sheeting Angle (°)	
Run No	m/s	Main Sail	Jib Sail	Main Sail	Jib Sail	Run No	m/s	Main Sail	Jib Sail	Main Sail	Jib Sail
211	zero	7	13	6	10	261	5	7	18	4	10
212	3	7	13	6	10	262	7	7	18	4	10
213	5	7	13	6	10	263	zero	7	18	4	12
214	7	7	13	6	10	264	3	7	18	4	12
215	zero	7	13	6	12	265	5	7	18	4	12
216	3	7	13	6	12	266	7	7	18	4	12
217	5	7	13	6	12	267	zero	7	18	4	14
218	7	7	13	6	12	268	3	7	18	4	14
219	zero	7	13	6	14	269	5	7	18	4	14
220	3	7	13	6	14	270	7	7	18	4	14
221	5	7	13	6	14	275	zero	7	18	6	10
222	7	7	13	6	14	276	3	7	18	6	10
227	zero	7	13	8	10	277	5	7	18	6	10
228	3	7	13	8	10	278	7	7	18	6	10
229	5	7	13	8	10	279	zero	7	18	6	12
230	7	7	13	8	10	280	3	7	18	6	12
231	zero	7	13	8	12	281	5	7	18	6	12
232	3	7	13	8	12	282	7	7	18	6	12
233	5	7	13	8	12	283	zero	7	18	6	14
234	7	7	13	8	12	284	3	7	18	6	14
235	zero	7	13	8	14	285	5	7	18	6	14
236	3	7	13	8	14	286	7	7	18	6	14
237	5	7	13	8	14	291	zero	7	18	8	10
238	7	7	13	8	14	292	3	7	18	8	10
259	zero	7	18	4	10	293	5	7	18	8	10
260	3	7	18	4	10	294	7	7	18	8	10

Table A.2.2 (continued): Run numbers for 20° AWA.

AWA 20°	Wind Speed	Twist Angle (°)		Sheeting Angle (°)		AWA 20°	Wind Speed	Twist Angle (°)		Sheeting Angle (°)	
Run No	m/s	Main Sail	Jib Sail	Main Sail	Jib Sail	Run No	m/s	Main Sail	Jib Sail	Main Sail	Jib Sail
295	zero	7	18	8	12	321	5	10	9	6	12
296	3	7	18	8	12	322	7	10	9	6	12
297	5	7	18	8	12	323	zero	10	9	6	14
298	7	7	18	8	12	324	3	10	9	6	14
299	zero	7	18	8	14	325	5	10	9	6	14
300	3	7	18	8	14	326	7	10	9	6	14
301	5	7	18	8	14	327	zero	10	9	8	10
302	7	7	18	8	14	328	3	10	9	8	10
303	zero	10	9	4	10	329	5	10	9	8	10
304	3	10	9	4	10	330	7	10	9	8	10
305	5	10	9	4	10	331	zero	10	9	8	12
306	7	10	9	4	10	332	3	10	9	8	12
307	zero	10	9	4	12	333	5	10	9	8	12
308	3	10	9	4	12	334	7	10	9	8	12
309	5	10	9	4	12	335	zero	10	9	8	14
310	7	10	9	4	12	336	3	10	9	8	14
311	zero	10	9	4	14	337	5	10	9	8	14
312	3	10	9	4	14	338	7	10	9	8	14
313	5	10	9	4	14	339	zero	10	13	4	10
314	7	10	9	4	14	340	3	10	13	4	10
315	zero	10	9	6	10	341	5	10	13	4	10
316	3	10	9	6	10	342	7	10	13	4	10
317	5	10	9	6	10	343	zero	10	13	4	12
318	7	10	9	6	10	344	3	10	13	4	12
319	zero	10	9	6	12	345	5	10	13	4	12
320	3	10	9	6	12	346	7	10	13	4	12

Table A.2.2 (continued): Run numbers for 20° AWA.

AWA 20°	Wind Speed	Twist Angle (°)		Sheeting Angle (°)		AWA 20°	Wind Speed	Twist Angle (°)		Sheeting Angle (°)	
Run No	m/s	Main Sail	Jib Sail	Main Sail	Jib Sail	Run No	m/s	Main Sail	Jib Sail	Main Sail	Jib Sail
347	zero	10	13	4	14	373	5	10	13	8	14
348	3	10	13	4	14	374	7	10	13	8	14
349	5	10	13	4	14	375	zero	10	18	4	10
350	7	10	13	4	14	376	3	10	18	4	10
351	zero	10	13	6	10	377	5	10	18	4	10
352	3	10	13	6	10	378	7	10	18	4	10
353	5	10	13	6	10	379	zero	10	18	4	12
354	7	10	13	6	10	380	3	10	18	4	12
355	zero	10	13	6	12	381	5	10	18	4	12
356	3	10	13	6	12	382	7	10	18	4	12
357	5	10	13	6	12	383	zero	10	18	4	14
358	7	10	13	6	12	384	3	10	18	4	14
359	zero	10	13	6	14	385	5	10	18	4	14
360	3	10	13	6	14	386	7	10	18	4	14
361	5	10	13	6	14	387	zero	10	18	6	10
362	7	10	13	6	14	388	3	10	18	6	10
363	zero	10	13	8	10	389	5	10	18	6	10
364	3	10	13	8	10	390	7	10	18	6	10
365	5	10	13	8	10	391	zero	10	18	6	12
366	7	10	13	8	10	392	3	10	18	6	12
367	zero	10	13	8	12	393	5	10	18	6	12
368	3	10	13	8	12	394	7	10	18	6	12
369	5	10	13	8	12	395	zero	10	18	6	14
370	7	10	13	8	12	396	3	10	18	6	14
371	zero	10	13	8	14	397	5	10	18	6	14
372	3	10	13	8	14	398	7	10	18	6	14

Table A.2.2 (continued): Run numbers for 20° AWA.

AWA 20°	Wind Speed	Twist Angle (°)		Sheeting Angle (°)		AWA 20°	Wind Speed	Twist Angle (°)		Sheeting Angle (°)	
Run No	m/s	Main Sail	Jib Sail	Main Sail	Jib Sail	Run No	m/s	Main Sail	Jib Sail	Main Sail	Jib Sail
399	zero	10	18	8	10	425	5	12	9	6	10
400	3	10	18	8	10	426	7	12	9	6	10
401	5	10	18	8	10	427	zero	12	9	6	12
402	7	10	18	8	10	428	3	12	9	6	12
403	zero	10	18	8	12	429	5	12	9	6	12
404	3	10	18	8	12	430	7	12	9	6	12
405	5	10	18	8	12	431	zero	12	9	6	14
406	7	10	18	8	12	432	3	12	9	6	14
407	zero	10	18	8	14	433	5	12	9	6	14
408	3	10	18	8	14	434	7	12	9	6	14
409	5	10	18	8	14	435	zero	12	9	8	10
410	7	10	18	8	14	436	3	12	9	8	10
411	zero	12	9	4	10	437	5	12	9	8	10
412	3	12	9	4	10	438	7	12	9	8	10
413	5	12	9	4	10	439	zero	12	9	8	12
414	7	12	9	4	10	440	3	12	9	8	12
415	zero	12	9	4	12	441	5	12	9	8	12
416	3	12	9	4	12	442	7	12	9	8	12
417	5	12	9	4	12	443	zero	12	13	4	10
418	7	12	9	4	12	444	3	12	13	4	10
419	zero	12	9	4	14	445	5	12	13	4	10
420	3	12	9	4	14	446	7	12	13	4	10
421	5	12	9	4	14	447	zero	12	13	4	12
422	7	12	9	4	14	448	3	12	13	4	12
423	zero	12	9	6	10	449	5	12	13	4	12
424	3	12	9	6	10	450	7	12	13	4	12

Table A.2.2 (continued): Run numbers for 20° AWA.

AWA 20°	Wind Speed	Twist Angle (°)		Sheeting Angle (°)		AWA 20°	Wind Speed	Twist Angle (°)		Sheeting Angle (°)	
Run No	m/s	Main Sail	Jib Sail	Main Sail	Jib Sail	Run No	m/s	Main Sail	Jib Sail	Main Sail	Jib Sail
451	zero	12	13	4	14	477	5	12	13	8	14
452	3	12	13	4	14	478	7	12	13	8	14
453	5	12	13	4	14	479	zero	12	18	4	10
454	7	12	13	4	14	480	3	12	18	4	10
455	zero	12	13	6	10	481	5	12	18	4	10
456	3	12	13	6	10	482	7	12	18	4	10
457	5	12	13	6	10	483	zero	12	18	4	12
458	7	12	13	6	10	484	3	12	18	4	12
459	zero	12	13	6	12	485	5	12	18	4	12
460	3	12	13	6	12	486	7	12	18	4	12
461	5	12	13	6	12	487	zero	12	18	4	14
462	7	12	13	6	12	488	3	12	18	4	14
463	zero	12	13	6	14	489	5	12	18	4	14
464	3	12	13	6	14	490	7	12	18	4	14
465	5	12	13	6	14	491	zero	12	18	6	10
466	7	12	13	6	14	492	3	12	18	6	10
467	zero	12	13	8	10	493	5	12	18	6	10
468	3	12	13	8	10	494	7	12	18	6	10
469	5	12	13	8	10	495	zero	12	18	6	12
470	7	12	13	8	10	496	3	12	18	6	12
471	zero	12	13	8	12	497	5	12	18	6	12
472	3	12	13	8	12	498	7	12	18	6	12
473	5	12	13	8	12	499	zero	12	18	6	14
474	7	12	13	8	12	500	3	12	18	6	14
475	zero	12	13	8	14	501	5	12	18	6	14
476	3	12	13	8	14	502	7	12	18	6	14

Table A.2.2 (continued): Run numbers for 20° AWA.

AWA 20°	Wind Speed	Twist Angle (°)		Sheeting Angle (°)		AWA 20°	Wind Speed	Twist Angle (°)		Sheeting Angle (°)	
Run No	m/s	Main Sail	Jib Sail	Main Sail	Jib Sail	Run No	m/s	Main Sail	Jib Sail	Main Sail	Jib Sail
503	zero	12	18	8	10	509	5	12	18	8	12
504	3	12	18	8	10	510	7	12	18	8	12
505	5	12	18	8	10	511	zero	12	18	8	14
506	7	12	18	8	10	512	3	12	18	8	14
507	zero	12	18	8	12	513	5	12	18	8	14
508	3	12	18	8	12	514	7	12	18	8	14

Table A.2.3 : Raw and corrected wind tunnel data for 28° AWA.

AWA 28	ZERO-ACQUIRED DATA				RAW WIND TUNNEL DATA				CORRECTED RAW DATA					VELOCITY
Run No	DF0 [N]	HF0 [N]	HM0 [Nm]	YM0 [Nm]	DF [N]	HF [N]	HM [Nm]	YM [Nm]	DFcorr.	HFcorr.	DF/HF	HMcorr.	YMcorr.	V (m/s)
516	-0.80733	3.27085	-4.26686	4.51454	1.70789	11.26699	2.34173	4.80267	2.51522	7.99614	0.3145543	6.60859	0.28813	3
517	-0.80733	3.27085	-4.26686	4.51454	4.50888	20.96452	8.67922	5.70829	5.31621	17.69367	0.3004583	12.94608	1.19375	5
518	-0.80733	3.27085	-4.26686	4.51454	5.80564	29.62109	12.04567	6.98046	6.61297	26.35024	0.2509643	16.31253	2.46592	7
520	-0.74187	3.15545	-4.21292	4.38964	1.66871	10.54814	1.9064	4.52623	2.41058	7.39269	0.3260762	6.11932	0.13659	3
521	-0.74187	3.15545	-4.21292	4.38964	4.19594	19.63395	7.78064	5.2018	4.93781	16.4785	0.2996517	11.99356	0.81216	5
522	-0.74187	3.15545	-4.21292	4.38964	5.31182	28.02586	11.03494	6.32131	6.05369	24.87041	0.2434093	15.24786	1.93167	7
524	-0.73971	3.02524	-4.20691	4.33281	1.50692	9.9432	1.61047	4.297	2.24663	6.91796	0.3247533	5.81738	-0.03581	3
525	-0.73971	3.02524	-4.20691	4.33281	3.70973	18.22792	6.96439	4.67768	4.44944	15.20268	0.2926747	11.17130	0.34487	5
526	-0.73971	3.02524	-4.20691	4.33281	4.33543	25.62915	9.57548	5.58366	5.07514	22.60391	0.2245249	13.78239	1.25085	7
528	-0.66323	2.9409	-4.19383	4.27565	1.45623	9.6435	1.21673	4.52714	2.11946	6.7026	0.3162146	5.41056	0.25149	3
529	-0.66323	2.9409	-4.19383	4.27565	3.55161	17.80193	6.18371	5.45871	4.21484	14.86103	0.2836169	10.37754	1.18306	5
530	-0.66323	2.9409	-4.19383	4.27565	4.35336	25.17855	8.39162	6.9059	5.01659	22.23765	0.2255899	12.58545	2.63025	7
532	-0.71054	2.64076	-4.11146	3.98541	1.37074	9.09934	1.05684	4.13412	2.08128	6.45858	0.3222504	5.16830	0.14871	3
533	-0.71054	2.64076	-4.11146	3.98541	3.26144	16.63161	5.6123	4.79685	3.97198	13.99085	0.2838984	9.72376	0.81144	5
534	-0.71054	2.64076	-4.11146	3.98541	3.7038	23.28072	7.38345	5.97686	4.41434	20.63996	0.2138735	11.49491	1.99145	7
536	-0.81767	2.3692	-4.0581	3.70159	1.09881	8.36766	0.80742	3.68426	1.91648	5.99846	0.3194953	4.86552	-0.01733	3
537	-0.81767	2.3692	-4.0581	3.70159	2.60132	15.07149	4.78937	4.04536	3.41899	12.70229	0.2691633	8.84747	0.34377	5
538	-0.81767	2.3692	-4.0581	3.70159	2.11227	19.71352	4.81559	4.88088	2.92994	17.34432	0.1689279	8.87369	1.17929	7
540	-0.67381	2.16136	-4.01968	3.60369	1.23969	8.2565	0.72618	3.8831	1.9135	6.09514	0.3139386	4.74586	0.27941	3
541	-0.67381	2.16136	-4.01968	3.60369	2.8827	15.36794	4.81286	4.84689	3.55651	13.20658	0.2692983	8.83254	1.2432	5
542	-0.67381	2.16136	-4.01968	3.60369	3.43427	22.01918	6.6179	6.32997	4.10808	19.85782	0.2068747	10.63758	2.72628	7
544	-0.49757	1.9892	-4.03451	3.45873	1.33853	7.80756	0.58973	3.61194	1.8361	5.81836	0.31557	4.62424	0.15321	3
445	-0.49757	1.9892	-4.03451	3.45873	2.81843	14.50502	4.42532	4.35715	3.316	12.51582	0.2649447	8.45983	0.89842	5
546	-0.49757	1.9892	-4.03451	3.45873	3.10411	20.58807	5.87721	5.59826	3.60168	18.59887	0.1936505	9.91172	2.13953	7
548	-0.52633	1.62195	-3.94442	3.14274	1.17601	7.05489	0.36304	3.17751	1.70234	5.43294	0.3133368	4.30746	0.03477	3

Table A.2.3 (continued): Raw and corrected wind tunnel data for 28° AWA.

AWA 28	BODY AXIS						WIND TUNNEL CORRECTIONS								VELOCITY
Run No	LIFT [N]	Cl	DRAG [N]	Cd	L/D	D/L²	Cd	β'	Cdi	Cds	BLOCKAGE	Cl	Cl²	Cd	V (m/s)
516	7.13691	1.09469	1.533152898	0.23516	4.65506	0.03010	0.2438576	28.0079	0.1127634	0.1310942	1.026426412	1.0665047	1.1374323	0.2375792	3
517	15.69099	0.86643	3.612740084	0.19949	4.34324	0.01467	0.204937	28.0063	0.0706404	0.1342967	1.027071977	0.8435914	0.7116464	0.1995352	5
518	22.83751	0.64339	6.531782409	0.18402	3.49637	0.01252	0.1870212	28.0047	0.0389527	0.1480685	1.029848151	0.6247441	0.3903052	0.1816008	7
520	6.63294	1.01739	1.342241919	0.20588	4.94169	0.03051	0.2133901	28.0074	0.0974	0.11599	1.023381658	0.9941422	0.9883186	0.2085146	3
521	14.60795	0.80663	3.376359694	0.18644	4.32654	0.01582	0.1911584	28.0059	0.0612253	0.1299331	1.026192353	0.7860377	0.6178552	0.1862793	5
522	21.47856	0.60511	6.330859236	0.17836	3.39268	0.01372	0.1810138	28.0044	0.0344549	0.146559	1.029543849	0.5877423	0.345441	0.1758194	7
524	6.20328	0.95148	1.264128942	0.19390	4.90715	0.03285	0.2004671	28.0069	0.0851901	0.115277	1.023237923	0.9298751	0.8646677	0.1959145	3
525	13.43383	0.74179	3.208603601	0.17717	4.18682	0.01778	0.1811667	28.0054	0.0517788	0.1293879	1.026082445	0.722937	0.5226379	0.1765616	5
526	19.34762	0.54507	6.130810306	0.17272	3.15580	0.01638	0.1748768	28.0040	0.0279573	0.1469195	1.029616536	0.5293935	0.2802574	0.1698466	7
528	5.98689	0.91829	1.275307992	0.19561	4.69447	0.03558	0.2017315	28.0067	0.0793507	0.1223808	1.024669936	0.8961854	0.8031482	0.1968746	3
529	13.07721	0.72210	3.255348146	0.17975	4.01715	0.01904	0.1835387	28.0052	0.0490662	0.1344725	1.027107415	0.7030429	0.4942694	0.1786947	5
530	19.04375	0.53651	6.010558233	0.16933	3.16838	0.01657	0.1714218	28.0039	0.027086	0.1443358	1.0290957	0.5213427	0.2717982	0.1665752	7
532	5.78478	0.88729	1.19445848	0.18321	4.84302	0.03569	0.1889242	28.0064	0.0740834	0.1148408	1.023149996	0.867217	0.7520654	0.1846496	3
533	12.31308	0.67991	3.061256034	0.16904	4.02223	0.02019	0.1723919	28.0049	0.0434996	0.1288923	1.025982545	0.6626885	0.439156	0.1680262	5
534	17.57721	0.49520	5.7922434	0.16318	3.03461	0.01875	0.164962	28.0036	0.0230749	0.1418871	1.028602078	0.4814255	0.2317705	0.1603749	7
536	5.36594	0.82305	1.123954988	0.17240	4.77416	0.03904	0.1773127	28.0060	0.063744	0.1135687	1.022893562	0.8046294	0.6474285	0.1733443	3
537	11.10294	0.61309	2.944574947	0.16259	3.77064	0.02389	0.165322	28.0044	0.0353695	0.1299525	1.026196271	0.5974347	0.3569282	0.1611018	5
538	14.45366	0.40720	5.555681546	0.15652	2.60160	0.02659	0.1577212	28.0030	0.0156026	0.1421186	1.028648747	0.3958561	0.1567021	0.1533285	7
540	5.43866	0.83420	1.171974682	0.17976	4.64059	0.03962	0.1848123	28.0061	0.0654834	0.119329	1.024054735	0.8146084	0.6635869	0.1804712	3
541	11.54446	0.63747	3.059901808	0.16896	3.77282	0.02296	0.1719114	28.0046	0.0382384	0.133673	1.026946255	0.6207386	0.3853164	0.1674006	5
542	16.85462	0.47484	5.695462442	0.16046	2.95931	0.02005	0.1620921	28.0034	0.0212167	0.1408754	1.028398138	0.461726	0.2131909	0.1576161	7
544	5.19555	0.79691	1.110374487	0.17031	4.67910	0.04113	0.1749225	28.0058	0.05976	0.1151625	1.023214845	0.7788339	0.6065823	0.1709538	3
445	10.91849	0.60290	2.947967357	0.16278	3.70373	0.02473	0.1654195	28.0044	0.034204	0.1312154	1.02645085	0.5873635	0.3449959	0.1611567	5
546	15.68607	0.44192	5.551545879	0.15640	2.82553	0.02256	0.1578186	28.0032	0.0183767	0.1394419	1.028109159	0.4298348	0.184758	0.1535037	7
548	4.84645	0.74337	1.047533827	0.16067	4.62654	0.04460	0.1646852	28.0054	0.051999	0.1126861	1.022715653	0.7268575	0.5283218	0.1610273	3

Table A.2.3 (continued): Raw and corrected wind tunnel data for 28° AWA.

AWA 28	ZERO-ACQUIRED DATA				RAW WIND TUNNEL DATA				CORRECTED RAW DATA					VELOCITY
Run No	DF0 [N]	HF0 [N]	HM0 [Nm]	YM0 [Nm]	DF [N]	HF [N]	HM [Nm]	YM [Nm]	DFcorr.	HFcorr.	DF/HF	HMcorr.	YMcorr.	V (m/s)
550	-0.52633	1.62195	-3.94442	3.14274	1.69651	17.17956	3.32775	4.39532	2.22284	15.55761	0.142878	7.27217	1.25258	7
552	-0.4638	1.60907	-3.98167	3.0934	1.96001	9.22269	2.27875	3.3387	2.42381	7.61362	0.3183518	6.26042	0.2453	3
553	-0.4638	1.60907	-3.98167	3.0934	4.51802	18.3423	8.19354	4.09008	4.98182	16.73323	0.2977202	12.17521	0.99668	5
554	-0.4638	1.60907	-3.98167	3.0934	5.65375	26.72997	11.38845	5.33564	6.11755	25.1209	0.2435243	15.37012	2.24224	7
556	-0.46727	1.36255	-3.88647	2.88501	1.9022	8.68784	2.08197	3.06935	2.36947	7.32529	0.3234643	5.96844	0.18434	3
557	-0.46727	1.36255	-3.88647	2.88501	4.3478	17.68466	7.84404	3.82383	4.81507	16.32211	0.2950029	11.73051	0.93882	5
558	-0.46727	1.36255	-3.88647	2.88501	5.55913	26.34125	11.24904	5.16576	6.0264	24.9787	0.2412616	15.13551	2.28075	7
560	-0.50354	1.28163	-3.88757	2.76037	1.87273	8.89467	2.2764	3.11051	2.37627	7.61304	0.3121316	6.16397	0.35014	3
561	-0.50354	1.28163	-3.88757	2.76037	4.39462	17.91791	8.03529	3.85065	4.89816	16.63628	0.2944264	11.92286	1.09028	5
562	-0.50354	1.28163	-3.88757	2.76037	5.44581	26.17169	10.99172	5.13915	5.94935	24.89006	0.2390251	14.87929	2.37878	7
564	-0.49255	1.25	-3.8283	2.64504	1.87839	8.67653	2.18256	2.95854	2.37094	7.42653	0.3192527	6.01086	0.3135	3
565	-0.49255	1.25	-3.8283	2.64504	4.34268	17.72342	7.93462	3.75008	4.83523	16.47342	0.2935171	11.76292	1.10504	5
566	-0.49255	1.25	-3.8283	2.64504	5.40409	26.10465	10.93899	5.0617	5.89664	24.85465	0.2372449	14.76729	2.41666	7
568	-0.49010	1.14047	-3.85031	2.61169	1.84468	8.377	1.9755	2.79612	2.33478	7.23653	0.3226381	5.82581	0.18443	3
569	-0.49010	1.14047	-3.85031	2.61169	4.20227	17.30529	7.5983	3.58424	4.69237	16.16482	0.2902828	11.44861	0.97255	5
570	-0.49010	1.14047	-3.85031	2.61169	5.32229	25.85988	10.75514	5.01484	5.81239	24.71941	0.2351347	14.60545	2.40315	7
572	-0.39801	1.18532	-3.86738	2.64033	1.93159	8.63883	2.0881	2.9966	2.3296	7.45351	0.3125507	5.95548	0.35627	3
573	-0.39801	1.18532	-3.86738	2.64033	4.31838	17.53516	7.69008	3.75978	4.71639	16.34984	0.288467	11.55746	1.11945	5
574	-0.39801	1.18532	-3.86738	2.64033	5.36227	25.88355	10.58825	5.11526	5.76028	24.69823	0.2332264	14.45563	2.47493	7
576	-0.4041	1.15333	-3.83565	2.58803	1.89589	8.39761	1.93941	2.85085	2.29999	7.24428	0.3174905	5.77506	0.26282	3
577	-0.4041	1.15333	-3.83565	2.58803	4.29744	17.45574	7.63975	3.70614	4.70154	16.30241	0.2883954	11.47540	1.11811	5
578	-0.4041	1.15333	-3.83565	2.58803	5.28187	25.79025	10.52573	5.06982	5.68597	24.63692	0.2307906	14.36138	2.48179	7
580	-0.66017	1.19371	-3.80387	2.44493	1.34039	7.84335	1.46291	2.59885	2.00056	6.64964	0.3008524	5.26678	0.15392	3
581	-0.66017	1.19371	-3.80387	2.44493	3.21842	15.94682	6.33465	3.29291	3.87859	14.75311	0.2628998	10.13852	0.84798	5
582	-0.66017	1.19371	-3.80387	2.44493	4.04328	24.06318	8.97733	4.86381	4.70345	22.86947	0.205665	12.78120	2.41888	7

Table A.2.3 (continued): Raw and corrected wind tunnel data for 28° AWA.

AWA 28	BODY AXIS						WIND TUNNEL CORRECTIONS								VELOCITY
Run No	LIFT [N]	Cl	DRAG [N]	Cd	L/D	D/L²	Cd	β'	Cdi	Cds	BLOCKAGE	Cl	Cl²	Cd	V (m/s)
550	12.79995	0.36061	5.341204253	0.15048	2.39645	0.03260	0.1514192	28.0026	0.0122365	0.1391827	1.028056917	0.3507663	0.123037	0.1472868	7
552	6.80725	1.04412	1.434280875	0.22000	4.74611	0.03095	0.2279074	28.0076	0.1025867	0.1253207	1.025262566	1.0183966	1.0371316	0.2222917	3
553	14.82063	0.81837	3.457089661	0.19089	4.28702	0.01574	0.1957547	28.0059	0.063021	0.1327337	1.026756896	0.7970429	0.6352774	0.1906534	5
554	21.69606	0.61123	6.392072135	0.18008	3.39421	0.01358	0.1827924	28.0044	0.0351562	0.1476362	1.029761009	0.5935688	0.352324	0.1775096	7
556	6.56469	1.00692	1.346897511	0.20659	4.87393	0.03125	0.2139504	28.0073	0.0954059	0.1185445	1.023896594	0.9834177	0.9671105	0.208957	3
557	14.43847	0.79727	3.411312024	0.18837	4.23253	0.01636	0.1929795	28.0058	0.0598129	0.1331667	1.026844184	0.7764246	0.6028351	0.1879346	5
558	21.55027	0.60713	6.405793952	0.18047	3.36418	0.01379	0.1831427	28.0044	0.0346853	0.1484574	1.029926541	0.5894854	0.3474931	0.1778211	7
560	6.78748	1.04109	1.47598391	0.22639	4.59861	0.03204	0.234258	28.0076	0.1019916	0.1322664	1.026662715	1.0140537	1.028305	0.2281743	3
561	14.71248	0.81240	3.485441789	0.19246	4.22112	0.01610	0.1972496	28.0059	0.0621047	0.1351449	1.027242967	0.7908524	0.6254476	0.1920184	5
562	21.45116	0.60433	6.432211104	0.18121	3.33496	0.01398	0.1838624	28.0044	0.034367	0.1494954	1.030135781	0.5866553	0.3441645	0.1784837	7
564	6.64270	1.01888	1.393128879	0.21368	4.76819	0.03157	0.2212174	28.0074	0.0976869	0.1235306	1.024901705	0.9941283	0.9882911	0.2158426	3
565	14.56236	0.80411	3.464547542	0.19131	4.20325	0.01634	0.1959986	28.0058	0.0608438	0.1351548	1.027244965	0.7827815	0.6127469	0.1908002	5
566	21.40266	0.60297	6.462127284	0.18205	3.31201	0.01411	0.1846932	28.0044	0.0342118	0.1504815	1.030334561	0.5852158	0.3424775	0.1792556	7
568	6.48271	0.99434	1.335856667	0.20490	4.85285	0.03179	0.2120743	28.0072	0.093038	0.1190362	1.02399572	0.9710436	0.9429256	0.2071046	3
569	14.26831	0.78787	3.445806511	0.19027	4.14077	0.01693	0.1947762	28.0057	0.0584114	0.1363648	1.027488875	0.7667929	0.5879713	0.1895652	5
570	21.26499	0.59909	6.473024285	0.18236	3.28517	0.01431	0.1849664	28.0043	0.0337731	0.1511933	1.03047806	0.5813706	0.3379918	0.1794957	7
572	6.64652	1.01947	1.442296276	0.22123	4.60829	0.03265	0.2287676	28.0074	0.0977993	0.1309683	1.026401023	0.9932474	0.9865403	0.2228832	3
573	14.41955	0.79622	3.511459739	0.19390	4.10643	0.01689	0.1984974	28.0058	0.0596562	0.1388412	1.027988075	0.7745445	0.5999191	0.1930931	5
574	21.22761	0.59804	6.509091276	0.18338	3.26122	0.01445	0.1859734	28.0043	0.0336544	0.1523189	1.03070496	0.5802209	0.3366562	0.1804332	7
576	6.47449	0.99308	1.370212819	0.21017	4.72517	0.03269	0.2173258	28.0072	0.0928023	0.1245235	1.02510186	0.968766	0.9385076	0.2120041	3
577	14.37725	0.79389	3.502304474	0.19339	4.10508	0.01694	0.1979649	28.0058	0.0593067	0.1386582	1.027951193	0.7722998	0.5964469	0.192582	5
578	21.15051	0.59586	6.54591981	0.18442	3.23110	0.01463	0.1869921	28.0043	0.0334104	0.1535817	1.030959508	0.5779709	0.3340504	0.1813768	7
580	5.89806	0.90467	1.355427246	0.20790	4.35144	0.03896	0.2138402	28.0066	0.0770132	0.136827	1.02758205	0.8803851	0.7750779	0.2081004	3
581	12.85798	0.70999	3.501573903	0.19335	3.67206	0.02118	0.197009	28.0052	0.0474348	0.1495742	1.030151665	0.689214	0.475016	0.1912427	5
582	19.39956	0.54654	6.583665965	0.18548	2.94662	0.01749	0.1876465	28.0040	0.0281076	0.1595389	1.032160395	0.5295065	0.2803771	0.1817998	7

Table A.2.4 : Run numbers for 28° AWA.

AWA 28°	Wind Speed	Twist Angle (°)		Sheeting Angle (°)		AWA 28°	Wind Speed	Twist Angle (°)		Sheeting Angle (°)	
Run No	m/s	Main Sail	Jib Sail	Main Sail	Jib Sail	Run No	m/s	Main Sail	Jib Sail	Main Sail	Jib Sail
515	zero	7	9	4	10	538	7	7	9	6	14
516	3	7	9	4	10	539	zero	7	9	8	10
517	5	7	9	4	10	540	3	7	9	8	10
518	7	7	9	4	10	541	5	7	9	8	10
519	zero	7	9	4	12	542	7	7	9	8	10
520	3	7	9	4	12	543	zero	7	9	8	12
521	5	7	9	4	12	544	3	7	9	8	12
522	7	7	9	4	12	545	5	7	9	8	12
523	zero	7	9	4	14	546	7	7	9	8	12
524	3	7	9	4	14	547	zero	7	9	8	14
525	5	7	9	4	14	548	3	7	9	8	14
526	7	7	9	4	14	549	5	7	9	8	14
527	zero	7	9	6	10	550	7	7	9	8	14
528	3	7	9	6	10	551	zero	7	13	4	10
529	5	7	9	6	10	552	3	7	13	4	10
530	7	7	9	6	10	553	5	7	13	4	10
531	zero	7	9	6	12	554	7	7	13	4	10
532	3	7	9	6	12	555	zero	7	18	4	10
533	5	7	9	6	12	556	3	7	18	4	10
534	7	7	9	6	12	557	5	7	18	4	10
535	zero	7	9	6	14	558	7	7	18	4	10
536	3	7	9	6	14	559	zero	10	9	4	10
537	5	7	9	6	14	560	3	10	9	4	10

Table A.2.4 (continued): Run numbers for 28° AWA.

AWA 28°	Wind Speed	Twist Angle (°)		Sheeting Angle (°)		AWA 28°	Wind Speed	Twist Angle (°)		Sheeting Angle (°)	
Run No	m/s	Main Sail	Jib Sail	Main Sail	Jib Sail	Run No	m/s	Main Sail	Jib Sail	Main Sail	Jib Sail
561	5	10	9	4	10	572	3	12	9	4	10
562	7	10	9	4	10	573	5	12	9	4	10
563	zero	10	13	4	10	574	7	12	9	4	10
564	3	10	13	4	10	575	zero	12	13	4	10
565	5	10	13	4	10	576	3	12	13	4	10
566	7	10	13	4	10	577	5	12	13	4	10
567	zero	10	18	4	10	578	7	12	13	4	10
568	3	10	18	4	10	579	zero	12	18	4	10
569	5	10	18	4	10	580	3	12	18	4	10
570	7	10	18	4	10	581	5	12	18	4	10
571	zero	12	9	4	10	582	7	12	18	4	10

APPENDIX A.3

Table A.3.1 : Geometric coordinates of main sail.

MAIN SAIL 1			MAIN SAIL 2			MAIN SAIL 3			MAIN SAIL 4		
X (mm)	**Y** (mm)	**Z** (mm)	**X** (mm)	**Y** (mm)	**Z** (mm)	**X** (mm)	**Y** (mm)	**Z** (mm)	**X** (mm)	**Y** (mm)	**Z** (mm)
396.8089	-348.9783	233.1773	134.2651	-128.2478	-109.7614	298.2728	761.7448	-530.9027	90.81265	1194.891	-910.7541
379.988	-357.291	211.6396	56.24748	-136.1348	-129.7244	285.9983	756.7743	-540.6208	71.72645	1191.493	-915.4431
343.0676	-372.7795	170.6194	-23.23089	-142.1707	-143.514	260.3623	747.4094	-558.9991	52.42803	1188.329	-919.354
276.9892	-391.2291	118.5719	-76.48368	-145.7027	-151.0234	218.4889	735.5004	-582.3164	39.51285	1186.284	-921.7489
201.5487	-403.8629	79.20951	-103.1419	-147.4139	-154.5916	173.6342	725.9234	-600.5504	33.04717	1185.264	-922.9049
121.1489	-412.4252	50.29702	383.2619	204.0252	-130.4305	127.1415	717.8587	-614.8954	114.0508	1327.244	-976.8452
38.13242	-418.7325	29.56836	366.8644	196.8074	-146.8652	79.68887	710.6499	-626.1699	111.046	1326.478	-978.3232
-46.48511	-422.8229	16.20072	331.8885	183.3008	-178.0077	31.57025	704.2432	-634.7442	104.9597	1325.013	-981.1592
-103.1579	-424.9689	9.285849	272.5078	166.6789	-217.4144	-0.6496837	700.1895	-639.7226	95.57704	1323.047	-984.954
-131.5259	-425.9759	6.045795	207.1385	154.2097	-247.7113	-16.77727	698.1841	-642.1179	85.9484	1321.326	-988.2108
399.9466	-250.306	173.3206	138.5425	144.5249	-270.8306	222.6693	1043.544	-743.9018	76.16863	1319.763	-991.0662
382.9357	-258.5415	152.4909	68.13551	136.4037	-288.2988	214.1983	1040.23	-749.7926	66.29005	1318.291	-993.6099
345.8289	-273.9042	112.8518	-3.466098	129.7857	-300.7407	196.6839	1033.948	-760.9556	56.33454	1316.904	-995.8858
280.1584	-292.3543	62.53699	-51.43041	125.7756	-307.6632	168.5989	1025.769	-775.2603	49.67837	1316.005	-997.3303
205.7318	-305.2864	24.27618	-75.44005	123.8146	-310.9682	138.8972	1018.925	-786.6792	46.34478	1315.553	-998.0252
126.6293	-314.378	-4.124252	346.5571	501.1543	-342.9942	108.282	1012.937	-795.9044	86.15703	1388.22	-1029.473
45.0212	-321.3387	-24.7964	331.8804	495.0374	-355.917	77.11682	1007.433	-803.4004	84.60217	1388.124	-1029.916
-38.15708	-326.2085	-38.517	300.9396	483.5646	-380.3501	45.55458	1002.379	-809.3795	81.49268	1387.933	-1030.801
-93.87827	-328.9041	-45.77376	249.5417	469.2458	-411.2085	24.42432	999.132	-812.951	76.82865	1387.646	-1032.13
-121.7711	-330.1896	-49.19532	193.8421	458.1363	-435.0376	13.84712	997.5183	-814.6751	72.16458	1387.357	-1033.459
399.6085	-64.21604	55.0175	135.8203	449.1306	-453.442	162.0489	1212.967	-880.5693	67.50103	1387.069	-1034.789
382.5411	-72.19608	35.75356	76.46713	441.3149	-467.5639	156.624	1211.058	-883.9018	62.8383	1386.783	-1036.123
345.6883	-87.11256	-0.8508327	16.21888	434.6256	-477.9099	145.5032	1207.427	-890.2369	58.17723	1386.503	-1037.464
281.6718	-105.2679	-47.31588	-24.12679	430.4692	-483.7764	127.9548	1202.635	-898.4574	55.07018	1386.32	-1038.36
210.0258	-118.4622	-82.92004	-44.32157	428.4229	-486.5867	109.6137	1198.541	-905.1733	53.51156	1386.223	-1038.789

Table A.3.2 : Geometric coordinates of jib sail.

JIB SAIL 1			JIB SAIL 2			JIB SAIL 3			JIB SAIL 4		
X (mm)	**Y** (mm)	**Z** (mm)	**X** (mm)	**Y** (mm)	**Z** (mm)	**X** (mm)	**Y** (mm)	**Z** (mm)	**X** (mm)	**Y** (mm)	**Z** (mm)
-169.1324	-478.3149	-85.00955	-457.4995	-248.4154	-331.366	-203.3319	324.8878	-578.3871	-63.01521	742.0713	-743.704
-187.0407	-484.7143	-94.39385	-474.114	-245.1028	-328.0449	-230.7744	328.4537	-576.1749	-72.98716	742.1022	-745.2687
-223.9653	-496.2475	-111.8197	-114.3813	-45.18184	-338.8965	-248.3661	332.1267	-572.0291	-83.07445	742.8287	-745.6627
-278.7946	-511.1645	-140.4354	-127.4706	-49.03333	-344.3987	-257.0099	334.1829	-569.6406	-92.98246	744.3649	-744.2856
-333.7419	-523.5423	-170.0584	-154.3085	-55.80642	-354.4103	-55.02343	494.2058	-620.2783	-99.33688	745.774	-742.5731
-391.024	-532.3048	-196.4629	-194.2003	-64.30385	-371.2775	-61.6306	492.8156	-622.1324	-102.465	746.5456	-741.6196
-452.0076	-536.097	-215.5057	-234.2085	-70.95554	-388.7193	-75.05722	490.4763	-625.3721	-27.41718	844.8283	-781.5914
-515.8364	-532.8248	-220.1596	-275.6187	-74.96636	-403.6139	-95.0704	487.7233	-631.1321	-29.20515	844.6203	-781.8964
-557.697	-526.7789	-215.3762	-319.0242	-75.39865	-412.9143	-115.1356	485.8497	-637.078	-32.80646	844.2949	-782.4098
-578.3098	-523.1223	-212.0947	-363.2351	-71.14247	-412.3878	-135.6386	485.2177	-641.7309	-38.18926	843.9666	-783.3686
-159.9552	-411.1916	-126.1833	-391.8012	-65.93882	-407.1785	-156.6312	486.2147	-643.6902	-43.57446	843.8231	-784.3627
-177.1498	-417.1536	-134.9087	-405.8448	-62.94434	-404.0155	-177.413	489.1519	-641.4519	-49.00702	843.9345	-785.0857
-212.5724	-427.86	-151.0658	-92.84669	143.5356	-441.3626	-190.7156	492.0305	-638.0611	-54.48002	844.3747	-785.2541
-265.1765	-441.6479	-177.6888	-103.7174	140.616	-445.4422	-197.2534	493.6276	-636.1382	-59.86703	845.2047	-784.5686
-317.9019	-452.9994	-205.2452	-125.9476	135.5436	-452.783	-42.86045	625.0038	-682.8316	-63.34346	845.9484	-783.7186
-372.8102	-460.8764	-229.665	-159.0153	129.2811	-465.3329	-47.76799	624.1032	-684.0126	-65.05915	846.3536	-783.2453
-431.1302	-463.9844	-246.9572	-192.1839	124.5397	-478.3027	-57.71226	622.6143	-686.044	-23.31416	938.7686	-821.0181
-491.8978	-460.3992	-250.5534	-226.3889	121.9709	-489.1156	-72.54961	620.9153	-689.7333	-23.64725	938.7832	-821.0608
-531.6424	-454.399	-245.5765	-261.9784	122.319	-495.2739	-87.41816	619.8423	-693.5425	-24.31343	938.8124	-821.1463
-551.2074	-450.8065	-242.2546	-297.8451	126.3586	-493.6069	-102.5464	619.6463	-696.4259	-25.31269	938.8562	-821.2745
-135.1008	-218.0149	-240.8424	-320.9145	130.8646	-488.7658	-117.9362	620.5903	-697.4031	-26.31196	938.9	-821.4027
-150.1713	-222.8223	-247.7843	-332.2511	133.4213	-485.9113	-133.0933	622.8695	-695.4723	-27.31122	938.9438	-821.531
-181.1418	-231.3661	-260.5269	-71.32001	338.0315	-542.4568	-142.7955	625.0199	-692.8829	-28.31049	938.9876	-821.6592
-227.1549	-242.2316	-281.7559	-79.85669	336.0048	-545.2376	-147.5665	626.2043	-691.4303	-29.30976	939.0314	-821.7874
-273.2927	-250.9662	-303.7208	-97.25731	332.5408	-550.1707	-33.50615	744.7962	-737.7283	-29.97593	939.0606	-821.8729
-321.1917	-256.6524	-322.8315	-123.1655	328.3645	-558.7644	-36.76314	744.2916	-738.3863	-30.30902	939.0752	-821.9156
-371.7201	-258.1791	-335.5717	-149.1486	325.3599	-567.6379	-43.34368	743.4744	-739.4995			
-423.7232	-254.0761	-336.6437	-175.8186	324.0198	-574.8112	-53.17231	742.579	-741.5665			

CURRICULUM VITAE

Name Surname: Ersin Danış

Address: London, UK

E-Mail: ersin.danis@yahoo.co.uk

B.Sc.: Shipbuilding and Ocean Engineering, ITU, 2008.

M.Sc.: Exchange Student in Ship Science at University of Southampton, 2010-2011.

M.Sc.: Naval Architecture and Marine Engineering, ITU, 2012.

Professional Experience and Rewards: 1 year work experience at SETA Naval Architecture and Marine Engineering Co.